

Acutely controlled inactivation reveals requirements for maintenance and subcompartmentalization of the mammalian Golgi ribbon

A thesis presented by

Timothy S. Jarvela

B.S., The College of New Jersey

to

The Department of Biological Sciences

Carnegie Mellon University

Pittsburgh, Pennsylvania

in partial fulfillment of the requirements for the degree of

Doctor of Philosophy

in the field of

Biological Sciences

September 20th, 2013

Thesis Advisor: Dr. Adam D. Linstedt

Abstract

The mammalian Golgi ribbon is a highly dynamic organelle, notoriously difficult to study and interpret. It is a nexus of the endomembrane system, with entry and exit at both ends of the stack. Cargo typically transports through the Golgi on the order of 20 minutes. However, traditional methods of cell biology used to determine the function of a protein through knockouts and knockdowns, result in aberrant end states that may be far removed from the initial functions. Further complicating efforts is that the Golgi undergoes complex rearrangements in response to the cell cycle, stress, development, and migration. Defects in a complex, interconnected membrane system at one level of the pathway can quickly cascade and compound into other secondary effects. Proper study requires analysis of the period immediately following loss of the protein of interest. One approach that allows for this is acute inactivation. Unfortunately, this tool has been mostly of limited use in mammalian cells as selectively targeted drugs and temperature sensitive mutants are difficult to come by. Instead, we have begun using a technique called Chromophore Assisted Light Inactivation (CALI) to acutely inactivate proteins. Though the practice and concepts of CALI have been around for the past 25 years, it has remained underused due to technical limitations and hazardous materials. Recently with the advent of KillerRed, a genetically encoded photosensitizer, we have been able to temporally control inactivation of specific protein complexes and observe the cell's response within the initial minutes post inactivation. Here we use KillerRed to address questions surrounding two different steps in Golgi biogenesis, ribbon formation and endoplasmic reticulum export.

Initially, we described the methods and effectiveness of using KillerRed tagged proteins to inactivate complexes of endogenous proteins in *trans* by expressing KillerRed tagged sec13, a component of the COPII coatomer which is required for vesicular transport from the endoplasmic reticulum. Irradiation of sec13-KillerRed expressing cells blocked export of cargo and Golgi proteins from the endoplasmic reticulum, consistent with long term inhibition experiments. Remarkably, the acute block of endoplas-

mic reticulum exit resulted in the distribution of early–but not late–Golgi residents to peripheral punctae that correspond to the endoplasmic reticulum-Golgi intermediate compartment. These results identify a omnipresent recycling pathway required for maintenance of the Golgi ribbon. Further, the return to the Golgi requires input from the endoplasmic reticulum.

Subsequently, we dissected the different roles that two mammalian Golgi tethers, GRASP65 and GRASP55, play in maintenance of the Golgi ribbon using a combination of KillerRed inactivation with Fluorescence recovery after photobleaching to measure Golgi ribbon integrity at discrete levels of the Golgi stack. Inhibition of GRASP65 which resides on the *cis*-Golgi, results rapid loss of fluorescence recovery after photobleaching of *cis*- but not *trans*-Golgi residents. GRASP55 inhibition resulted in a rapid loss of *trans*- but not *cis*-Golgi resident recovery. The distinction of duties was functionally significant, as rescuing the loss of GRASP65 from the *cis*-Golgi with redistributed GRASP55 restored integrity of the ribbon but sacrificed compartmentalization and proper glycosylation of exported cargo. These data identify GRASPs as novel regulators of Golgi subcompartmentalization identity. Thus the division of duties among two GRASPs in Golgi ribbon forming cells is important for proper processing of cargo.

Collectively, the use of KillerRed has given evidence to old predictions as well been useful in framing more traditional molecular biology experiments.

Contents

Contents	iii
List of Figures	iv
1 Introduction	1
2 Golgi GRASPs: moonlighting membrane tethers	5
2.1 Introduction	6
2.2 GRASP structural features	8
2.3 Structuring the Golgi	14
2.4 Regulation of GRASP activity	18
2.5 Chaperoning secretion and processing	20
2.6 Unconventional secretion	22
2.7 Conclusion	25
3 Irradiation-induced protein inactivation reveals Golgi enzyme cycling to cell periphery	27
3.1 Introduction	27
3.2 Results	29
Targeted acute inactivation blocks ER exit	29
Acute dependence of Golgi integrity on ER exit	32
GalNAcT2-GFP cycles to the cell periphery	34

Cycling is through the ER-Golgi intermediate compartment	36
Cycling involves cis- but not trans-Golgi proteins	38
3.3 Discussion	42
3.4 Materials and Methods	43
3.5 Movie Figure Legends	46
4 The Role of GRASPs in cisternae specific linking	49
4.1 Introduction	50
4.2 Results	52
4.3 Discussion	65
4.4 Materials and Methods	69
4.5 Movie Legends	72
5 Conclusions and Future Directions	73
6 Appendix on the use of KillerRed for acute inactivation	79
Bibliography	87

List of Figures

2.1 Overview of the unconventional and conventional secretory pathways .	8
2.2 Mammalian GRASP65 and GRASP55	10
2.3 GRASP65 tethering and 2 step phospho-regulation	17
2.4 GRASP65 and GRASP55 work sequentially to promote C-terminal valine motif cargo through the secretory pathway	21

2.5	Speculative model of GRASP function in unconventional secretion . . .	23
3.1	Acute inactivation at the onset of Golgi assembly	31
3.2	Acute inactivation at steady state	33
3.3	Golgi at 4.5 hours after Sec13–KR inactivation	35
3.4	Evidence for GalNAcT2–GFP cycling	37
3.5	Progressive loss of ERGIC53-positive puncta after Sec13-KR inactivation.	38
3.6	GalNAcT2 redistribution to the ER-Golgi intermediate compartment	39
3.7	Preferential peripheral cycling of <i>cis</i> Golgi components	40
3.8	Endogenous <i>cis</i> Golgi proteins co-label GalNAcT2-GFP-positive recycling intermediates	41
4.1	Localization and bleaching of KR constructs. Pre- and post-bleach images of each KR indicated	54
4.2	Inactivation of GRASP proteins blocks Golgi ribbon formation	55
4.3	GRASP inactivation blocks Golgi ribbon maintenance	57
4.4	GRASPs are required for integrity of distinct levels of the Golgi stack	58
4.5	The GM130-45 chimera rescues Golgi ribbon integrity after GM130 knockdown	61
4.6	C-terminus of golgin-45 recruits GRASP55 to mitochondrial membranes	63
4.7	Expression of the GM130-45 chimera increases marker colocalization .	64
4.8	Decreased glycan processing in cells expressing the GM130-45 chimera	66

Acknowledgements

Over the course of an endeavor such as this, it becomes necessary to rely on many people for help and guidance.

First and foremost I must thank Dr. Adam D Linstedt for his support, guidance, and input throughout the years spent working in his lab. He has been constant in challenging me to become a better scientist and communicator of ideas. I would like to also thank him for allowing me to function primarily as a microscopist in a lab that he has built on biochemistry and molecular biology.

I would like to thank my committee members Dr. John Woolford and Dr. Manojkumar Puthenveedu for their guidance throughout my graduate career. I also thank Dr. Simon Watkins for serving as my external committee member for my thesis examination.

Drs James Fitzpatrick, Haibing Teng, and Simon Watkins have each been extremely helpful in expanding my knowledge and understanding of the principles and practice of microscopy, for that I am very grateful.

One does not spend 6 years in a career without developing friends and colleagues to rely on for daily support and help. I have many past and present members of the Linstedt lab to thank: Dr. Tim Feinstein, Dr. Debrup Sengupta, Dr. Steve Truschel, Dr. Yusong Guo, Dr. Smita Yadav, Dr. Somshuvra Mukhopadhyay, Cassandra Hall and Collin Bachert. They have each been valuable lab mates to have around for conversation and troubleshooting experiments. Also, the members of the Lee and Puthenveedu labs, especially Dr. Jeanne Morin-Leisk and Dr. Kaitlyn Dykstra, have been great for support.

Most importantly, I have to thank all my friends and family who have constantly believed in me and been there to support me whenever the challenges seemed too daunting or the hours became too long. Most of all, I need to thank my fiancée Alys Cheatle for her constant love, support, and understanding.

Introduction

The Golgi

The mammalian Golgi ribbon is a complex structure consisting of stacks of flattened cisternae which are linked laterally to form a contiguous lumen. The stacked membrane system is structured to promote sequential processing of cargos ([Mellman and Simons, 1992](#)) while the lateral linking is thought to be important in equalizing cargo and enzyme loads within a cisternal layer ([Puthenveedu et al., 2006](#)). The central positioning and formation of the Golgi ribbon are important for directed secretion ([Bergmann et al., 1983](#)) which is important in many processes, among them cell polarity and wound repair.

Controversy still surrounds how different proteins function in formation of the Golgi. Membrane tethers, namely the GRASPs and golgins, have been implicated at each step of Golgi assembly: subcompartmentalization, stacking of membranes, positioning, and formation of lateral linkages between adjacent stacks.

Models of trafficking through the Golgi

Diverse models have been proposed to explain how the flow of membranes, enzymes, and cargo, proceeds through the Golgi stack. Secretory cargo enters the Golgi at the cis-face and progresses towards the trans, encountering processing enzymes throughout, and then exits into the trans Golgi network (TGN) for further sorting and export to final cellular destinations. The cisternal progression model hypothesizes that cargo enters the Golgi as

the formation of a new cisternae which is then populated by recycling early Golgi enzymes. This continues with later enzymes replacing earlier enzymes, and earlier enzymes recycling to and fusing with newer cisternae. This allows cargo to traverse the stack without leaving the lumen of the original cisternae, as has been seen when observing trafficking of large aggregates (Bonfanti et al., 1998). The vesicular trafficking model suggests that secretory cargo moves forward through the stack in anterograde vesicles while the enzymes remain within their original cisternae.

Two other models have been proposed to explain additional data which do not fit into either of the previous. The rapid-partitioning model states that upon entering the Golgi, secretory cargo rapidly diffuses throughout all layers of the stack and that the Golgi is separated into processing and export domains. This can explain how the export of some cargoes follows exponential kinetic rates (Patterson et al., 2008).

Regulation and maintenance of the mammalian Golgi apparatus

One of the most striking aspects of the mammalian Golgi ribbon is the changes in structure that it undergoes prior to mitosis. The Golgi ribbon first fragments and then unstacks and vesiculates into small vesicles and tubular components (Colanzi and Corda, 2007). This process is repeated every time a cell divides and is required for a cell to undergo division. The reformation of the Golgi post mitosis occurs in a few discrete stages: subcompartmentalization, stacking of cisternae, minus end directed motility, and ribbon formation. While these stages can be discretely resolved from one another through different knockdowns (Puthenveedu and Linstedt, 2001; Feinstein and Linstedt, 2008; Yadav et al., 2009) and drug treatments (Cole et al., 1996; Puri and Linstedt, 2003), they are thought to be continually occurring throughout the steady state secretory pathway, with the additional step of membrane and cargo input into this system through the COPII vesicles budding from the ER.

Acute manipulations are required to understand dynamic systems

Understanding dynamic systems such as the Golgi requires experiments that can address questions on relevant time scales. For the Golgi, that scale would be minutes to hours.

Pharmacological inhibition or activation of proteins and pathways is still the gold standard for on demand manipulations of the cellular milieu. However, drug discovery and characterization of targets are tedious to a researcher who has a protein target already in mind. In yeast and other genetically tractable organisms, temperature sensitive mutations allow for a quick targeted approach. Temperature sensitive mutants have been used with success in mammalian systems. Indeed, the temperature sensitive secretory protein VSV-G tagged with GFP has been thoroughly used to study secretory trafficking (Presley et al., 1997). But finding new temperature sensitive mutants is still a daunting task.

Other methods to acutely inactivate protein function have been by microinjection of dominant negative proteins (Miles et al., 2001) or of degradation inducing antibodies (Puthenveedu et al., 2006). These have come with their own technological drawbacks due to the difficulties of microinjection and the added stresses it adds to cells. In contrast, the genetically encoded photosensitizer KillerRed (Bulina et al., 2005) can be tagged to proteins targeted for inactivation by chromophore assisted light inactivation (CALI). The principles of CALI rely on the generation of reactive oxygen species which aggressively react with protein sidechains and the peptide backbone resulting in inactivation of the protein (Jay, 1988; Liao et al., 1994; Surrey et al., 1998).

The numerous controversies surrounding Golgi structure and function can only be untangled with more powerful and robust assays to study Golgi dynamics immediately post inactivation. This thesis puts forward the use of KillerRed as a tool for specific protein inactivation in studying membrane trafficking pathways. First, we will introduce the GRASP proteins and the many pathways in which they play a part. Using acute inactivation and probing for one specific pathway, ribbon formation, we can address the role of that GRASPs play in ribbon formation without worrying about downstream effects. Additionally, we used

acute inactivation to study the dependence of the Golgi on export from the ER. In both cases, acute inactivation yields phenotypes distinct from long term knockdown, but which fit within current models of Golgi structure and function.

Overview

In the next chapter, we first review the many functions of Golgi reassembly and stacking proteins. The GRASPs are ideal targets for acute inactivation techniques due to their prevalence in a variety of cellular trafficking pathways ([Jarvela and Linstedt, 2012a](#)). Following this, in chapter three we will first show the efficacy of KillerRed by inactivating ER exit and examine the role it plays in maintaining the Golgi apparatus. Acute inactivation of *sec13*, a component of the COPII coat, revealed a robust recycling pathway of early Golgi proteins to the cell periphery ([Jarvela and Linstedt, 2012b](#)). Chapter four focuses on the use of KillerRed to acutely inactivate each GRASP independently to study its role in ribbon formation. These experiments reveal a novel role for GRASPs to play in subcompartmentalization of the Golgi. In the final chapter, we will address how these data achieved by acute inactivation fit with previously published results and potential future directions for research into Golgi maintenance.

Golgi GRASPs: moonlighting membrane tethers

The identification of mammalian Golgi reassembly stacking proteins (GRASPs) 15 years ago was followed by experiments implicating them in diverse functions, including two differing structural roles in Golgi biogenesis and at least two distinct roles in the secretion of proteins. GRASP65 and GRASP55 are localized to cis and medial/trans Golgi cisternae, respectively. They are both required for stacking of Golgi membranes in a Golgi reassembly assay. Depletion of either GRASP from cultured cells prevents the linking of Golgi membranes into their normal ribbon-like network. While GRASPs are not required for transport of secretory cargo per se, they are required for ER-to-Golgi transport of certain specific cargo, such as those containing a C-terminal valine motif. Surprisingly, GRASPs also promote secretion of cargo by the so-called unconventional secretory pathway, which bypasses the Golgi apparatus where the GRASPs reside. Furthermore, regulation of GRASP activity is now recognized for its connections to cell cycle control, development, and disease. Underlying these diverse activities is the structurally conserved N-terminal GRASP domain whose crystal structure was recently determined. It consists of a tandem array of atypical PSD95–DlgA–Zoo-1 (PDZ) domains, which are well-known protein–protein interaction motifs. The GRASP PDZ domains are used to localize the proteins to the Golgi as well as GRASP-mediated membrane tethering and cargo interactions. These activities are regulated, in part, by phosphorylation of the large unstructured C-terminal domain.

2.1 Introduction

Proteins translated in association with the endoplasmic reticulum (ER) are packaged into vesicles for export to the Golgi apparatus. This protein cargo may bear exit signals promoting selective concentration during exit ([Bonifacino and Glick, 2004](#)).

In mammalian cells, ER exit sites are both centrally located and distributed throughout the cell periphery. Vesicles leaving the ER coalesce into the ER-Golgi intermediate compartment (ERGIC) ([Presley et al., 1997](#)). From the ERGIC, there is both recycling to the ER and transfer of cargo-bearing membrane to the centrally located Golgi apparatus ([Appenzeller-Herzog and Hauri, 2006](#)).

The Golgi apparatus is structured to promote sequential processing of the arriving cargo ([Mellman and Simons, 1992](#)). Flattened membranes called cisternae are in close apposition to one another, forming a stack. The first Golgi enzymes to act on the cargo are enriched in the entry, or cis-cisternae. Enzymes enriched in the medial cisternae of the stack carry out the next processing steps. The last events occur in the trans-cisternae and trans-Golgi network (TGN). In the TGN, the processed cargo is packaged for exit from the Golgi apparatus. The stacked structure of the Golgi apparatus is evident in most eukaryotes.

Mammalian Golgi stacks are positioned near the centrosome-based microtubule-organizing center and they are laterally linked to form a ribbon-like membrane network ([Lowe, 2011](#)). Dynamic tubular membranes connect adjacent analogous cisternae within this network promoting uniform, yet cisternae-specific distribution of Golgi enzymes across the entire Golgi ribbon. Discontinuities, if prolonged, lead to nonuniform enzyme distribution and under-processing of secretory cargo ([Puthenveedu et al., 2006](#)). Positioning of Golgi membranes near the centrosome allows the secretion to be efficiently directed to the most proximal plasma membrane domain or cell leading edge ([Bergmann et al., 1983](#)). This directed secretion is needed for cell polarity and cell migration for wound repair. It is also involved in muscle differentiation, immunological synapse formation, and neuritic process extension ([Kupfer et al., 1982, 1983](#); [DeAnda et al., 2005](#)).

In preparation for mitosis, the mammalian Golgi ribbon is unlinked, and the resulting stacks then vesiculate, leaving dispersed vesicles and clusters of vesicles (Jesch and Linstedt, 1998; Colanzi et al., 2007; Feinstein and Linstedt, 2008). These vesicles and vesicle clusters are partitioned equally into daughter cells, whereupon they reassemble into the stacked and laterally linked interphase membrane network. The Golgi ribbon is also extensively fragmented during apoptosis, and unlinking of the ribbon is thought to occur transiently during reorientation of the organelle as cells define a new leading edge (Lane et al., 2002; Bisel et al., 2008b).

Interestingly, certain secretory cargo molecules entirely bypass the Golgi apparatus en route to secretion (Nickel, 2003; Giuliani et al., 2011). Examples include fibroblast growth factors 1 and 2 (Prudovsky et al., 2002; Zehe et al., 2006), interleukins 1 α and β (Keller et al., 2008; Dupont et al., 2011), integrin α PS1 (Schotman et al., 2008), acyl-CoA binding protein (Duran et al., 2010; Manjithaya et al., 2010; Kinseth et al., 2007; Cabral et al., 2010), and galectins (1 and 3) (Cooper and Barondes, 1990; Sato et al., 1993; Hughes, 1999; Mehul et al., 1995). Unconventional secretion occurs by multiple routes. For some unconventional cargo, secretion begins with transmembrane proteins translated in association with the ER or cytosolic proteins internalized into autophagic membranes (Nickel, 2005). Membranes derived from the ER or the autophagic membranes then dock and fuse directly with the plasma membrane to transfer their content.

Since their discovery 15 years ago, experimental evidence indicates that mammalian Golgi reassembly stacking proteins (GRASPs) may participate in a surprising number of the processes just described (Figure 2.1). Mammalian cells express two GRASPs and both are encoded by distinct genes. GRASP65 is localized to cis-Golgi cisternae and GRASP55 is localized to medial and trans-Golgi cisternae (Shorter et al., 1999). The GRASPs contain a conserved N-terminal GRASP domain. Simpler eukaryotes express a single GRASP, which is also defined by the presence of this domain. The key feature of the GRASP domain is its two PSD95-DlgA-Zo-1 (PDZ) domains, which interact with PDZ ligands in partner

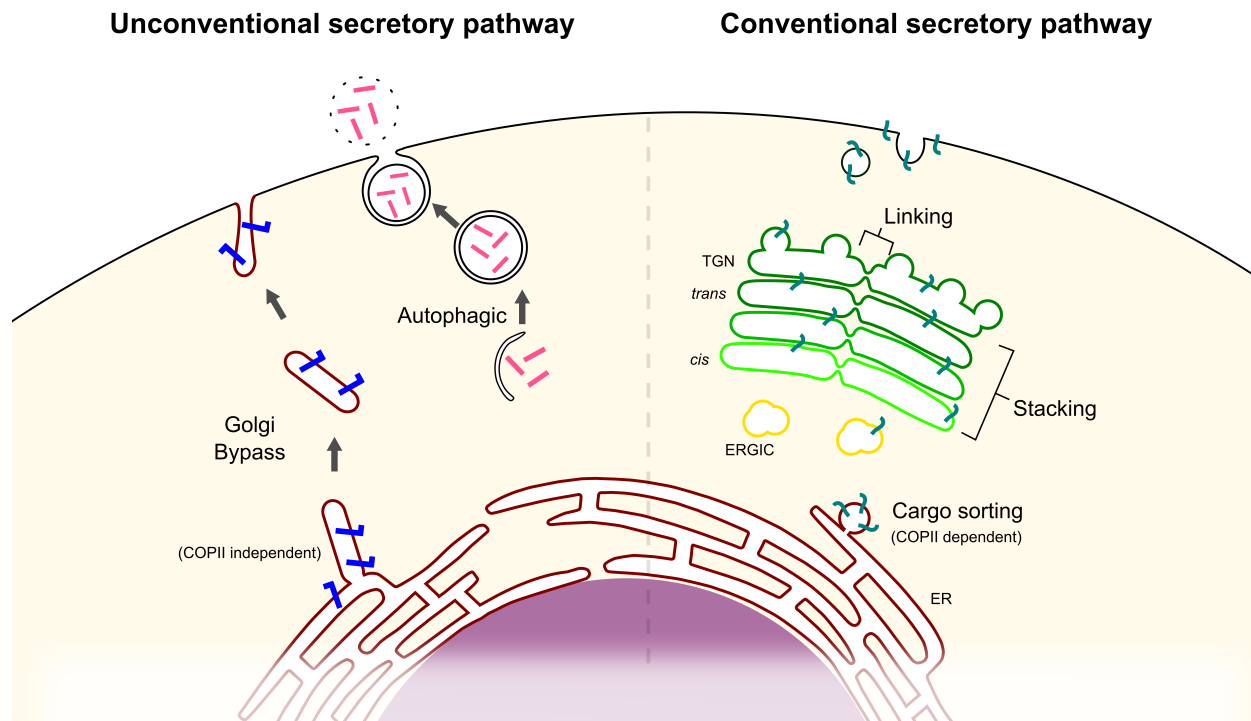


Figure 2.1: **Overview of the unconventional and conventional secretory pathways.** Three types of cargo are shown passing through the secretory pathway. Unconventional transmembrane cargo (blue) are exported from the ER in a COPII independent fashion and directly tether with the plasma membrane prior to fusion. Cytosolic cargo (pink) is first internalized in autophagic membranes before tethering and fusing to the plasma membrane. Traditional cargo (teal) progresses through the canonical secretory pathway.

proteins (Figure 2.2A and B). Following the GRASP domain, GRASPs have a nonconserved, serine and proline rich (SPR) domain comprising about half of the protein (Figure 2.2A). A simplifying assumption is that the GRASP domain mediates functional interactions regulated by the SPR domain.

2.2 GRASP structural features

The GRASP domain

The GRASP domain is a striking feature conserved across GRASP homologues. It is comprised mostly of two PDZ domains in tandem (Figure 2.2B). PDZ domains share a conserved

globular structure in which an α -helix and β -strand form a hydrophobic binding groove. Many proteins contain PDZ domains, and most PDZ-containing proteins contain multiple such domains that are present in arrays. The domain mediates protein–protein interactions and, as such, its presence in multiple copies confers the ability to scaffold the assembly of large complexes (Wang et al., 2010). Typically, the ligands that bind the groove fall into one of three categories. Canonical ligands are present at a protein’s C-terminus. The four C-terminal residues insert into the PDZ groove, forming a β -strand that completes a β -sheet. The carboxyl group at the C-terminus is coordinated within the PDZ binding pocket by a Gly–Leu–Gly–Phe sequence and water molecule (Oschkinat et al., 1999). The second and third types are internal sequences. They may form a β -finger with a tight hairpin and usually an acidic amino acid to mimic the free C-terminus (Hillier et al., 1999) or they might simply be flexible sequence stretches that contain glycines, for example, that decrease steric constraints and project side chains into the pocket (Runyon et al., 2007; Zhang et al., 2009).

The structure of the GRASP55 GRASP domain was recently solved (Truschel et al., 2011) and unexpectedly revealed that the GRASP PDZ domains lack the typical $\beta\beta\beta\alpha\beta\beta\alpha\beta$ secondary structure organization of eukaryotic PDZ domains. Instead, the two PDZ domains are circularly permuted, which has two important consequences. First, although not evident among metazoan PDZ domains, circular permutation is present in prokaryotic PDZs. In fact, the overall structures of the GRASP PDZ domains align remarkably well with prokaryotic PDZ domains as well as with one another (Prudovsky et al., 2002). Second, this unusual arrangement of a metazoan PDZ revealed that the key β 2 strands of the binding grooves lay outside the previously predicted PDZ-like regions. This calls into question the interpretation of experiments based on incorrect assignment of the domains. In fact, a recent study failed to include the key β 2 strands in its GRASP PDZ domain constructs even though this work was published after the structure was known (Gee et al., 2011). Inexplicably, the constructs were binding competent, but this binding could not have been due to a PDZ interaction.

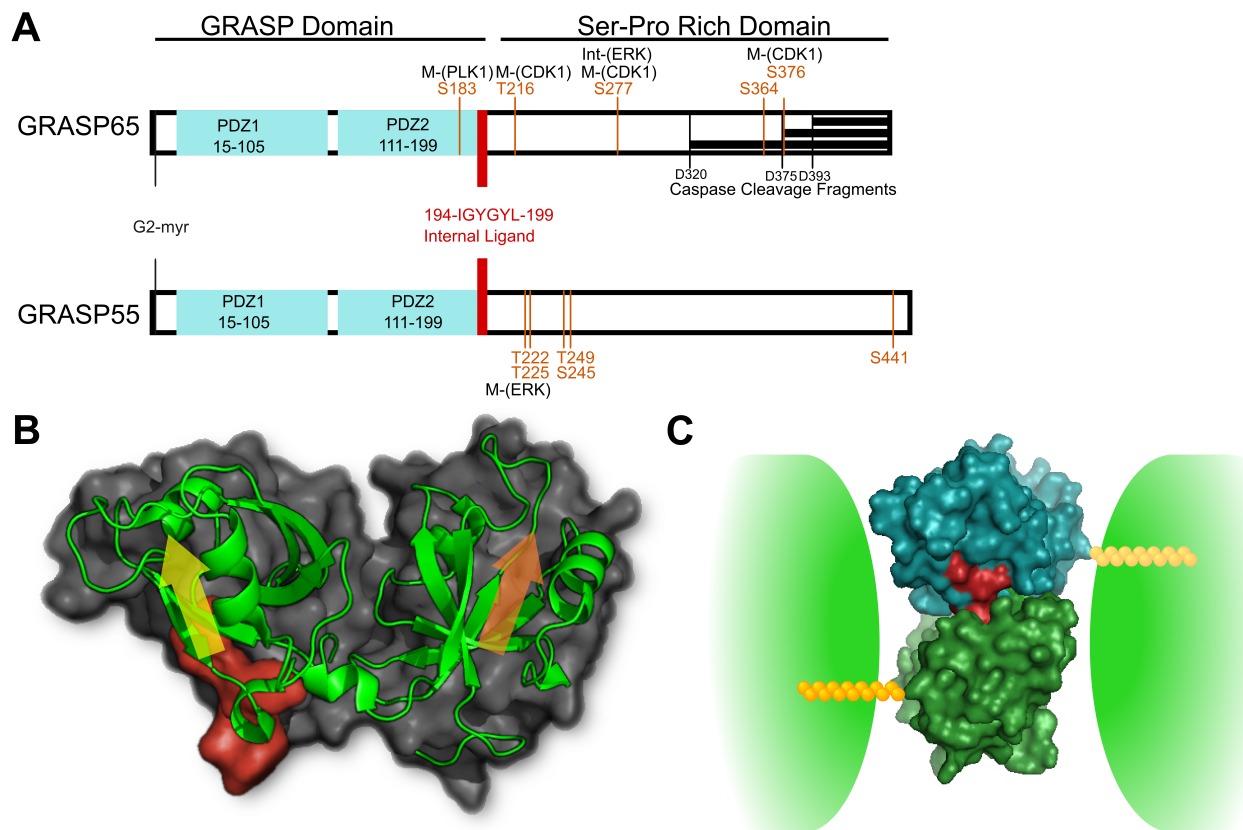


Figure 2.2: **Mammalian GRASP65 and GRASP55.** (A) Schematic of mammalian GRASP functional domains and features. N-terminal myristoylation (gray), PDZ1 and PDZ2 (blue), phosphorylation sites (orange), internal ligand (red), and caspase cleavage sites (black) are show with indicated residue numbers. (B) A cartoon representation of the GRASP domain of GRASP55 1-208 overlaid on spacefill model. PDZ1 (orange arrow) and PDZ2 (yellow arrow) binding grooves are highlighted. The internal ligand is highlighted in red. (C) Schematic of GRASP domain tethering mechanism. Two apposed Golgi cisternal rims are shown (green) each bearing a GRASP protein. The internal ligand (red) of one GRASP domain is docked in the PDZ1 binding pocket of the second GRASP domain. Myristoylation (yellow) anchors the domains and is hypothetically placed.

Although the two PDZ domains in the GRASP domain are similar in overall structure, there are significant differences in the binding grooves, which reflect the specificities of their interactions. The interface between the second α -helix and second β -strand of the PDZ1 binding domain contains a deep depression resembling a pocket (Truschel et al., 2011). In contrast, the PDZ2 groove contains a phenylalanine occluding the pocket. Evidence suggests that while PDZ2 of GRASP65 binds a C-terminal ligand present in the coiled-coil Golgi protein GM130, PDZ1 interacts with a novel type of internal PDZ ligand. Remarkably, this ligand is present on the surface of the PDZ2 domain and forms a conspicuous surface protrusion that appears to fit into the pocket of PDZ1 (Figure 2.2C). As described in more detail below, the separation of function of the two PDZ domains in GRASP65 allows targeting of the protein to the Golgi via PDZ2 and homodimer formation via PDZ1. Together these activities allow the protein to mediate homotypic membrane tethering. Residues flanking PDZ2 may also stabilize the interaction of PDZ2 with GM130. Mutation of these residues blocks binding to GM130 (Barr et al., 1998), and flanking regions are known to stabilize the ligand-pocket interaction of other PDZ domains by making the PDZ domain less dynamic (Wang et al., 2010). Paralleling the activities of GRASP65, GRASP55 self-interacts and binds a coiled-coil Golgi protein, golgin45. Nevertheless, it remains to be determined whether these activities map to PDZ1 and PDZ2, respectively, and whether the golgin45 interaction mediates Golgi localization of GRASP55 (Short et al., 2001).

N-terminal membrane attachment

The mammalian GRASPs are myristoylated at their N-termini. This modification is required along with golgin binding for their localization to the Golgi (Barr et al., 1998). Thus, dual contact with the membrane stabilizes membrane binding. The N-terminal myristic acid is immediately adjacent to the PDZ1 module. Mutation of the glycine residue that becomes myristoylated blocks membrane tethering by PDZ1, even if the protein is stably anchored to the membrane by other means. Substituting a transmembrane domain for the

myristoylation site restores activity, which indicates that the N-terminus of PDZ1 must be membrane anchored for PDZ1-mediated membrane tethering (Sengupta et al., 2009). Interestingly, membrane binding of the N-terminus is conserved, even though certain species express GRASPs without the myristoylation sequence (Behnia et al., 2007; Struck et al., 2008). The GRASP homologue in *Plasmodium falciparum* expresses a splice variant with an N-terminal signal anchor, and the *Saccharomyces cerevisiae* version has an amphipathic helix that is acetylated to mediate membrane association.

There appears to be additional significance to the dual-anchoring of GRASP65 by the N-terminal myristic acid and GM130 binding (Puthenveedu et al., 2006). The two contact points of membrane binding might orient the GRASP65 homotypic binding interface to promote trans interactions across two membranes (Bachert and Linstedt, 2010). Subsequent membrane fusion then imparts a torque on the complex because of the dual anchors. In other words, membrane rearrangement forces an unfavorable cis configuration leading to partner dissociation. Because they are relatively weak, PDZ interactions (Nourry et al., 2003) might lend themselves to regulation by membrane dynamics. Interestingly, by their shared requirement for dual anchoring, localization of the tether and tether activity are linked. Thus, only dually anchored GRASP65 molecules are on the Golgi, thereby ensuring that cis interactions do not interfere with trans pairing.

GRASP55 has at least one additional fatty acid modification (Kuo et al., 2000). It is palmitoylated although the functional relevance of this modification is unclear. The longer acyl chain could affect the distribution and preference of GRASP55 in the membrane, making it prefer the thicker, late Golgi membranes (Greaves and Chamberlain, 2007).

Internal ligand

GRASP55 and GRASP65 share a conserved sequence stretch IGYGYL at the end of PDZ2 that binds PDZ1 (Sengupta and Linstedt, 2010; Truschel et al., 2011) (Figure 2.2A–C). The glycines likely contribute to rotational flexibility, allowing the surface projecting tyrosine

and leucine side chains to fit precisely into the deep pocket present in the PDZ1-binding groove (Truschel et al., 2011). Extensive van der Waals contacts may provide the stability to the interaction, nullifying the need for coordination of a carboxyl group seen in other PDZ interactions. Because the proteins do not bind one another, it is puzzling that the surface projecting ligand is identical in GRASP65 and GRASP55. There may be residues flanking the ligand sequence that play an important role in ligand specificity. Importantly, the GRASP ligand is a target of mitotic regulation. In GRASP65 a nearby serine is phosphorylated during mitosis likely inducing a conformational change that blocks the ligand from binding PDZ1 (Sengupta and Linstedt, 2010).

Serine proline-rich (SPR) domain

The C-terminal half of the GRASP proteins is enriched in serine and proline residues. This region appears to be unstructured. In striking contrast to the GRASP domain, the SPR domain is not conserved at the sequence level. Noteworthy in this region are multiple phosphorylation and caspase cleavage sites (Acharya et al., 1995, 1998; Cheng et al., 2010; Feinstein and Linstedt, 2008, 2007; Jesch et al., 2001; Kano et al., 2000; Lane et al., 2002). Cyclin-dependent kinase 1/cyclin B (CDK1), a MEK/ERK cascade, and Polo-like kinase 1 (PLK1) each phosphorylates one or both GRASP proteins (Feinstein and Linstedt, 2007; Jesch et al., 2001; Kano et al., 2000). ERK directly phosphorylates GRASP55, and inhibition of its upstream activator MEK1 blocks both GRASP55 phosphorylation and G2-phase Golgi unlinking (Feinstein and Linstedt, 2008, 2007; Jesch et al., 2001). Furthermore, mutation of ERK phosphorylation sites in GRASP55 to mimic the phosphorylated state blocks GRASP55 activity in both Golgi ribbon formation and self-association (Feinstein and Linstedt, 2007). GRASP65 is directly phosphorylated at multiple sites by CDK1, ERK, and PLK1, and phosphorylation blocks its homo-oligomerization in vitro (Jesch et al., 2001; Wang et al., 2005, 2003; Yoshimura et al., 2005). Interestingly, the PLK family of kinases initially binds substrates and becomes activated through their Polo box domains. Once acti-

vated, the kinases can phosphorylate distant sites (Barr et al., 2004; Elia et al., 2003; Lowery et al., 2005). In the case of GRASP65, mitotic phosphorylation of the SPR domain creates a PLK1 binding site (Preisinger et al., 2005). The activated PLK1 then phosphorylates a site adjacent to the internal GRASP65 PDZ ligand and blocks its ability to mediate GRASP65 self-interaction (Sengupta and Linstedt, 2010).

2.3 Structuring the Golgi

The role of GRASPs in Golgi structure

Stacking of Golgi cisternae is heterotypic in that Golgi stacks consist of cisternae of differing membrane compositions. Stacking connections might be initiated as new cis-cisternae form and might be broken as the membranes of trans-cisternae remodel, giving rise to budding membranes. During mammalian cell mitosis, as the Golgi vesiculates, the stacked architecture of the Golgi is lost, which suggests inhibition of the stacking mechanism. In contrast to stacking, Golgi ribbon formation is a homotypic reaction. Analogous cisternae among Golgi stacks are dynamically linked to one another by tubular membrane projections that undergo fusion and fission. Specificity of fusion in ribbon formation is needed to preserve compositional differences between cis-, medial-, and trans-cisternae. The lateral ribbon-forming contacts between analogous cisternae are disrupted as cells prepare for cell division and rebuilt after cell division (Bonazzi et al., 2005).

Originally, GRASP65 and then GRASP55 were shown to be required individually for the in vitro assembly of stacked Golgi membranes (Barr et al., 1998). Surprisingly, however, knockdown of either GRASP65 or GRASP55 in cultured cells leaves the Golgi with normal stacks (Feinstein and Linstedt, 2008; Puthenveedu et al., 2006). Only depletion of both proteins perturbs the stacked architecture (Xiang and Wang, 2010). GRASP proteins have the ability to link membranes through their homotypic interactions, but the membrane junctions evident when GRASP proteins are used to tether mitochondrial membranes to

one another are morphologically distinct from those of Golgi cisternae (Sengupta et al., 2009). Even more perplexing, *Saccharomyces cerevisiae* does not have a stacked Golgi and yet expresses a GRASP homologue, and *Pichia pastoris* has a stacked Golgi, yet its stacked architecture does not depend on GRASPs (Connerly et al., 2005; Glick and Nakano, 2009; Levi et al., 2010). In *Drosophila*, depletion of the lone GRASP homologue dGRASP decreases but does not abolish cisternal stacking (Kondylis et al., 2005). Overall, it seems that another mechanism is primarily responsible for Golgi stacking, the GRASP proteins providing an additional contribution.

Mammals and other vertebrates that form Golgi ribbon networks express two GRASP proteins. Depletion of either breaks the ribbon into individual Golgi stacks. Because each protein interacts only with itself, the proteins could act in parallel reactions: GRASP65 supports membrane fusion to link laterally and elongate cis-cisternae, and GRASP55 maintains these contacts in medial cisternae. From an evolutionary perspective, functional divergence that gives rise to compartment specific tethering by the GRASP proteins might be for the maintenance of Golgi subcompartments in the face of microtubule-based motility, thereby bringing Golgi ministacks into close proximity in the region of the microtubule organizing center. In lower eukaryotes, a single GRASP gene is present and Golgi membranes, even when present as stacked cisternae, are neither confined to a central position nor fused laterally to form a ribbon-like membrane network. Possibly, ribbon formation in vertebrates is a more extreme form of cisternal elongation carried out by simpler eukaryotes (Pelletier et al., 2002). If so, homotypic membrane-tethering mediated by membrane-anchored PDZ1 could represent the fundamental mechanism of GRASP65 action. The physical distance separating Golgi elements in simpler eukaryotes may prevent lateral fusion which, given the presence of only a single GRASP, might otherwise impair maintenance of subcompartment identity.

GRASP-tethering mechanism

GRASPs contribute to Golgi structure by homotypic oligomerization, an ability that was first observed for purified GRASP65 either in isolation or on the surface of beads (Wang et al., 2005, 2003). The GRASP domain mediates oligomerization. In order to understand the mechanism of GRASP-mediated tethering on the surface of membranes and in physiological conditions, GRASP65 has been targeted to the outer membrane of mitochondria (Sengupta et al., 2009). Paralleling its activity at the Golgi, GM130 recruits GRASP65, and GRASP65 is necessary and sufficient for mitochondrial tethering, which depends on the PDZ1-binding groove and the PDZ2 surface-projecting ligand. The same mutations of these elements that block mitochondrial clustering also block GRASP-mediated Golgi ribbon formation. Thus, the mechanism involves an internal PDZ–ligand within a GRASP65 partner on one membrane binding to the first of two PDZ binding pockets in a GRASP65 partner on the opposing membrane (Figure 2.3A). The binding groove of PDZ2 is expendable for tethering membranes, but it is needed to localize GRASP65 to cis-cisternae by binding GM130. Both the N- and C-termini of the GRASP domain require anchoring to the membrane for efficient tethering, the former by myristoylation and the latter by a golgin.

This orients the internal ligand and PDZ1 pocket into a conformation that promotes a trans-interaction between GRASPs on separate membranes (Bachert and Linstedt, 2010). Loss of either anchor point allows free rotation of the GRASP molecule in the plane of the membrane, which allows interactions in cis and decreases the propensity for functional trans-pairing.

As mentioned above, the crystal structure of the GRASP domain yields a model for the tethering interface. The internal ligand present on the surface of PDZ2 projects its side chains into the deep binding pocket of PDZ1 (Truschel et al., 2011). A significant feature of the GRASP domain structure is that the internal ligand for self-interaction is on the surface opposite that of the PDZ1 groove to which it binds. This provides a structural explanation for the observed tendency of GRASP65 to form multimers (Wang et al., 2003) and suggests

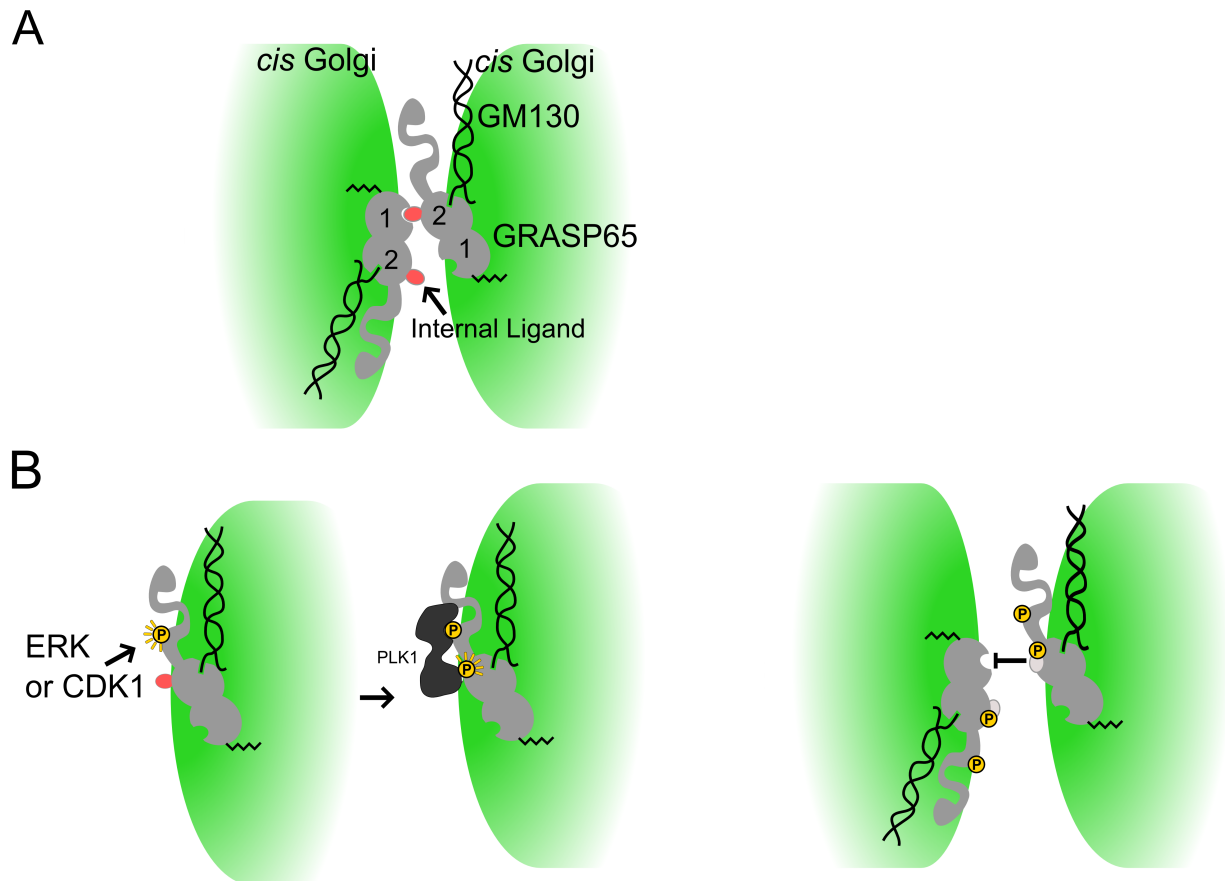


Figure 2.3: **GRASP65 tethering and 2 step phospho-regulation.** (A) Schematic diagram of GRASP65 tethering at the rims of two cis Golgi cisternae (green). The internal ligand (shown as a red protrusion) of one GRASP65 binds to the PDZ1 pocket of the other. Each is anchored to the membrane to promote trans interactions through N-terminal myristoylation and a PDZ2-GM130 interaction. (B) Two step model for GRASP65 inactivation. ERK1/2 or CDK1 phosphorylate a site in the SPR domain creating a binding site for PLK1. PLK1 (shown in dark grey) docks and phosphorylates Ser-189 near the internal ligand. This phosphorylation causes a conformational change in the ligand, which prevents its binding to the PDZ1 pocket.

that interdigitation of the molecules may occur during tethering.

2.4 Regulation of GRASP activity

Mitotic regulation of GRASP tethering activity

The homotypic tethering activity of both GRASP65 and GRASP55 is regulated during the cell cycle. As mentioned, both GRASP65 and GRASP55 are phosphorylated during mitosis. GRASP65 is a major target of Plk-1 (Barr et al., 1998). GRASP55 is phosphorylated by MEK/ERK (Feinstein and Linstedt, 2008, 2007; Jesch et al., 2001). In the case of GRASP65, a two-step phosphorylation process inhibits its homotypic tethering activity (Figure 2.3B). First, the SPR region is phosphorylated by ERK (in late G2) or CDK1 (in M phase), resulting in a docking site for Plk-1 (Bisel et al., 2008b; Preisinger et al., 2005). Plk-1 then phosphorylates Ser-189, which has been shown to block homotypic tethering and cause unlinking of the Golgi ribbon (Sengupta and Linstedt, 2010). The proximity of Ser-189 to the internal ligand suggests that phosphorylation of Ser-189 causes a conformational change in the ligand that prevents its binding to the PDZ1 pocket. GRASP55 also has a serine at 189 but whether it is mitotically phosphorylated at this position is not known. GRASP55 does not appear to interact with Plk-1 during mitosis (Preisinger et al., 2005).

GRASP regulation during cell motility

Certain cell types respond to an external motility cue by repositioning their microtubule-nucleating centrosome. Golgi membranes also move, presumably because cytoplasmic dynein keeps them near the minus ends of microtubules. Intriguingly, expression of a version of GRASP65 that cannot be phosphorylated by ERK blocks cellular reorientation to a scratch wound (Bisel et al., 2008b). Because GRASP65 maintains Golgi structure and is phospho-inhibited, it is thought that GRASP65 is phosphorylated under these conditions to break transiently the Golgi membrane network, thereby removing a physical barrier that Golgi

membranes might exert over centrosomal movement. This view is supported by the finding that Golgi disassembly by brefeldin A treatment bypasses the requirement for GRASP65 phosphorylation (Bisel et al., 2008b).

GRASP regulation during development

In migrating granule neurons of the developing nervous system, polyubiquitination of GRASP65 PDZ1 by the Golgi-localized Cul7-Fbxw8 E3-ubiquitin ligase decreases GRASP65 protein levels (Litterman et al., 2011). Interestingly, reducing GRASP65 levels causes an increase in dendritic size and branching. Because GRASP65 knockdown increases Golgi fragmentation, possibly increasing its secretory ability (Wang, 2008), it may be that ubiquitination of GRASP65 is a regulated step that governs morphogenesis of the Golgi apparatus and development of dendrites in the brain.

GRASPs and AIDS progression

Hiyoshi and colleagues have shown that GRASP65 is a critical downstream target in human immunodeficiency virus (HIV) to acquired immunodeficiency syndrome (AIDS) progression in macrophages. HIV-1 Nef is a steric activator of Hck, a Src kinase in macrophages. By reducing the surface level of the receptor Fms, Hck inhibits macrophage colony stimulating factor signaling (Hiyoshi et al., 2008). The reduced signaling disables the anti-inflammatory state (Hamilton, 2008), thereby allowing more viral replication (Herbein et al., 2010). The reduction in Fms surface levels is attributed to Golgi accumulation of a hypo-N-glycosylated form of the protein (Kuo et al., 2000). The cause of this accumulation appears to be disruption of the Golgi ribbon through phosphorylation of GRASP65 by ERK (Hiyoshi et al., 2012), which is consistent with other experiments showing reduced glycosylation upon perturbation of the Golgi ribbon (Puthenveedu et al., 2006). In sum, inhibition of GRASP65-mediated cisternal linking appears to play a role in the virulence of AIDS. These experiments also

show that glycosylation defects arising from perturbed Golgi ribbon maintenance can have physiologically significant effects.

2.5 Chaperoning secretion and processing

C-terminal valine motif cargoes

Although GRASPs are not required for traffic of model cargo, such as the viral protein VSVG, the situation is different for processing and transport of specific proteins. One type of protein that is dependent on GRASPs contains a C-terminal valine motif. These include CD8- α , Frizzled4 (Mellman and Simons, 1992), and TGF- α (Kuo et al., 2000). Their efficient transport is thought to involve GRASP65 chaperoning ER-to-Golgi transit and GRASP55 chaperoning intra-Golgi trafficking (figure 2.4A).

The C-terminal valine motif matches the minimal consensus for a C-terminal PDZ-ligand, and these cargoes bind PDZ1 of both GRASP65 and GRASP55 (Behnia et al., 2007; D'Angelo et al., 2009). In the absence of GRASP65, the cargo molecules accumulate at ER exit sites, whereas GRASP55 depletion results in the retention of these cargoes at the Golgi (D'Angelo et al., 2009). The interaction with GRASP65 might serve as an exit signal, as the yeast GRASP has been shown to localize to exit sites and interact with the inner COPII coat complex sec23/24 (Behnia et al., 2007; Levi et al., 2010). However, it is unknown how GRASP55 depletion decreases exit from the Golgi of C-terminal valine motif cargoes (D'Angelo et al., 2009). One hypothesis is that interaction with GRASP55 is needed to free these cargoes from their interaction with GRASP65, which holds them in the cis-Golgi.

An intriguing aspect of these findings is that cargo levels could influence Golgi ribbon integrity (Guo and Linstedt, 2006; Trucco et al., 2004). Increasing occupancy of PDZ1 by C-terminal valine-bearing cargo would prevent homotypic GRASP interactions. Consequently, the ribbon would transiently fragment, thereby exposing greater surface areas for the purpose of cargo transit.

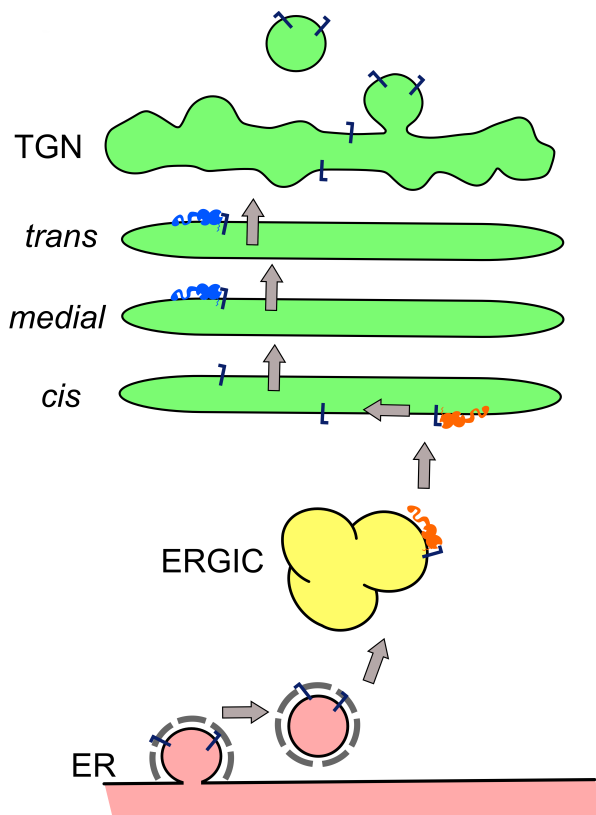


Figure 2.4: **GRASP65 and GRASP55 work sequentially to promote C-terminal valine motif cargo through the secretory pathway.** Cargo with a C-terminal di-valine motif interacts with GRASP65 (orange) at the ERGIC to somehow promote transport to the cis Golgi. Once at the Golgi, GRASP55 (blue) binds the cargo and somehow promotes its transport through the stack. Only PDZ1 of the GRASP proteins is shown for simplification.

Cargo adaptors

GRASPs also interact with the p24 family of cargo receptors (Barr et al., 2001). This family of cargo receptors is important for secretion of luminal cargo, and they interact with both the COPI and COPII vesicle coats (Dominguez et al., 1998). Interestingly, their cytoplasmic C-termini also match a minimal consensus for PDZ ligands, and they bind the GRASP proteins. Loss of GRASP binding by mutation of the C-terminal VV to AA results in an increased surface expression of these cargo receptors (Barr et al., 2001) and would presumably decrease the secretion efficiency of p24-specific cargoes. GRASP65 was found in complexes containing both GM130 and p24 family members. GRASP55 was found in complexes with

either golgin-45 or p24 family members, but not both at the same time.

Processing efficiency

Interactions between GRASPs and cargo can also increase cargo-processing efficiency. A minor population of GRASP55 is found in cells interacting with the cytoplasmic domain of furin and the cytoplasmic domain of a matrix metalloproteinase (MT1-MMP) (Roghi et al., 2010). The latter involves the sequence LLY near the C-terminus of MT1-MMP possibly binding PDZ2 of GRASP55. Furin also binds PDZ2, which suggests that dimerization of GRASP55 through PDZ1 generates a scaffold that brings furin and MT1-MMP together. This allows furin to cleave to the N-terminal inhibitory prodomain peptide of MT1-MMP. Because MMPs are often regulated during development (Vu and Werb, 2000), binding of GRASP55 to MT1-MMP could be developmentally regulated.

2.6 Unconventional secretion

While the majority of secreted proteins follow the canonical secretory pathway, some proteins follow an unconventional pathway. This pathway includes both cytoplasmic and membrane spanning cargo. The former lack a signal sequence and do not incorporate into the ER during synthesis, whereas the latter are translated in association with the ER. Transport of both types for secretion excludes the Golgi apparatus, and despite being predominately Golgi localized, GRASP proteins are required in this process (Figure 2.5). Unconventional secretion is regulated by stress (Giuliani et al., 2011).

Autophagic secretion

In *Dictyostelium discoideum*, knockout of its GRASP homologue GrpA blocks secretion of acyl coenzyme A binding protein (AcbA) causing decreased sporulation (Kinseth et al., 2007).

AcbA lacks a signal sequence, which indicates that it is secreted unconventionally. AcbA

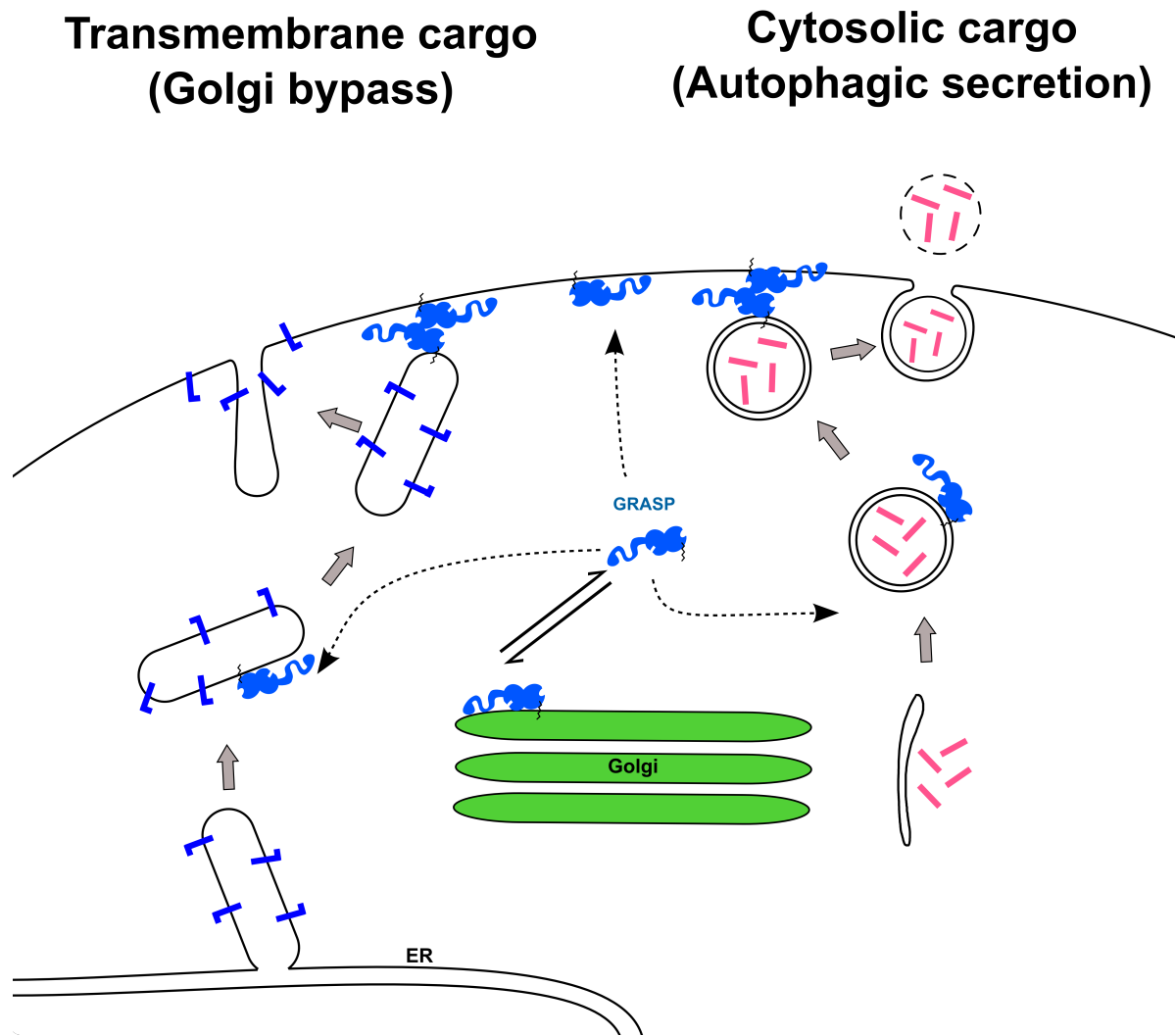


Figure 2.5: **Speculative model of GRASP function in unconventional secretion.** Unconventionally secreted transmembrane cargo exits the ER through a COPII independent process (left). GRASP is recruited to the unconventional carrier as well as the plasma membrane. GRASPs then tether the membranes prior to fusion. Cytosolic cargo is first internalized into autophagic membranes (right). GRASP is recruited to these membranes and the plasma membrane. GRASPs function as a tether prior to fusion.

secretion is induced by the spore differentiation factor 2 (SDF-2), and there is cytoplasmic build-up of AcbA in the absence of GrpA. Further analysis shows that stimulation with SDF-2 results in AcbA incorporation into vesicles prior to secretion and that GrpA is required for the fusion of these vesicles, not their formation (Cabral et al., 2010). Significantly, the secretion of the AcbA homologue in yeast, Acb1, requires the yeast GRASP Grh1, as well as autophagosomal and early endosomal machinery (Duran et al., 2010; Manjithaya et al., 2010). It also requires Bug1, the yeast homologue to GM130, which suggests that, in this pathway too, the GRASP requires a golgin for its attachment to membranes.

During the inflammatory response in macrophages, caspase-1 is activated and cleaves the precursor to the interleukin cytokine IL-1 β . The cytokine is processed in the cytosol and secreted, bypassing the normal secretory pathway. Induction of autophagy stimulates secretion causing a partial redistribution of GRASP55 from the Golgi to the autophagic membranes (Dupont et al., 2011). Knockdown of GRASP55 reduces the number of autophagic punctae and reduces secretion. The mechanism of GRASP55 in autophagy related unconventional secretion is currently unknown.

Golgi bypass

During *Drosophila* embryogenesis, dGRASP is required for unconventional secretion of α PS1 integrin to confer adhesion to a specific plasma membrane zone during epithelial remodeling (Schotman et al., 2008). The remodeling event causes a triangular void where the cells pull apart. At this stage, dGRASP and dGM130 change their localization from the Golgi to the zone of contact and nearby transitional ER, and the gap is repaired. Embryos homozygous at loss of dGRASP show a block in α PS1 secretion and a disorganized epithelium. Because dGRASP becomes localized to the plasma membrane, it may function there as a membrane tether that links membranes of unconventional secretory pathway to the plasma membrane (Giuliani et al., 2011). Because dGM130 is also present, it may act, as it does at the Golgi, to localize dGRASP (Schotman et al., 2008). It has been speculated that unconventional

secretion provides a means of modulating integrin adhesivity because glycosylation increases integrin adhesion to the extracellular matrix.

Additionally, GRASPs may play a role as chaperones of cargo, recruiting them to the unconventional secretory pathway. This could be similar to the binding of C-terminal valine motif cargoes in the conventional secretory pathway (D'Angelo et al., 2009). GRASP55 depletion during interleukin-1 β secretion decreases autophagic punctae, but not the maturation of these punctae (Dupont et al., 2011), which suggests that GRASP55 plays a role early in the unconventional secretory pathway, presumably in the organization of membrane and capture of cargo.

Therapeutic target?

The tantalizing possibility of using GRASP55 to enhance unconventional secretion as a means of treating cystic fibrosis recently emerged (Gee et al., 2011). It is well known that a common form of the disease is caused by a mutation in the cystic fibrosis transmembrane conductance regulator (CFTR), which prevents its exit from the ER even though the protein retains activity. Interestingly, CFTR has a C-terminal PDZ ligand consensus sequence and undergoes unconventional secretion during the stress of an unfolded protein response. GRASP55 is required for this pathway of CFTR secretion. Furthermore, GRASP55 overexpression enhanced surface expression of the mutated CFTR, even rescuing growth defects in a mouse model (Gee et al., 2011).

2.7 Conclusion

The GRASP proteins are important components in maintaining the integrity of the Golgi apparatus. In this capacity, they sustain the ribbon-like membrane network, which is important for Golgi processing and secretion kinetics, and they contribute to Golgi stacking. GRASPs are regulated during the cell cycle, in development, and in disease, which has a

significant impact on the Golgi membrane network and the processes that depend on this network. Additionally, GRASPs play an important, if less understood, role in specialized secretion events. In several of these cases, there is a strong indication that PDZ interactions occur between the GRASP and the secretory cargo. However, the purpose of these interactions remains an exciting and potentially clinically significant area for future work.

Irradiation-induced protein inactivation reveals Golgi enzyme cycling to cell periphery

Abstract

Acute inhibition is a powerful technique to test proteins for direct roles and order their activities in a pathway, but as a general gene-based strategy, it is mostly unavailable in mammalian systems. As a consequence, the precise roles of proteins in membrane trafficking have been difficult to assess *in vivo*. Here we used a strategy based on a genetically encoded fluorescent protein that generates highly localized and damaging reactive oxygen species to rapidly inactivate exit from the endoplasmic reticulum (ER) during live-cell imaging and address the long-standing question of whether the integrity of the Golgi complex depends on constant input from the ER. Light-induced blockade of ER exit immediately perturbed Golgi membranes, and surprisingly, revealed that cis-Golgi-resident proteins continuously cycle to peripheral ER-Golgi intermediate compartment (ERGIC) membranes and depend on ER exit for their return to the Golgi. These experiments demonstrate that ER exit and extensive cycling of cis-Golgi components to the cell periphery sustain the mammalian Golgi complex.

3.1 Introduction

The mammalian Golgi complex is composed of stacks of flattened cisternae linked through tubules to form a contiguous juxtannuclear ribbon. The stacked cisternae reflect the compart-

mentalization of Golgi enzymes for the processing of transiting cargo (Mellman and Simons, 1992; Puthenveedu and Linstedt, 2005). Cargo movement through the stack has been variously suggested to occur in vesicles, in maturing cisternae, or by tubular connections between cisternae (Malhotra et al., 1989; Mollenhauer and Morr e, 1991; Glick et al., 1997; Allan and Balch, 1999; Pelham and Rothman, 2000; Trucco et al., 2004). Although not exclusive of other processes, maturation has gained recent support (Emr et al., 2009). This model starts with the creation of cargo-containing cis-Golgi cisternae. The cargo stays within these cisternae and is sequentially processed when the cis enzymes are replaced with medial enzymes, which are subsequently replaced with trans enzymes. As cisternae progress through the Golgi stack, this change in enzyme composition is mediated by recycling vesicles. For example, cis enzymes are removed by recycling vesicles that bud from cis cisternae, whereas medial enzymes are delivered by fusion of another set of recycling vesicles, which originate from maturing medial cisternae. Thus formation of new cis cisternae is predicted to rely on both input from the ER and the recycling of cis-Golgi residents to a pre-Golgi compartment. The extent of Golgi residents cycling to the ER remains controversial (Cole et al., 1998; Storrie et al., 1998; Miles et al., 2001; Pecot and Malhotra, 2004; Rhee et al., 2005; Pecot and Malhotra, 2006). Further, if Golgi residents cycle, it is unclear whether they do so in the same vesicles as well-known recycling proteins such as the KDEL receptor and members of the p24 family (Martinez Men rquez et al., 1999; Lanoix et al., 2001; Malsam et al., 2005). Although yeast Golgi cisternae have been visualized undergoing the predicted composition changes (Losev et al., 2006; Matsuura-Tokita et al., 2006; Glick and Nakano, 2009) and mammalian Golgi cisternae support movement of large cargo trapped inside (Bonfanti et al., 1998), the role of constant membrane input from the ER to form new cisternae and the existence of robust enzyme cycling between cisternae have not been convincingly demonstrated. This is probably due to temporal and spatial resolution constraints. In mammalian systems, few approaches allow acute inactivation and as a consequence the immediate effects of a blockade of membrane trafficking are largely unknown. Similarly, the reason that recycling vesicles have not

been directly imaged might be because available live-cell imaging approaches cannot resolve vesicles within the short distances of their travel between cisternae.

Improvements in fluorescence microscopy offer an exciting avenue to address these shortcomings, particularly when combined with acute manipulations of the underlying molecular machinery. Therefore, we sought a technique for rapid protein inactivation while carrying out live-cell imaging experiments to better understand Golgi dynamics. Chromophores can inactivate proteins upon illumination by producing reactive oxygen species that can generate adducts, break peptide bonds and induce crosslinking (Jay, 1988; Liao et al., 1994; Surrey et al., 1998). Further, with a half maximal reactive distance of approximately 4 nm, the damage can be largely limited to a target protein and its interacting partners (Bulina et al., 2005). This approach has been of limited value because targeting proteins of interest mostly relied on micro-injection of fluorophore-conjugated antibodies (Surrey et al., 1998; Jay and Sakurai, 1999). However, the development of Killer Red, a derivative of the Hydrazoan jellyfish chromoprotein anm2CP that generates at least 1000-fold increase in reactive oxygen species over green fluorescence protein (GFP), presents the possibility of simply expressing Killer Red fusion proteins (Bulina et al., 2005; Carpentier et al., 2009; Pletnev et al., 2009; Serebrovskaya et al., 2009; Destaing et al., 2010; Teh et al., 2010). Here, we used Killer Red to impose an abrupt block in ER export and determine its effect on the Golgi complex. Our results indicate that the Golgi is sustained by both the constant input of membrane from the ER and a surprising level of peripheral cycling of cis-Golgi components.

3.2 Results

Targeted acute inactivation blocks ER exit

To impose an acute block of ER exit during live-cell imaging, we fused Killer Red to the coatamer protein (COP) II coat subunit Sec13 (Sec13-KR). As controls, we also generated a cytosolic version of Killer Red (Cyto-KR) and a version fused to the Golgi-localizing

3. IRRADIATION-INDUCED PROTEIN INACTIVATION REVEALS GOLGI ENZYME CYCLING TO CELL PERIPHERY

membrane anchor of giantin (KR-GTN). The constructs were expressed in cells expressing a GFP-tagged version of the Golgi enzyme N-acetylgalactosaminyl transferase- 2 (GalNAcT2-GFP), which localizes to all Golgi cisternae (Storrie et al., 1998). Upon expression, the localization of Sec13-KR was similar to endogenous Sec13 in both its appearance (Figure 3.1A) and in its quantified distribution relative to the Golgi (Figure 3.1B). Further, Sec13-KR colocalized with the COPII adaptor Sec23, confirming its localization at ER-exit sites (Figure 3.1C). Experiments were restricted to cells expressing Killer Red fusion proteins at comparable levels to GalNAcT2-GFP and with proper localization (Figure 3.1D, pre-bleach). Nevertheless, increased levels of protein expression (up to 50% higher expression by fluorescence intensity) were non-toxic and yielded similar results. The antioxidant Trolox was added as a quenching agent to further reduce the likelihood of off-target effects (Bisby et al., 1999). Trolox concentration and irradiation time and power were optimized using the Golgi-localized control construct to achieve bleaching without affecting Golgi morphology. As shown, illumination of the entire cell with a mercury arc lamp through a 535–585 nm filter for 30 seconds at 2 W/cm² in 375 mM Trolox bleached the Killer Red fluorescence of each target protein whereas the GalNAcT2-GFP fluorescence remained (Figure 3.1D, post-bleach). Because Sec13 functions in a complex, there is a reasonable expectation that bleaching would damage not only the transfected construct, but also its endogenous partners, including Sec31 (Bulina et al., 2005). Previous work using knockdown of Sec13 failed to block ER exit suggesting the importance of complete inactivation of the Sec13– Sec31 complex (Townley et al., 2008).

To test the effectiveness of Sec13-KR in blocking ER exit, we used an assay in which the Golgi assembles out of the ER upon washout of brefeldin A (BFA), an inhibitor of Arf1 activation that reversibly redistributes Golgi enzymes into the ER (Lippincott-Schwartz et al., 1989; Peyroche et al., 1999). Immediately after drug washout, the Killer Red fusion proteins were bleached for 30 seconds and GalNAcT2-GFP was imaged for 90 minutes (Figure 3.1E, supplementary material Movie 1). Cells expressing the control constructs, Cyto-KR

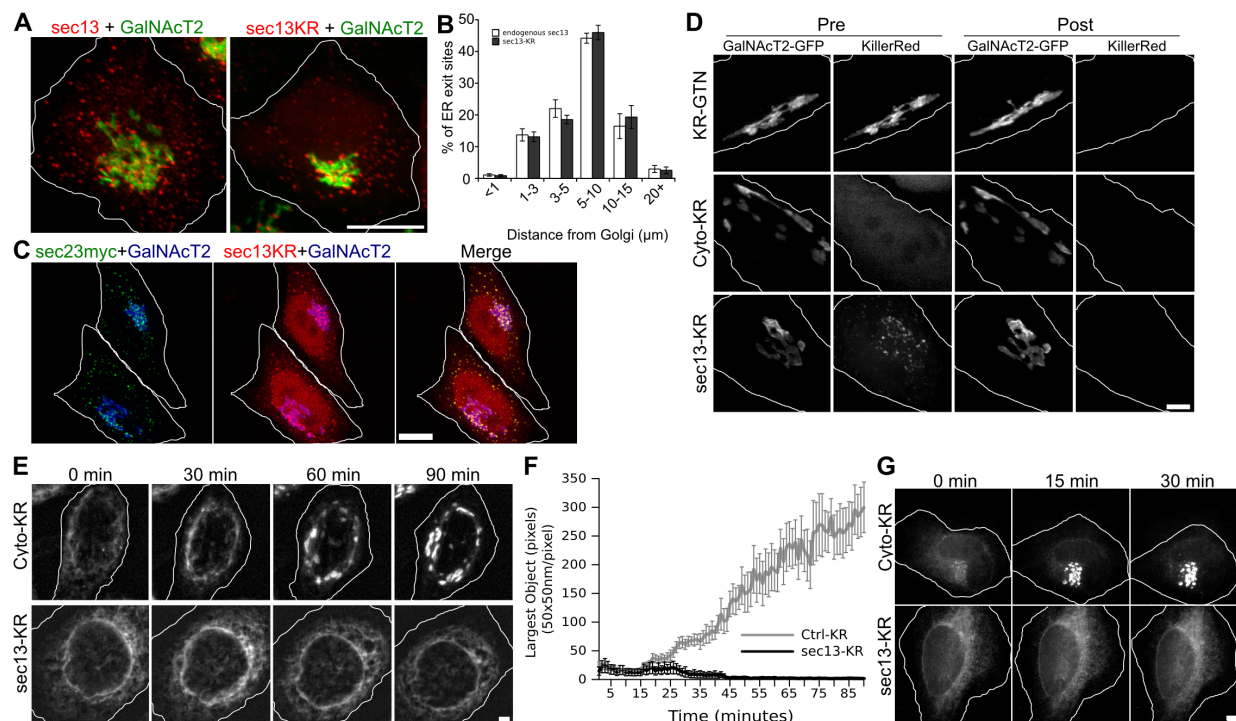


Figure 3.1: Acute inactivation at the onset of Golgi assembly. (A) HeLa cells stably expressing GalNAcT2–GFP as a Golgi marker were fixed and stained with antibodies against Sec13 (left) or transiently transfected with Sec13–KR and fixed. Endogenous Sec13 and Sec13KR expression show similar patterns of ER exit sites. Scale bar: 10 μm. (B) Distribution of these exit sites was quantified by distance of each site from the center of the Golgi. The percentage of total ER exit sites within each radius is shown for both proteins. (C) Cells were transiently co-transfected with Sec13–KR and Sec23–Myc and fixed and stained with anti-Myc antibodies. Scale bar: 10 μm.

or KR–GTN, showed full assembly of the Golgi with kinetics similar to untransfected cells. In striking contrast, bleaching of Sec13–KR blocked the exit of GalNAcT2–GFP from the ER, indicating the inactivation of this essential COPII subunit. Golgi assembly was quantified by determining the size of the largest fluorescent Golgi object at each time point and confirmed a robust and reproducible block by Sec13–KR inactivation (Figure 3.1F). ER-exit blockade was also demonstrated using the temperature-sensitive vesicular stomatitis virus G protein (VSVG) transport assay (Presley et al., 1997). Cells expressing VSVG–GFP were shifted from 40 °C to 32 °C and simultaneously photo-inactivated. Control cells transported VSVG–GFP to the Golgi by 15 minutes, whereas VSVG–GFP was trapped in the ER in

Sec13–KR-inactivated cells, where it remained for at least 90 minutes (Figure 3.1G).

Acute dependence of Golgi integrity on ER exit

Having established its effectiveness, we used Sec13–KR inactivation to test the acute dependence of the Golgi complex on ER exit. Golgi labeled with GalNacT2–GFP was imaged for 10 minutes to establish a base line. The control and Sec13–KR constructs were then bleached, and the Golgi was followed for another 60 minutes. Bleaching of KR–GTN yielded little effect on the stability or dynamics of the Golgi ribbon, whereas photobleaching of Sec13–KR had an immediate effect, causing both a fragmentation of the Golgi ribbon and a concomitant accumulation of GalNacT2–GFP in small peripheral objects (Figure 3.2A, supplementary material Movie 2). Integrity of the ribbon was assayed using fluorescence recovery after photobleaching. Whereas KR–GTN inactivated cells showed diffusion of GalNacT2–GFP equivalent to untreated cells, Sec13–KR inactivated cells exhibited little or

Continued from 3.1 on the preceding page

(D) Pre- and post-bleach images for the indicated Killer Red constructs. HeLa cells stably expressing GalNacT2–GFP as a Golgi marker were transiently transfected with Killer Red constructs and, after 2 days, were placed in medium containing 375 μ M Trolox. Cells were selected based on comparable Killer Red and GalNacT2–GFP fluorescence signals and proper localization of the constructs. Pre-bleach images of the selected cells were acquired in each channel and then the cells were irradiated with 535–580 nm light at an intensity of 2 W/cm² for 30 seconds followed by the immediate acquisition of post-bleach images in each channel. Scale bar: 2 μ m. **(E)** Time course of Golgi assembly after bleaching of the indicated Killer Red constructs. Cells were transfected with Killer Red constructs and, after 2 days, GalNacT2–GFP was redistributed to the ER by exposure to 2 μ g/ml brefeldin A for 15 minutes, followed by washing in PBS and immediate mounting in imaging medium for a 30 seconds bleaching of the Killer Red fluorescence. Imaging of GalNacT2–GFP was then at 1 minute intervals for 90 minutes. Max value Z-projections are shown for the indicated time points and the corresponding full time course is shown in supplementary material Movie 1. Scale bar: 2 μ m. **(F)** Golgi assembly was measured for the indicated constructs by determining the largest fluorescent object present at each time point with the threshold set above the level of GalNacT2–GFP fluorescence in the ER (n=10, mean \pm s.e.m.). **(G)** Time course of VSVG–GFP transit from the ER to Golgi initiated by temperature shift immediately before bleaching of the indicated Killer Red constructs. Imaging of VSVG–GFP was at 1 minute intervals for 90 minutes. Max value Z-projections are shown for the indicated time points. Scale bar: 2 μ m.

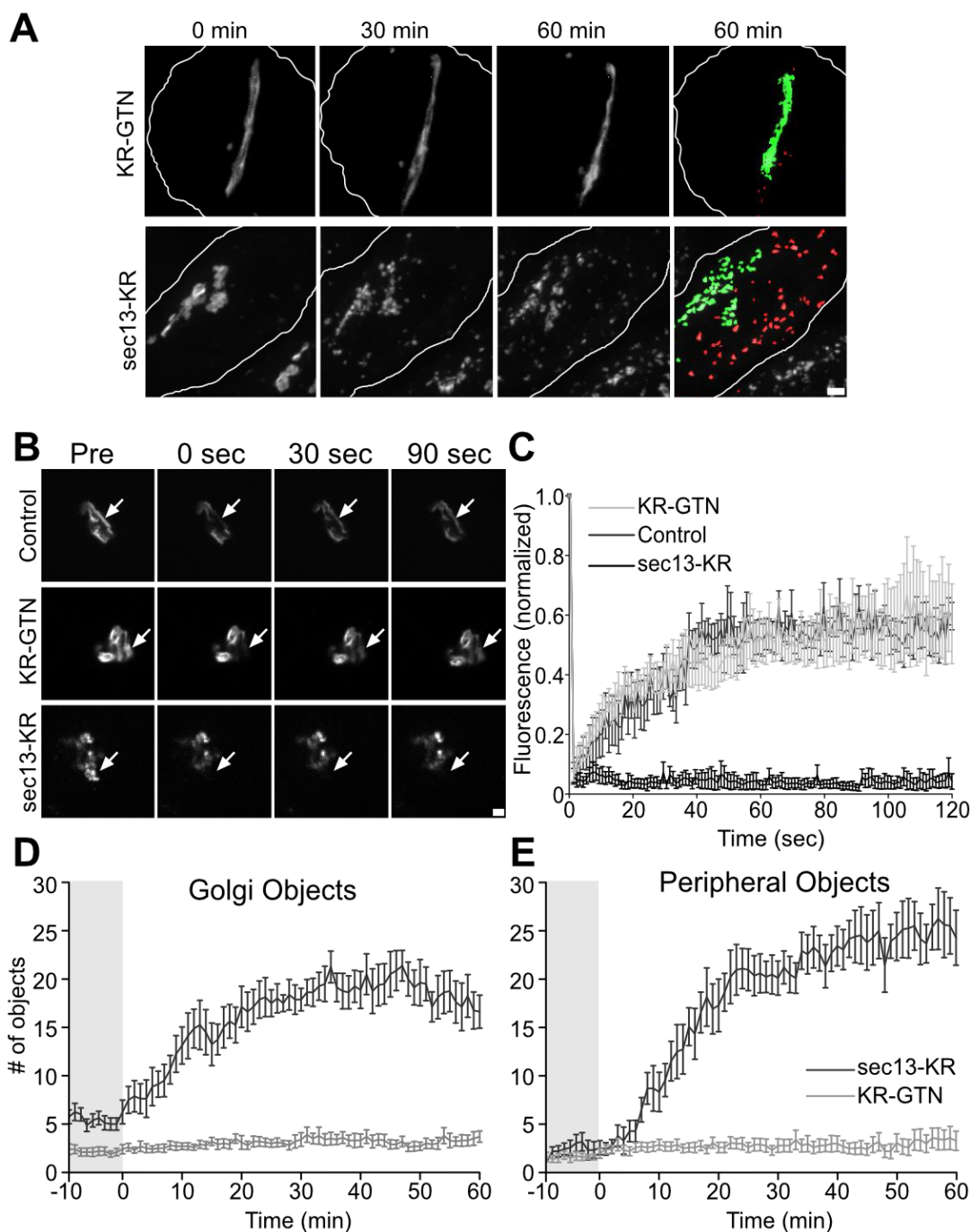


Figure 3.2: Acute inactivation at steady state. (A) Time course of Golgi integrity after bleaching of the indicated Killer Red constructs. Cells transfected with Killer Red constructs were imaged to observe GalNAcT2-GFP at 1 minute intervals for 10 minutes before a 30 second bleaching and then for a further 60 minutes. Max value Z-projections are shown for the indicated time points and the 60 minute time point is also shown after pseudo-coloring to indicate objects that visibly detached from the Golgi (green) and objects that appeared in the periphery (red). The corresponding full time course is in supplementary material Movie 2 (gray scale) and Movie 3 (pseudo-colored). Scale bar: 2 μ m. (B) Analysis of Golgi integrity by fluorescence recovery after photobleaching. Cells were subjected to no treatment, inactivation of KR-GTN or inactivation of Sec13-KR. After 15 minutes images were acquired before and after a small region of GalNAcT2-GFP fluorescence on the Golgi was bleached (arrows) and the indicated time points are shown. Scale bar: 2 μ m. (C) Fluorescence was measured in bleached zone and is plotted versus time (n=33 cells, mean \pm s.e.m.). (D,E) Golgi disassembly was measured by determining the number of total (D) and peripheral (E) fluorescent objects present at each time point using the ImageJ ‘Analyze particles’ function with the threshold set above the level of GalNAcT2-GFP fluorescence in the ER (n=10, mean \pm s.e.m.). Pre- and post-bleach periods are indicated.

no GalNAcT2–GFP diffusion into the bleached zone, indicating loss of ribbon architecture (Figure 3.2B,C). To analyze the appearance of GalNAcT2–GFP in the cell periphery after Sec13–KR inactivation, we first used an algorithm that highlights objects contiguous with the original Golgi in green and any peripheral objects that arise in red (Figure 3.2A last panels, supplementary material Movie 3). Golgi objects corresponded to pixel sets that intersected with pixel sets in previous frames extending back in time to the original pixel set defining the Golgi and peripheral objects corresponded to all other above-threshold objects. The fluorescence in each group was quantified (Figure 3.2D,E), confirming the reproducibility of both the fragmentation of the Golgi ribbon and the appearance of peripheral objects with each effect exhibiting a $t_{1/2}$ of <10 minutes. Although there was extensive redistribution to the periphery, GalNAcT2–GFP was not detectable in the ER until the post-inactivation incubation was extended to 4.5 hours, at which time most of the fluorescence was present in the ER (Figure 3.3). A slow rate of ER redistribution in response to an ER exit block is in accord with previously published longer-term experiments (Storrie et al., 1998; White et al., 1999), whereas the immediate effects in disrupting Golgi integrity and causing redistribution to peripheral punctae have not been previously observed. To provide further evidence that ER exit was blocked by Sec13–KR and did not contribute to the appearance of the peripheral punctae, we specifically bleached the Golgi GalNAcT2–GFP immediately after Sec13–KR inactivation. These cells showed no GalNAcT2–GFP accumulating in the periphery (supplementary material Movie 4) confirming a Golgi origin for the peripheral fluorescence rather than exit of the residual ER pool.

GalNAcT2–GFP cycles to the cell periphery

The redistribution of GalNAcT2–GFP to peripheral punctae upon ER exit blockade suggests that it constantly cycles to peripheral structures and depends on ER exit for its return to the Golgi. In an attempt to visualize GalNAcT2–GFP cycling directly, we carried out faster time-lapse imaging using binning and greater laser power to boost sensitivity. During a

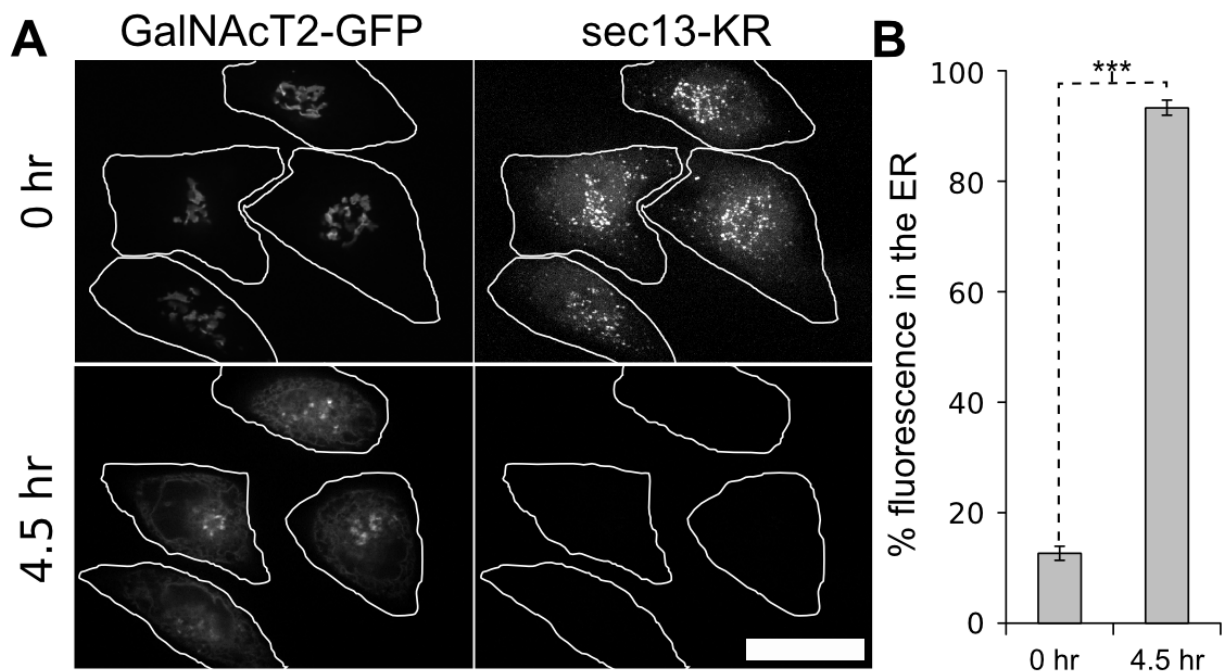


Figure 3.3: **Golgi at 4.5 hours after Sec13-KR inactivation.** (A) Representative Z-slices of GalNAcT2-GFP are shown before and 4.5 hours after inactivation. Scale bar: 10 μm . (B) The percentage fluorescence in the ER was calculated by measuring total cell fluorescence and subtracting any above-threshold fluorescent objects with the threshold manually set to exclude the nuclear envelope but retain remnant Golgi objects ($n=8$ cells, mean \pm s.e.m.). Statistical significance was measured using the paired Student's t-test (** $P=0.0000003$).

15 minute pre-inactivation period, the enhanced imaging revealed a multitude of small, dim GalNAcT2-GFP objects leaving the Golgi and arriving at the Golgi. Figure 3.4A-C presents images cropped around the Golgi region to highlight a few examples where objects left the Golgi and moved towards the periphery (black arrowheads) or moved from the periphery inward to the Golgi (white arrowheads). The full extent of these events is better observed in supplementary material Movie 5. Following this imaging, either KR-GTN or Sec13-KR was then inactivated and the cells were imaged for another 15 minutes. In the case of the KR-GTN control, inward and outward traffic persisted (Figure 3.4A) and the distribution of objects remained constant (Figure 3.4D). By contrast, after Sec13-KR inactivation there was a loss of inward-directed motility (Figure 3.4B), and a significant and progressive increase in peripheral object size (Figure 3.4D) because some objects approached each other and

appeared to fuse (Figure 3.4B, white arrow). To test the role of the COPI vesicle coat in generating the GalNAcT2–GFP objects leaving the Golgi, this experiment was repeated in the presence of 1,3-cyclohexanebimethylamine, which causes COPI membrane dissociation and blocks COPI function (Hu et al., 1999; Puthenveedu and Linstedt, 2001; Zhang et al., 2009). This treatment blocked the Sec13–KR-induced increase of peripheral GalNAcT2–GFP objects (Figure 3.4C,D, supplementary material Movie 6). To further test the dependence on Arf- dependent COPI function, we added BFA to cells immediately after inactivation of Sec13–KR. In the 15 minute post-inactivation period there was extensive tubulation and then collapse of the Golgi into the ER. Peripheral punctae did not arise during tubulation and were not evident after Golgi collapse (supplementary material Movie 7). Thus, GalNAcT2–GFP continuously cycled to the cell periphery with the outward path requiring COPI and the inward return dependent on ER exit. Respectively, these dependencies probably reflect COPI-mediated budding of GalNAcT2-containing vesicles from the Golgi and a demand for new membrane and/or transport factors.

Cycling is through the ER-Golgi intermediate compartment

Previously it was hypothesized that cycling vesicles containing Golgi components fuse with ERGIC membranes (Love et al., 1998; Lin et al., 1999; Marra et al., 2001; Puthenveedu and Linstedt, 2001), therefore we wished to test whether the peripheral GalNAcT2–GFP objects were positive for ERGIC markers. However, the ERGIC collapses in the absence of ER exit (Aridor and Balch, 2000; Lee and Linstedt, 2000). This was confirmed in the case of Sec13–KR inactivation after 30 minutes (Figure 3.5); nevertheless, at 15 minutes after inactivation, the ERGIC markers ERGIC53 and Yip1A were still evident in peripheral punctae, so we asked whether these were positive for trapped GalNAcT2–GFP. As a control, a parallel set of cells was stained at the same time point to visualize ER- exit sites using transfected, Myc-tagged Sec23. After thresholding the images, the Golgi region was ignored and all peripheral GalNAcT2–GFP objects were scored for overlap with ERGIC53, Yip1A,

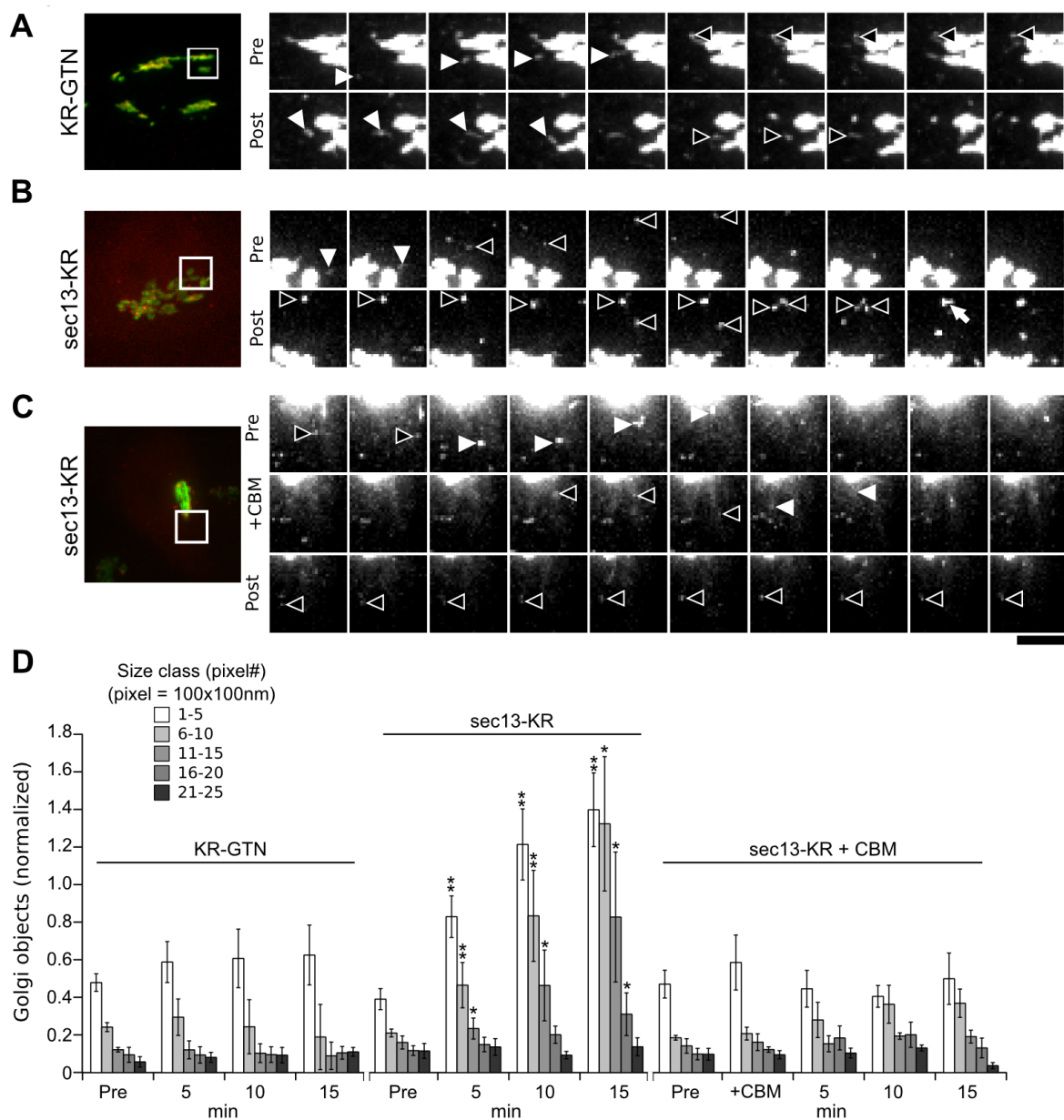


Figure 3.4: **Evidence for GalNAcT2-GFP cycling.** (A–C) Time course of structures detaching from the Golgi or moving back to the Golgi during pre- and post-bleaching periods in untreated cells expressing KR-GTN (A) or Sec13-KR (B), or in cells treated with 1,3-cyclohexanebimethylamine for 5 minutes before Sec13-KR inactivation (C). GalNAcT2-GFP was imaged every 15 seconds with 4× binning of the acquired signal for 10 minutes before (Pre) and 10 minutes after (Post) a 30 second bleaching. Representative max value Z-projections are shown for consecutive time points with inward objects indicated by white arrowheads and outward by black arrowheads. The corresponding full time courses are in supplementary material Movies 5, 6. Scale bar: 1 μm. (D) The distribution of small Golgi objects in size classes is shown for the indicated time points following bleaching of the KR-GTN control or the Sec13-KR construct. Values are the number of objects normalized to the value in the pre-inactivation segment (n=10, mean ± s.e.m., *P<0.005 and **P<0.0005).

3. IRRADIATION-INDUCED PROTEIN INACTIVATION REVEALS GOLGI ENZYME CYCLING TO CELL PERIPHERY

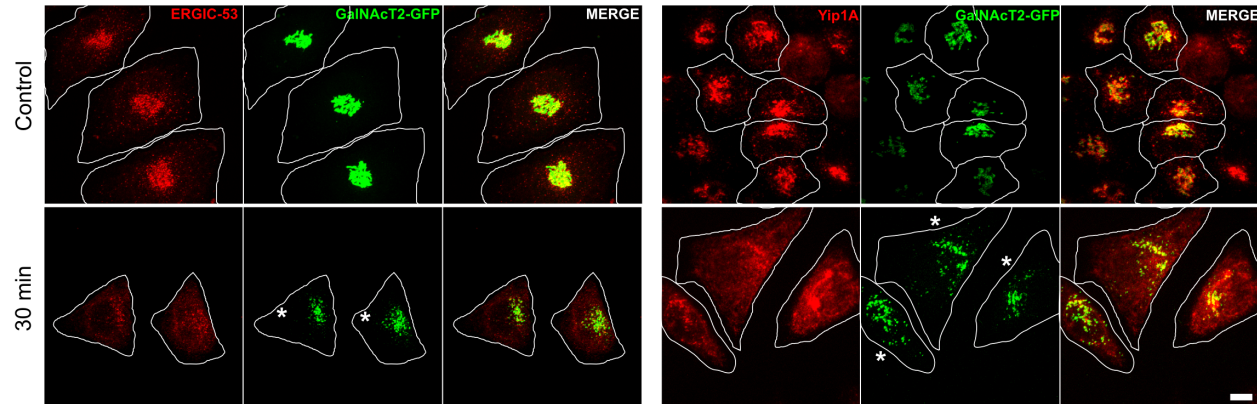


Figure 3.5: **Progressive loss of ERGIC53-positive puncta after Sec13-KR inactivation.** Cells were fixed at 30 minutes post inactivation of Sec13-KR and stained for ERGIC53 or Yip1A. Max-value Z-projections are shown and inactivated cells are marked with *. Note diminution of ERGIC53 and Yip1A positive punctate structures. Scale bar: 10 μ m.

or Sec23 punctate fluorescence. Whereas few GalNAcT2-GFP punctae colocalized with Sec23, there was extensive colocalization with ERGIC markers ERGIC53 and Yip1A (Figure 3.6A,B). Thus, GalNAcT2-GFP probably cycles to ERGIC membranes, which in the absence of continued ER exit become depleted, leading to accumulation of GalNAcT2-GFP in the cell periphery.

Cycling involves cis- but not trans-Golgi proteins

Next, we tested whether additional Golgi markers traffic in the pathway made evident by inactivation of Sec13-KR to see whether there might be preferential involvement of cis-Golgi proteins. First, we compared GalNAcT2-GFP to the cis-Golgi protein GPP130-GFP. Each responded to Sec13-KR inactivation by rapid accumulation in peripheral punctae with GPP130-GFP slightly preceding GalNAcT2-GFP (Figure 3.7A,B, supplementary material Movies 8, 9). Redistribution was also confirmed for endogenous cis-localized proteins. Endogenous giantin, GPP130 and GRASP65 each accumulated in GalNAcT2-GFP-positive peripheral punctate structures after Sec13-KR inactivation (Figure 3.8). By contrast, two trans-Golgi markers, galactosyltransferase tagged with yellow fluorescent protein

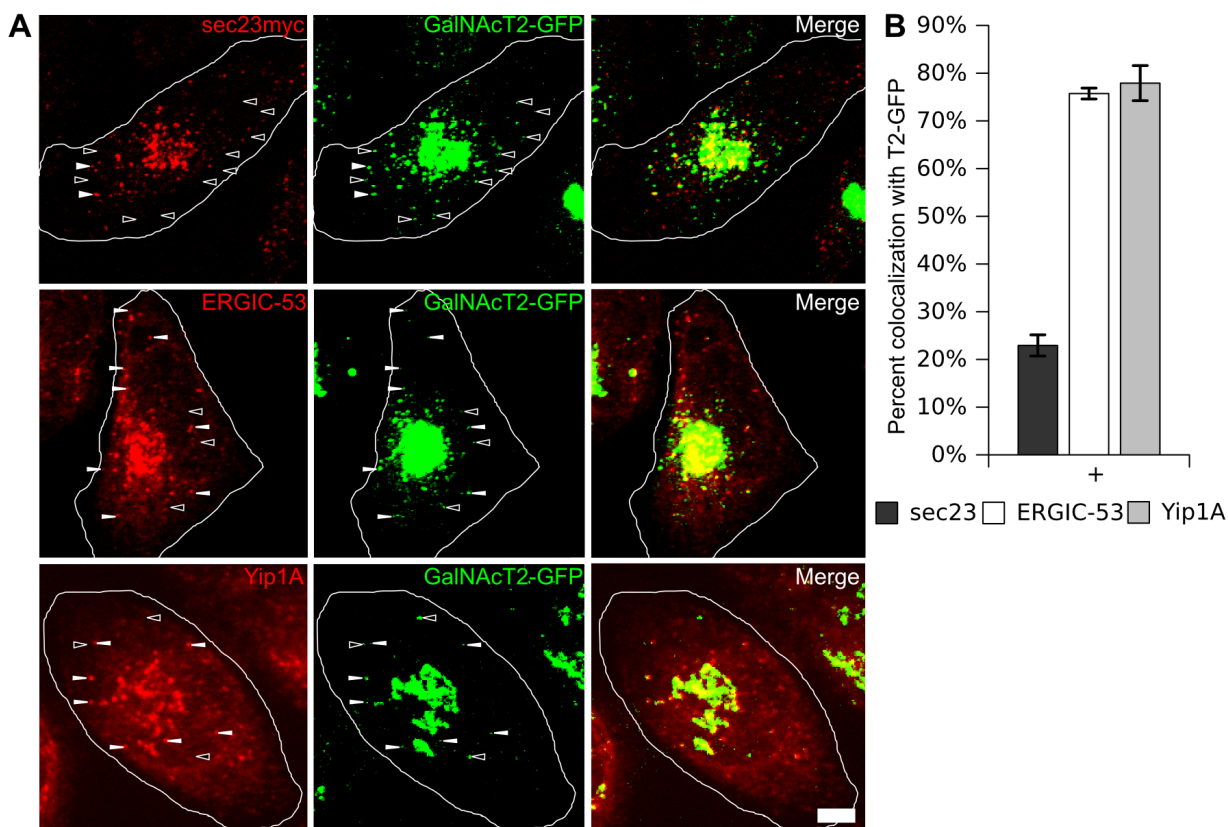


Figure 3.6: GalNAcT2 redistribution to the ER-Golgi intermediate compartment. (A) Cells were fixed for 15 minutes after inactivation of Sec13-KR and stained for transfected Sec23-Myc or endogenous ERGIC-53. Max-value Z-projections are shown with representative GalNAcT2-GFP-positive objects which co-label peripheral punctae with Sec23-Myc or ERGIC-53 (filled arrowheads) and or lack Sec23 or ERGIC-53 (empty arrowheads). Scale bar: 2 μ m. (B) GalNAcT2-GFP objects were scored for colocalization with Sec23 or ERGIC-53 based on overlap of punctate fluorescence above background in single Z-sections (n=15 cells objects >250).

(GalT-YFP) and globotriaosylceramide synthase (GB3S-GFP), showed delayed and relatively minimal accumulation in peripheral punctae (Figure 3.7C,D, supplementary material Movies 8, 9). Thus, if these trans components cycle, their cycling is probably restricted to the Golgi region and is therefore not discernible. These experiments strongly suggest that cycling of cis-Golgi-localized proteins to ERGIC membranes sustains Golgi biogenesis.

3. IRRADIATION-INDUCED PROTEIN INACTIVATION REVEALS GOLGI ENZYME CYCLING TO CELL PERIPHERY

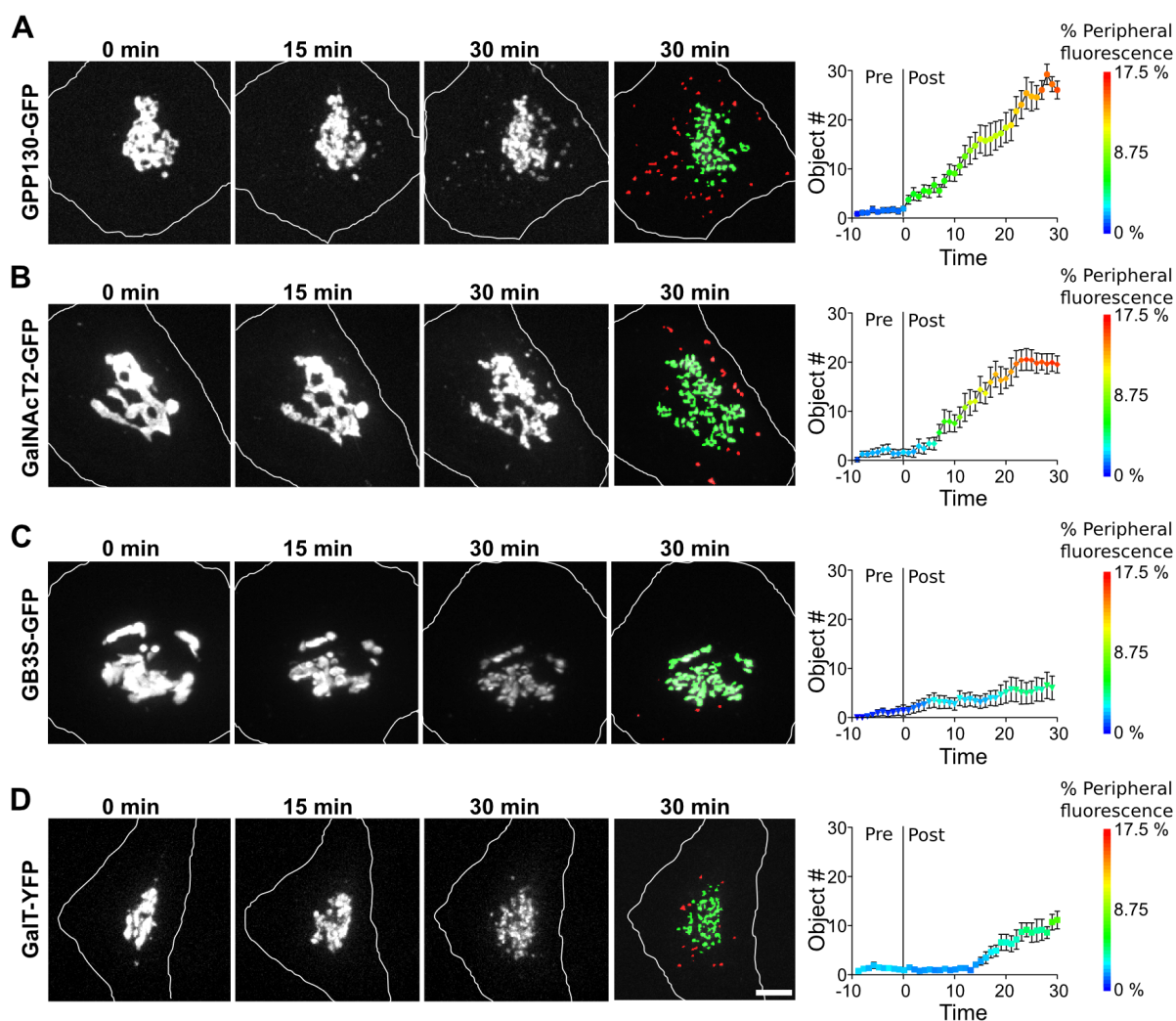


Figure 3.7: **Preferential peripheral cycling of cis Golgi components.** (A–D) Cells expressing GPP130–GFP (A), GalNAcT2–GFP (B), GB3S–GFP (C) or GalT–GFP (D) were imaged at 1 minute intervals for 10 minutes before a 30 second bleaching of Sec13–KR and then for a further 30 minutes. Max value Z-projections are shown for the indicated time points and the 30 minute time point is also shown after pseudo-coloring to indicate objects that visibly detached from the Golgi (green) and objects that appeared in the periphery (red). The corresponding full time course is in supplementary material Movie 7 (gray scale) and Movie 8 (pseudo-colored). Scale bar: 2 μ m. Quantification of the number of peripheral objects (y-axis) and percent of total fluorescence in peripheral objects (color axis) is shown for each construct (n=10 cells, mean \pm s.e.m.)

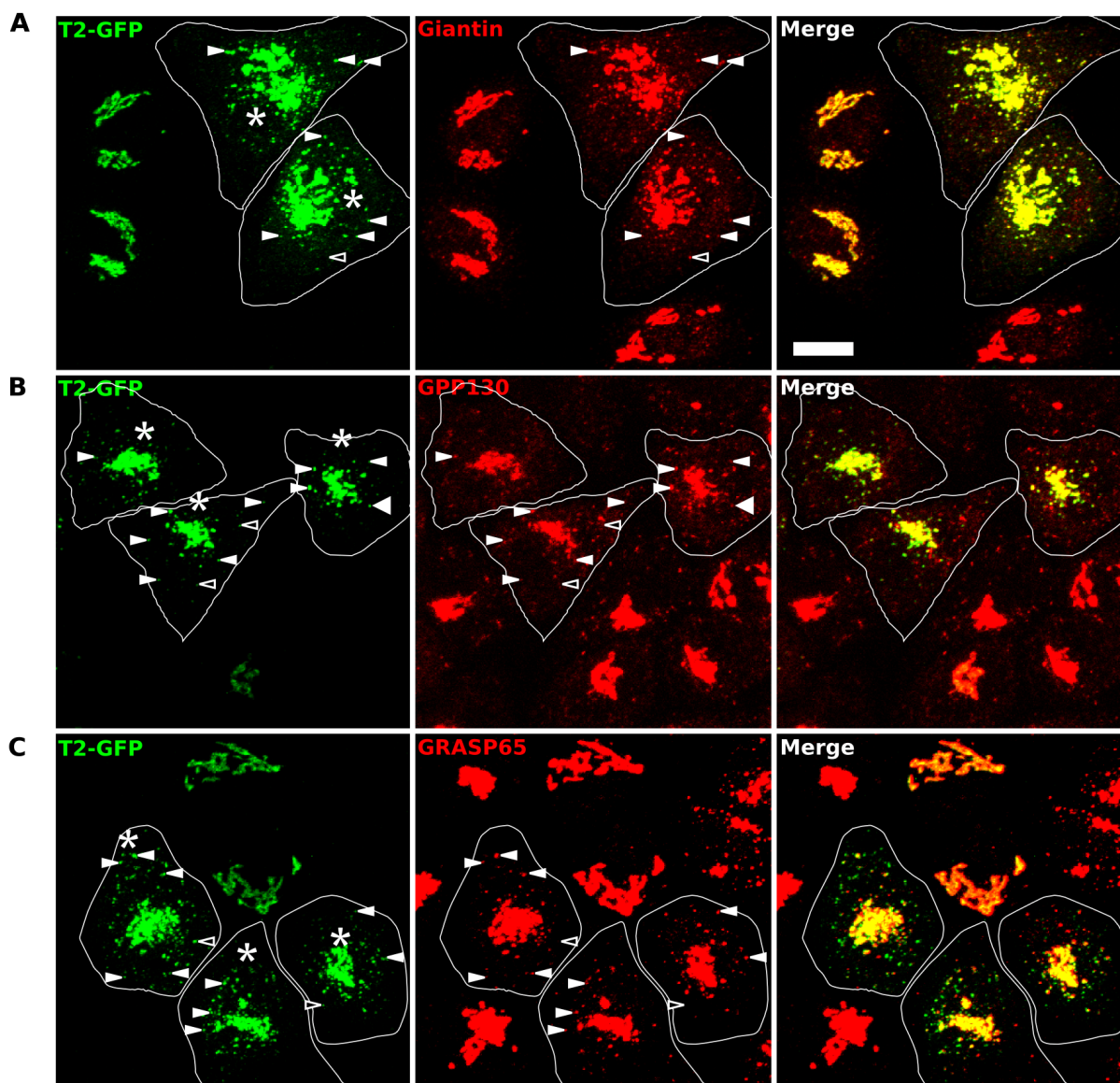


Figure 3.8: **Endogenous cis Golgi proteins co-label GalNAcT2-GFP-positive recycling intermediates.** Cells were fixed 30 minutes post inactivation of Sec13-KR and stained for endogenous cis-Golgi proteins giantin (A), GPP130 (B) and GRASP65 (C). Max-value Z-projections are shown and inactivated cells are marked with *. Example GalNAcT2-GFP objects are highlighted to indicate either co-labeling with an endogenous marker (filled arrowheads) or lack of co-labeling (empty arrowheads). Scale bar: 10 μ m.

3.3 Discussion

These experiments demonstrate the technical feasibility of using a 30 second photo-inactivation of a crucial component in a dynamic system while carrying out live-cell fluorescent imaging. Although specificity of inactivation using Killer Red is not absolute, several considerations increase confidence in our conclusions. Chromophore-assisted light inactivation has a successful history and is based on validated physical theory (Surrey et al., 1998; Jay and Sakurai, 1999). The Killer Red variation of the technique increases specificity because it more precisely targets the chromophore. It also avoids micro-injection, which is less reproducible and might impair cell viability. Although micro-injection can, in principle, impose an immediate block, the need to allow cell recovery could explain why previous reports of blockade of ER exit using a dominant-negative version of Sar1 involved analysis 4–6 hours following micro-injection (Storrie et al., 1998; Miles et al., 2001). The inactivation done in the steady state analysis used the same parameters and set-up as the Golgi biogenesis and VSVG–GFP transport assays confirming its effectiveness. Finally, our conclusions do not require highly specific inhibition of the single targeted component Sec13. Indeed, this would be unlikely given the proximity of Sec13 to its binding partners at an ER exit site. Rather, the conclusions rest on effective inhibition of ER export – a process that depends on Sec13 and its binding partners. Given that the approach we describe is based on a genetically encoded fluorescent protein whose localization and expression level are readily verified, we expect Killer-Red-mediated inactivation during live imaging to be widely adopted and of particular significance where temporally or spatially restricted inactivation of proteins and their binding partners is required.

Acute inactivation revealed the Golgi to be sustained by both ER exit and a surprisingly high rate of continuous cycling of cis-Golgi components to ERGIC membranes. These observations fulfill previously unmet expectations of the maturation model in which new cisternae are constantly built by the fusion of cargo-bearing membrane from the ER and cis-enzyme-bearing recycling membrane from the Golgi. Certain trafficking components were previously

visualized in ERGIC-directed tubules but the tubules were devoid of Golgi enzymes (Marra et al., 2001), except when BFA was used to induce their appearance (Mardones et al., 2006). Significantly, COPI was required to generate the cycling membranes, whereas ER export was required for their inward return to the Golgi. Arguably, ER export is required to contribute membrane and transport factors that sustain the ERGIC and are essential for the progression ERGIC membranes towards biogenesis of cis-Golgi cisternae.

Our results help resolve controversies concerning cycling of Golgi proteins through the ER (Altan-Bonnet et al., 2004; Patterson et al., 2008; Budnik and Stephens, 2009; Emr et al., 2009; Wei and Seemann, 2009). Evidence in support of cycling through the ER (Cole et al., 1998; Storrie et al., 1998; Miles et al., 2001; Ward et al., 2001; Rhee et al., 2005) can be reinterpreted as showing the importance of ER exit in supporting Golgi enzyme cycling through the ERGIC with redistribution into the ER being a secondary, longer-term effect. Evidence against cycling through the ER, such as lack of Golgi enzyme trapping by ER- localized binding partners (Pecot and Malhotra, 2004, 2006), although supported by our findings, missed the importance of ER exit in sustaining the robust cycling of enzymes through the ERGIC.

In conclusion, in contrast to longer-term inhibition experiments, photo-inactivation revealed that the mammalian Golgi complex is sustained by ER exit and extensive Golgi protein recycling.

3.4 Materials and Methods

Cell Imaging. Cells were transferred to imaging medium (MEM, 7% FBS, 375 mM Trolox) and placed on a 37 °C heated stage under a blood gas mixture (5% CO₂, 95% air) on a Zeiss Axiovert 200 with a heated 1006 Plan-Apo NA 1.4 oil objective (Zeiss, Thornwood, NY) attached to an UltraView spinning-disk confocal system (Perkin- Elmer, Shelton, CT). Cells expressing properly localized Killer Red constructs at brightness levels matching Gal-

3. IRRADIATION-INDUCED PROTEIN INACTIVATION REVEALS GOLGI ENZYME CYCLING TO CELL PERIPHERY

NacT2-GFP were identified. Cells expressing low levels or levels high enough to cause gross mistargeting were ignored because, upon photo-inactivation, the former failed to exhibit an effect and the latter sometimes resulted in cell death. Bleaching of Killer Red fluorescence was by epifluorescence light through a 535–585 nm filter at 2 W/cm² for 30 seconds. Capture parameters before and after bleaching are indicated in the figure legends. Enhanced images were taken using 4x binning to increase camera sensitivity. FRAP experiments were carried out in OptiMEM containing 7% FBS and 375 mM Trolox at 37 °C under ambient CO₂. Acquisition was performed on an Andor Revolution XD system (Andor Technology, Belfast, UK). Killer Red was bleached at 100% laser power (561 nm) for 90 mseconds per pixel and GFP was bleached at 80% laser power (488 nm) for 20 mseconds per pixel. To stain inactivated cells, cells on glass-bottomed dishes were returned to a 37 °C incubator for the indicated times after pre- and post-inactivation images had been acquired and then the cells were fixed in 3% paraformaldehyde at room temperature or a methanol/acetone (2:1 mixture) at -20 °C. Antibodies were: rabbit anti-GRASP65 ([Bachert and Linstedt, 2010](#)), rabbit anti-Yip1A([Dykstra et al., 2010](#)), mouse anti-GPP130 ([Linstedt et al., 1997](#)), mouse anti-alpha-tubulin (Sigma), mouse anti-giantin([Linstedt and Hauri, 1993](#)), mouse anti-ERGIC53 ([Schweizer et al., 1990](#)), mouse anti-Myc ([Evan et al., 1985](#)) and Cy5-labeled secondary antibodies (Invitrogen).

Cloning. Sec13-KR was constructed by PCR amplifying KR from pKillerRed-N (Evrogen) and inserting it into the XhoI and XbaI sites of pCS2-Sec13 (kind gift of Tina Lee, Dept. of Biological Sciences, Carnegie Mellon Univ.). KR was also cloned into the BamHI and EcoRI sites of pCS2 to generate Cyto-KR. For KR-Gtn, the sequence encoding the last 100 amino acids was amplified and cloned into the EcoRI and XbaI sites of Cyto-KR. GPP130-GFP was as described ([Mukhopadhyay et al., 2010](#)). GalT-YFP was created by inserting the localization domain of GalT (residues 1-75) along with YFP into the pIRES vector. GB3S-GFP was created by its insertion into pEGFP.

Cell Culture and Transfection. HeLa cells stably expressing GalNacT2-GFP were

cultured in MEM (Thermo Scientific) with 10% FBS (Atlanta Biologicals). Prior to experiments, cells were passed to 30-50% confluency in a 60 mm dish, and transfected with JetPEI (PolyPlus) according to the manufacturers protocol. After 24 h the cells were passed onto 35 mm coverslips and at 36-72 h post-transfection the coverslips were mounted in an imaging chamber or 35 mm glass-bottomed dish (Matek). Brefeldin A (Sigma) was added at 2 $\mu\text{g}/\text{ml}$ where indicated. Where indicated, 1,3-cyclohexanebis(methylamine) (Acros Organics) was added at 10 mM final concentration.

Analysis. ImageJ (<http://rsbweb.nih.gov/ij>) was used to carryout analysis of the max value projected images. To determine the largest object size during Golgi assembly, images were thresholded to exclude ER-localized GalNAcT2-GFP fluorescence (value set using the 0 min time point) and the “Analyze Particles” function was used to find the largest object in each cell for each time point. To determine the number and size of Golgi objects after steady-state inactivation, the images were enhanced using the spot-enhancing-filter plugin ([Sage et al., 2005](#)), manually thresholded to maximize object recovery (single threshold/series), and analyzed using the “Analyze Particles” function. To pseudo-color objects based on continuity with the starting Golgi, the spot-enhanced and thresholded images were converted to binary and object continuity over time, that is overlapping pixels, was determined using the “3D Object counter” plugin. All objects contiguous with the starting Golgi were added as a green layer on top of the original grayscale image and all other objects were added as a red layer. Colocalization analysis was performed after background subtraction and generation of an average projection of the Z-stack using the “Manders Coefficients” plugin. To determine size distribution of cycling objects, the 4X binned images were thresholded and analyzed using the “Analyze Particles” function with max object size set to 25 pixels. Analysis of FRAP data was performed using ImageJ “Measure” function over the bleached area after background subtraction. Values were normalized to pre-FRAP intensity and also corrected for photobleaching using an adjacent unbleached area. Statistical analysis used a one-tailed paired T-test.

3.5 Movie Figure Legends

Movie 1. Acute inactivation at the onset of Golgi biogenesis. Experiment is described in Figure 3.1. Each frame corresponds to 1 minute of the experiment. Total time is 90 minutes.

Movie 2. Acute inactivation at steady-state. Experiment is described in Figure 3.2. Each frame corresponds to 1 minute of the experiment. White triangle at the top marks the frames surrounding the bleaching event. Total time is 70 minute.

Movie 3. Pseudo-colored steady-state inactivation. The data are the same as Movie2 except objects arising in continuity with the Golgi are colored green and objects arising in the periphery are red.

Movie 4. Bleaching of Golgi GalNAcT2-GFP prevents appearance in peripheral punctae. Sec13-KR was inactivated in the two cells shown. For the cell on the left, immediately afterwards the GalNAcT2-GFP fluorescence was bleached in a restricted region corresponding to the Golgi. Each frame corresponds to 30 seconds. Note that appearance of GalNAcT2-GFP in peripheral objects required Golgi GalNAcT2-GFP.

Movie 5. Acute inactivation at steady-state with enhanced imaging. Experiment is described in Figure 3.4. Each frame corresponds to 20 seconds of the experiment. Triangle at the top marks the frames surrounding the bleaching event. Total time is 30 minutes.

Movie 6. Appearance of peripheral punctae requires COPI. Experiment is described in Figure 3.4. Each frame corresponds to 15 seconds of the experiment. Square at the top right marks the addition of 1,3-cyclohexanebimethylamine), triangle at the top right marks the frame surrounding the sec13-KR bleaching event. Total time is 35 minutes

Movie 7. Addition of BFA blocks peripheral punctae appearance prior to Golgi collapse. Cells were inactivated immediately before the addition of brefeldin A to a final concentration of 2 $\mu\text{g}/\text{ml}$. Max value z-projections are shown. Each frame corresponds

to 20 seconds. Total time is 15 minutes

Movie 8. Response of cis and trans markers to Sec13-KR inactivation. Experiment is described in Figure 3.6. Each frame corresponds to 1 minute of the experiment. The central circle marks the time points surrounding inactivation.

Movie 9. Pseudo-colored response of cis and trans markers to sec13-KR inactivation. The data are the same as Movie 8 except objects in continuity with the Golgi are green and those appearing in the periphery are red.

The Role of GRASPs in cisternae specific linking

Abstract

Homotypic membrane tethering by the GRASP proteins is required for the lateral linkage of mammalian Golgi ministacks into a ribbon-like membrane network. Although GRASP65 and GRASP55 are specifically localized to cis and medial/trans cisternae, respectively, it is unknown whether each GRASP mediates cisternae-specific tethering and whether such specificity is necessary for Golgi compartmentalization. Here, each GRASP was tagged with KillerRed (KR), expressed in HeLa cells, and inhibited by a 1 min exposure to light. Significantly, inactivation of either GRASP unlinked the Golgi ribbon, but the immediate effect of GRASP65-KR inactivation was a loss of cis rather than trans Golgi integrity, whereas inactivation of GRASP55-KR first affected the trans and not the cis Golgi. Thus, each GRASP appears to play a direct and cisternae specific role in linking ministacks into a continuous membrane network. To test the consequence of loss of cisternae specific tethering, we generated Golgi membranes with a single GRASP on all cisternae. Remarkably, the membranes exhibited the full connectivity of wildtype Golgi ribbons but were decompartmentalized and defective in glycan processing. Thus, the GRASP isoforms specifically link analogous cisternae to ensure Golgi compartmentalization and proper processing.

4.1 Introduction

Intracellular organelles connected by membrane trafficking pathways allow cargo molecules to sequentially move between way stations optimized for processing. The abundant membrane trafficking connecting compartments must be tightly controlled to prevent rapid breakdown of compartment integrity. Of critical importance is specificity during membrane fusion. Without this specificity, mistakes in the fusion of vesicles with compartments and in compartments with other compartments would quickly intermix membranous organelles. Membrane tethers, proteins that form a transient molecular bridge between membranes prior to fusion, are thought to contribute to the specificity of fusion because tethering complexes contact the two membranes with specificity ([Whyte and Munro, 2002](#)). However, there is very little direct evidence showing that tethers impact fusion specificity and compartment integrity.

The assembly of the mammalian Golgi apparatus into a ribbon-like membrane network provides an important example of organelle tethering and fusion. Whereas other cell types have many isolated Golgi stacks distributed throughout the cytoplasm, mammalian Golgi stacks are collected near the minus-ends of microtubules and laterally linked by dynamic fusion events to form the Golgi ribbon ([Ladinsky et al., 1999](#)). Golgi stacks consist of flattened cisternae, each with high membrane curvature at their perimeters, called Golgi rims. Membrane tubules extend from the rims forming the lateral linkages between adjacent stacks. Based on their appearance in electron micrographs, the contact areas are termed non-compact zones ([Rambourg et al., 1987](#)). In addition to the tubular connections, the non-compact zones also contain vesicles. The lateral linkage is considered a product of homotypic fusion because analogous cisternae connect to one another([Thorne-Tjomsland et al., 1998](#)). That is, membrane continuity is observed among most cis cisternae in a Golgi ribbon, but cis cisternae rarely exhibit connections to medial or trans cisternae. Whether and how the contacts are restricted to homotypic fusion and whether this preserves compartment integrity is not known.

The linkages forming the Golgi ribbon are physiologically important, in part, because

they promote uniform distribution of Golgi enzymes throughout the entire network of their respective cisternae (Puthenveedu et al., 2006). For example, in a Golgi assembly assay, the individual Golgi stacks that arise in the cell periphery are differentially enriched in Golgi markers and then, as the stacks move inward and link to form the ribbon, these markers become evenly distributed. If the linkages are blocked from forming, there is a disproportioning of the markers. As a consequence there are defects in glycan processing presumably due to under-processing in isolated Golgi stacks containing diminished levels of processing enzyme (Puthenveedu et al., 2006). From an evolutionary perspective, the need for homotypic lateral fusion to distribute Golgi enzymes may have arisen when the Golgi acquired the characteristic of moving inward on microtubule tracks. Inward Golgi movement physically separates mammalian Golgi membranes from ER exit sites. In contrast, the distributed ministacks of other cell types are positioned immediately adjacent to sites of ER exit and may use recycling through the ER to ensure proper enzyme distribution. Thus, the specificity of homotypic, cisterna-cisterna fusion is hypothetically required for both Golgi compartmentalization and proper processing.

The Golgi localized GRASP proteins are thought to be the membrane tethers involved in fusion of analogous cisternae to form the Golgi ribbon (Klumperman, 2011; Vinke et al., 2011; Wilson et al., 2011). GRASP65 is localized to cis cisternae and GRASP55 is localized to medial and trans cisternae (Shorter et al., 1999). GRASP65 localization depends on its N-terminal myristic acid and its ability to bind to GM130 on the cis Golgi (Barr et al., 1998; Shorter et al., 1999; Puthenveedu et al., 2006). GRASP55 localization involves its N-terminal myristic acid and its binding to med/trans Golgi localized proteins including golgin-45 (Short et al., 2001). Knockdown of either GRASP unlinks the ribbon while leaving other aspects of Golgi organization largely intact (Puthenveedu et al., 2006; Feinstein and Linstedt, 2008; Xiang and Wang, 2010). Each protein specifically self-interacts using its N-terminal GRASP domain (Wang et al., 2005). The GRASP domain is a tandem set of atypical PDZ domains (Truschel et al., 2011). The binding groove of the first PDZ domain

mediates the self-interaction by binding an internal PDZ ligand present on the surface of the second PDZ domain (Sengupta et al., 2009; Truschel et al., 2011). At least for GRASP65, the binding groove of the second PDZ domain binds a C-terminal PDZ ligand in its Golgi-localized receptor GM130 (Bachert and Linstedt, 2010). Thus the model for cisternae-specific membrane tethering during ribbon formation invokes isoform specific localization and self-interaction of the GRASP proteins thereby providing an opportunity to test the role of membrane tethering in the specificity of membrane fusion and compartment maintenance.

However, given the small distances and dynamic aspects involved, testing the cisternae specific roles of the GRASP proteins is challenging. We sought to overcome these limitations using a combination of chromophore assisted light inactivation (CALI), fluorescence recovery after photobleaching (FRAP), and high resolution structured illumination microscopy (SIM). KillerRed mediated CALI of either GRASP protein coupled with FRAP of cisternae-specific markers reported Golgi ribbon integrity in the immediate moments after GRASP inactivation and showed that GRASP65 and GRASP55 mediate Golgi ribbon formation in the early and late Golgi cisternae, respectively. Further, SIM analysis of Golgi markers in cells expressing a single GRASP throughout the Golgi indicated that compartmentalization of the Golgi ribbon depends on the separation of duty by the GRASP isoforms.

4.2 Results

Rapid GRASP inactivation blocks Golgi ribbon formation

Although the Golgi ribbon is unlinked by depletion of either GRASP using siRNA (Feinstein and Linstedt, 2008; Puthenveedu et al., 2006; Xiang and Wang, 2010), these experiments involve a long time course of inhibition leaving open the question of whether Golgi ribbon integrity acutely depends on GRASP function. Recently, we demonstrated a rapid and specific block of ER exit using a 30 sec illumination the KR-tagged COPII component Sec13 (Jarvela and Linstedt, 2012b). Irradiation of KR with green light ($561\pm 20\text{nm}$) results in the genera-

tion of reactive oxygen species (ROS) that can break bonds and denature proteins (Jay, 1988; Liao et al., 1994; Surrey et al., 1998). ROS have a half maximal distance of 4nm, meaning this damage is spatially limited to the tagged protein and its interacting factors (Bulina et al., 2005). Thus, our strategy here was to express either GRASP65 or GRASP55 tagged with KR, inactivate the tagged protein using 561 nm light, and then immediately assess integrity of the Golgi ribbon. Because the GRASP proteins form homo-oligomers our hope was that irradiation would not only inactivate the expressed chimeric construct but also its endogenous counterpart. An important aspect of this technique is confirming the proper localization and expression level of the KR constructs and this was carried out on a cell-by-cell basis before each trial. Only cells that exhibited at least 50% of their total GRASP-KR fluorescence on the Golgi, which was demarcated using the Golgi enzyme N-acetylgalactosaminyltransferase T2 tagged with the green fluorescent protein (GalNAcT2-GFP) (Storrie et al., 1998), were chosen and illuminated to specifically bleach the KR fluorescence (Figure 4.1).

Several permutations of the experiment were employed. In the first, we monitored Golgi assembly upon brefeldin A washout in cells following inactivation of either of the GRASP protein. Golgi reassembly involves many factors and several distinct steps. Thus, whether reassembly proceeds normally up to, but not including, a point where GRASP proteins link the Golgi is a test of whether inactivation is specific, effective and supports a direct role for GRASPs in linking. The C-terminus of either GRASP was tagged with KR and expressed in cells expressing GalNAcT2-GFP to mark Golgi membranes. GalNAcT2-GFP is present in all cisternae of the stack (Storrie et al., 1998). A cytoplasmic version of KR (Cyto-KR) was used as a control. The constructs were irradiated immediately after drug washout and GalNAcT2-GFP was imaged at 1 min intervals to follow Golgi assembly. In irradiated cells expressing Cyto-KR, GalNAcT2-GFP emerged from the ER and accumulated in punctate structures that moved inward eventually coalescing into a Golgi ribbon (Figure 4.2A, movie1). Similar to non-irradiated cells, or cells not expressing KR constructs, the entire assembly occurred in about 90 min. In contrast, irradiated cells expressing either GRASP-KR protein showed

Supplemental Figure S1

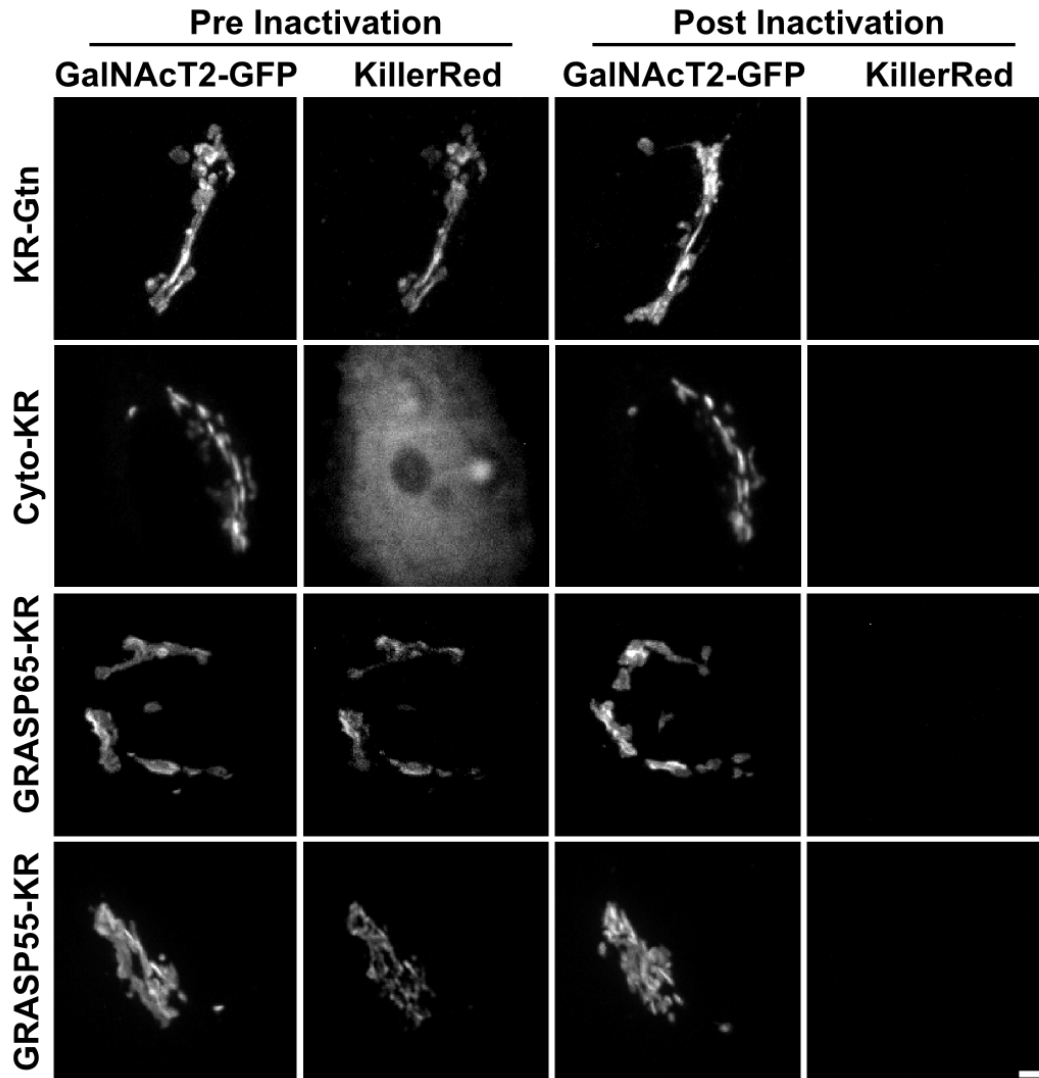


Figure 4.1: **Localization and bleaching of KR constructs.** Pre- and post-bleach images of each KR indicated. HeLa cells stably expressing GalNAcT2-GFP as a Golgi marker were transiently transfected with the indicated KR constructs. After 48 h, media was replaced with imaging media and Pre-bleach images were acquired. Cells were then irradiated with green light and post bleach images were acquired. Maximum value Z-projections are shown for the indicated pre and post bleach periods. Scale bar = 2 μ m.

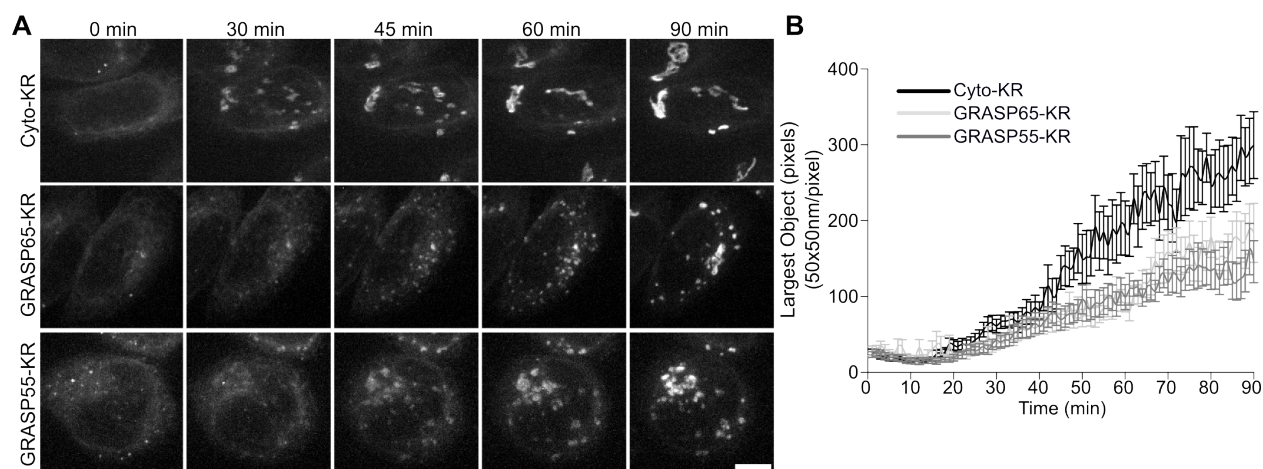


Figure 4.2: Inactivation of GRASP proteins blocks Golgi ribbon formation. (A) Cells stably expressing GalNAcT2-GFP were transfected with KR constructs. After two days, GalNAcT2-GFP was redistributed to the ER with 20 $\mu\text{g}/\text{ml}$ brefeldin A for 20 min. Cells were then quickly washed and placed in imaging medium and irradiated with 535-580nm light at an intensity of 2 W/cm^2 for 30 sec. Average value Z-projections of GalNAcT2-GFP fluorescence are shown for the indicated times after inactivation. Scale bar= 5 μm . (B) Golgi assembly was quantified by determining the size of the largest GalNAcT2-GFP object at each time point, with the threshold set above the level of GalNAcT2-GFP fluorescence in the ER (n=10, mean \pm s.e.m.).

GalNAcT2-GFP exiting from the ER and moving inward in puncta, but these objects failed to coalesce into an intact Golgi ribbon (Figure 4.2A, Movie 1). The experiment was quantified by determining the size of the largest GalNAcT2-GFP object at each time point for each cell analyzed (Figure 4.2B). As can be seen, the GRASP-KR inactivated cells failed to reestablish a Golgi of normal size; instead they exhibited a collection of mostly perinuclear Golgi fragments. These Golgi fragments had the characteristic fluorescence pattern of a stacked Golgi, with the fluorescence of cis-Golgi localized GPP130 being slightly offset from the medially enriched GalNAc-T2GFP (Figure 4.2C) when pixel intensity line plots are taken. The resulting pattern was essentially identical to that observed after depletion of either GRASP using siRNA (Feinstein and Linstedt, 2008; Puthenveedu et al., 2006). In comparison to the siRNA experiments, the relatively short time course of inactivation by KR supports a direct role for the GRASPs in establishing the Golgi ribbon.

In the second permutation, we asked whether inactivation of either GRASP would affect an intact Golgi and, if so, with what time course. As a control we used a previously described construct (Jarvela and Linstedt, 2012b) in which KR contains at its C-terminus the membrane anchor of the Golgi protein giantin (KR-Gtn) yielding a Golgi localized and cytoplasmically disposed KR. The control or GRASP-KR constructs were expressed in GalNAcT2-GFP expressing cells and irradiated followed by live cell imaging of GalNAcT2-GFP at 1 min intervals. The results clearly indicated that Golgi fragmentation consistent with unlinking took place after irradiation of either GRASP but not after irradiation of the control (Figure 4.3A, Movie 2). To quantify the experiment the number of GalNAcT2-GFP objects was determined at each time point in each cell analyzed. The number of objects was also determined for every frame of a pre-movie acquired before the inactivation. The resulting plot shows that the GalNAcT2-GFP pattern yields a small number of objects in untreated or control inactivated cells whereas there was a large, statistically significant, increase in object number in GRASP-KR inactivated cells (Figure 4.3B). The fragmentation became detectable at around 10 min after inactivation and continued to increase for the next 20 min. As addressed in the next section, this analysis may underestimate the rate because Golgi unlinking is only detectable once individual Golgi objects move far enough away from one another to be resolved. Nevertheless, the fact that fragmentation became detectable within 10-30 min of GRASP-KR inactivation provides strong evidence that ongoing function of these proteins is required to maintain integrity of the Golgi ribbon.

GRASP Inactivation Unlinks Specific Golgi cisternae

In the third and final permutation of the KR experiment, we addressed the question of whether the two GRASP proteins play compartment specific roles in linking the Golgi ribbon. For this purpose we analyzed compartment specific integral proteins. GFP-tagged GPP130 (GPP130-GFP) was used to monitor the cis Golgi (Mukhopadhyay et al., 2010) and an YFP-tagged galactosyltransferase transmembrane domain (GalT-YFP) was used to

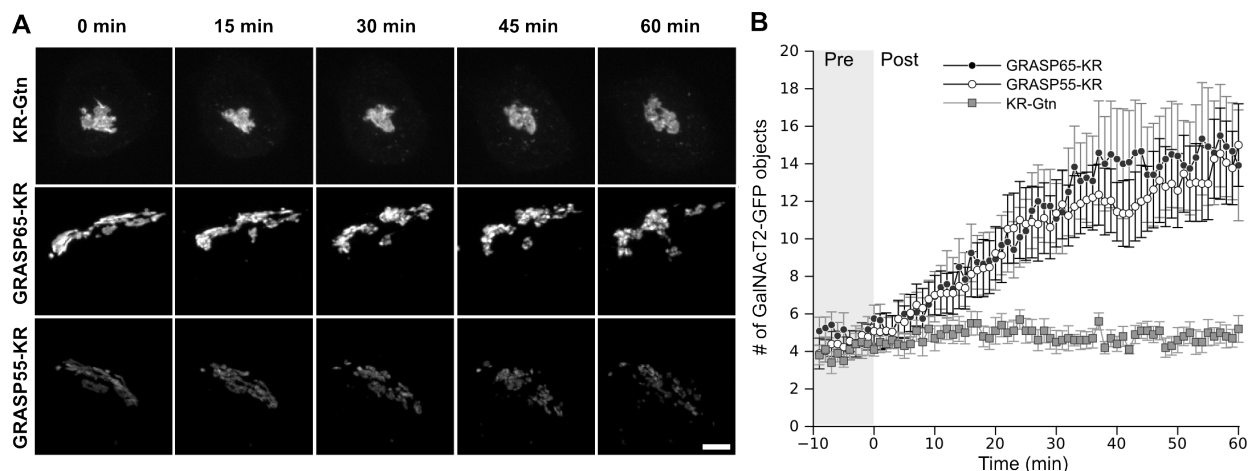


Figure 4.3: **GRASP inactivation blocks Golgi ribbon maintenance.** (A) Cells expressing the indicated KR constructs were irradiated with 535-580nm light at an intensity of 2 W/cm² for 30 sec. Z-stacks were acquired at one min intervals for 10 min prior to and 60 min post inactivation. Maximum value Z-projections are shown for the indicated time points. Scale bar = 5μm. (B) The total number of discrete Golgi objects at each time point was quantified using the ImageJ “analyze particles” function (n=10, mean ± s.e.m.).

monitor the trans Golgi (Jarvela and Linstedt, 2012b). To increase temporal sensitivity, we altered the assay to assess Golgi ribbon connectivity using fluorescence recovery after photobleaching (FRAP). We previously demonstrated that intact Golgi ribbons show rapid recovery of GalNAcT2-GFP fluorescence, whereas unlinked Golgi ribbons do not (Feinstein and Linstedt, 2008; Puthenveedu et al., 2006). Thus, our plan was to follow KR inactivation with photobleaching of the GFP and YFP signals in a small region of the Golgi and then record recovery with rapid 10 sec acquisition intervals. To test for an immediate effect on Golgi integrity the photobleaching was carried out 1 min after the KR inactivation. Compartment specific linking by GRASP65 predicts its inactivation would produce loss of FRAP for cis-localized GPP130-GFP but not for trans-localized GalT-YFP (Figure 4.4A). The opposite outcome is predicted for inactivation of GRASP55-KR.

The results for the cis Golgi marked by GPP130-GFP are shown in Figure 4.4B. As expected, rapid recovery was observed after inactivation of the control construct KR-Gtn. Inactivation of GRASP55-KR was also followed by rapid recovery of GPP130-GFP fluorescence indicating that the cis Golgi remained intact. In contrast, inactivation of GRASP65-KR led

4. THE ROLE OF GRASPs IN CISTERNAE SPECIFIC LINKING

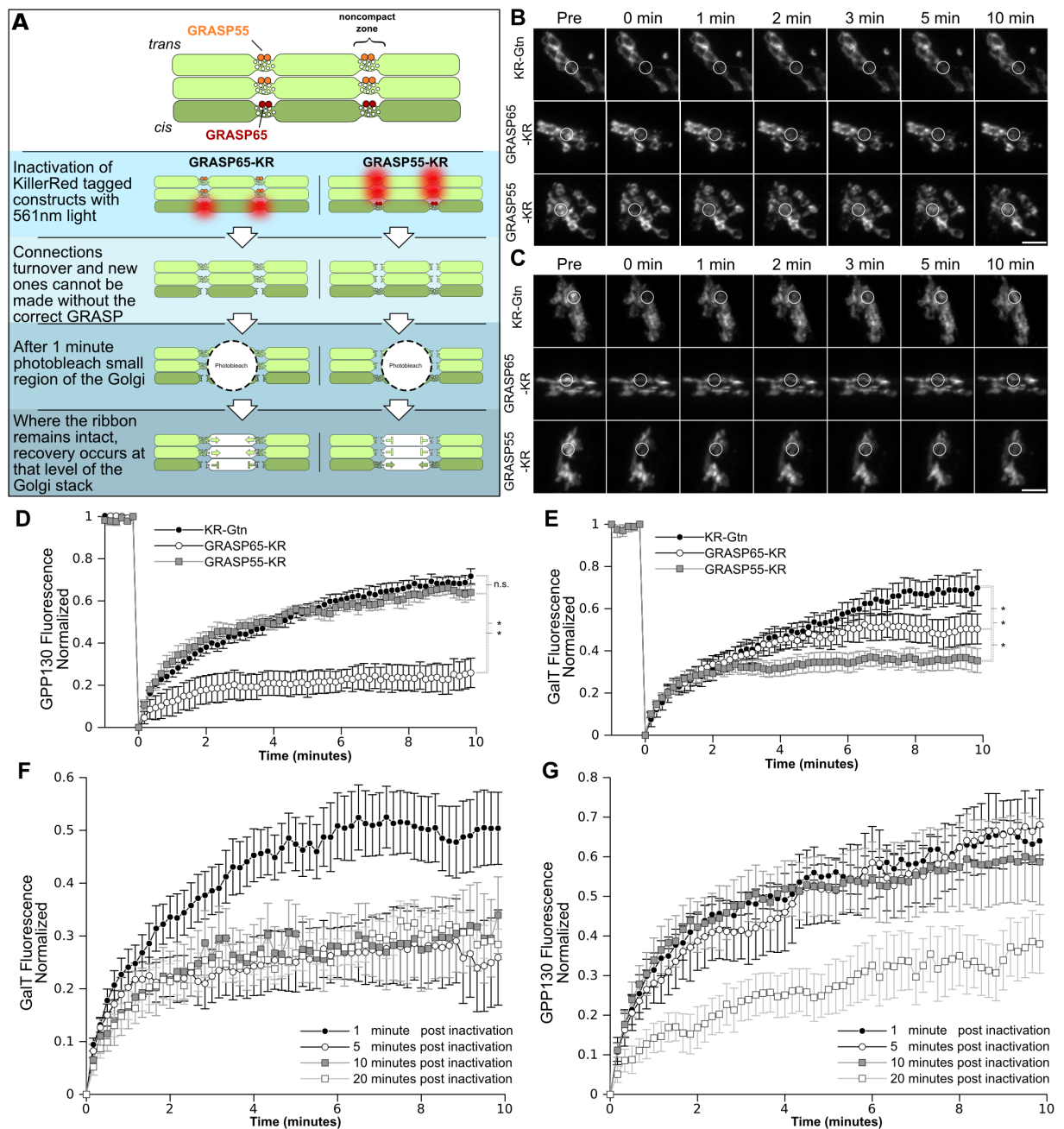


Figure 4.4: **GRASPs are required for integrity of distinct levels of the Golgi stack.** (A) A schematic of the experiment is shown in which KR constructs were inactivated and 1 min post inactivation, a small segment of the Golgi was photobleached. If the Golgi ribbon remained intact at the cis-Golgi, GPP130-GFP fluorescence was expected to recover. If the trans-Golgi ribbon remained interconnected, GalT-YFP fluorescence was expected to recover. (B-C) Cells expressing the indicated KR constructs were irradiated with 15.8 mW of a 561nm laser for 45µsec per pixel repeated six times. GPP130-GFP fluorescence to mark the cis Golgi (B) or GalT-YFP fluorescence to mark the trans Golgi

Continued from [4.4 on the preceding page](#) (**C**) was recorded at 10 second intervals for 1 min, then the outlined segment was bleached with 27.3mW 488nm laser light for 20 μ sec repeated 60 times, and then fluorescence recovery was recorded for a further 10 min at 10 second intervals. Average value Z projections are shown for the indicated time points. Bar = 5 μ m. (**D-E**) GPP130-GFP (**D**) and GalT-YFP (**E**) fluorescence was measured in the bleached zone and plotted versus time (n=10 cells, mean \pm s.e.m.). Results were compared for statistical significance using a two-tailed Students T-test (*P<0.05, n.s. = not significant). (**F**) Trans marker GalT-YFP FRAP is shown after being carried out at the indicated times post inactivation of GRASP65-KR (n>5, mean \pm s.e.m.). (**G**) Cis marker GPP130-GFP FRAP is shown after being carried out at the indicated times post inactivation of GRASP55-KR (n>5, mean \pm s.e.m.)

to a pronounced block in recovery. The intimate role of GRASP65 in linking cis cisternae is strongly supported by these data given that the FRAP component of the assay was initiated only 1 min after inactivation and that recovery was significantly delayed even at the earliest time points. The results for the trans Golgi marker GalT-YFP also supported cisternal specific roles for the GRASPs but were less pronounced (Figure 4.4C). GRASP65-KR inactivation yielded recovery that was similar to the control yet the final extent of recovery was somewhat reduced. GRASP55-KR inactivation clearly had a more profound effect on GalT-GFP recovery than did either the KR-Gtn or GRASP65 and this block was also significant compared to its lack of effect on GPP130-GFP. There are several possible explanations for the residual recovery in the inactivated cells including imprecise targeting of the constructs and recycling of the markers by vesicular trafficking.

Because acute inactivation of either GRASP protein yielded cisternae specific unlinking whereas longer term depletion of either GRASP unlinks the entire Golgi ribbon we tested whether acute inactivation would lead to unlinking of all cisternae if given sufficient time. For example, if GRASP65 initiates linking as Golgi cisternae elongate on the cis face of the ribbon and GRASP55 maintains these linkages as cisternae mature then loss of GRASP65 function would ultimately destabilize the entire ribbon. Indeed, whereas GRASP65-KR inactivation had no effect on the trans marker GalT-YFP recovery at 1 min post inactivation, by 5 min there was already a marked reduction and this was also observed at 10 and 20 min post inactivation (Figure 4.4D). The level of loss in recovery was similar to that reached by GRASP55-KR inactivation, suggesting that disruption at the cis face propagates to the late

Golgi. Interestingly, inactivation of GRASP55-KR also propagated but this occurred with a slower time course. GRASP55-KR inactivation had no effect on the cis marker GPP130-GFP recovery at 1, 5 and 10 min post inactivation, but recovery became impaired by 20 min post inactivation (Figure 4.4E). This time course matched that shown above (Figure 4.3A-B) for Golgi unlinking assessed by fragmentation of GalNAcT2-GFP fluorescence into resolvable Golgi objects. One possibility is that once late Golgi cisternae become physically separated from one another, GRASP65 can no longer effectively initiate linking of cisternae. In any case, these results reveal a rapid time course leading from the acute disruption phenotype to the longer-term knockdown phenotype, and taken together, the photoinactivation experiments strongly support a direct role for the GRASP proteins in cisternae specific linking.

“Single-GRASP” Golgi yields intact ribbon with loss of compartmentalization

Unlike mammalian cells, which express two GRASP proteins and generate Golgi ribbon networks, non-vertebrate cells express a single GRASP and typically contain isolated ministacks (Wei and Seemann, 2010). To gain insight into why two GRASP proteins are required in HeLa cells we attempted to generate Golgi membranes containing a single GRASP localized to all cisternae. First, we took advantage of the fact that GRASP65 can be removed from Golgi membranes by depletion of its membrane receptor GM130 (Puthenveedu et al., 2006). As expected, transfection with GM130 siRNA caused loss of GRASP65 and unlinked the Golgi (Figure 4.5A-C).

Second, we expressed in these cells a myc-tagged GM130 replacement construct in which we substituted the GRASP55 binding site from golgin-45 in place of the GM130 C-terminal GRASP65 binding site. As expected, the GM130-45 chimera was Golgi localized and failed recruit GRASP65 (Figure 4.5A-B). Significantly, the continuity of the Golgi ribbon was rescued in cells expressing the GM130-45 chimera as assayed by determining the number

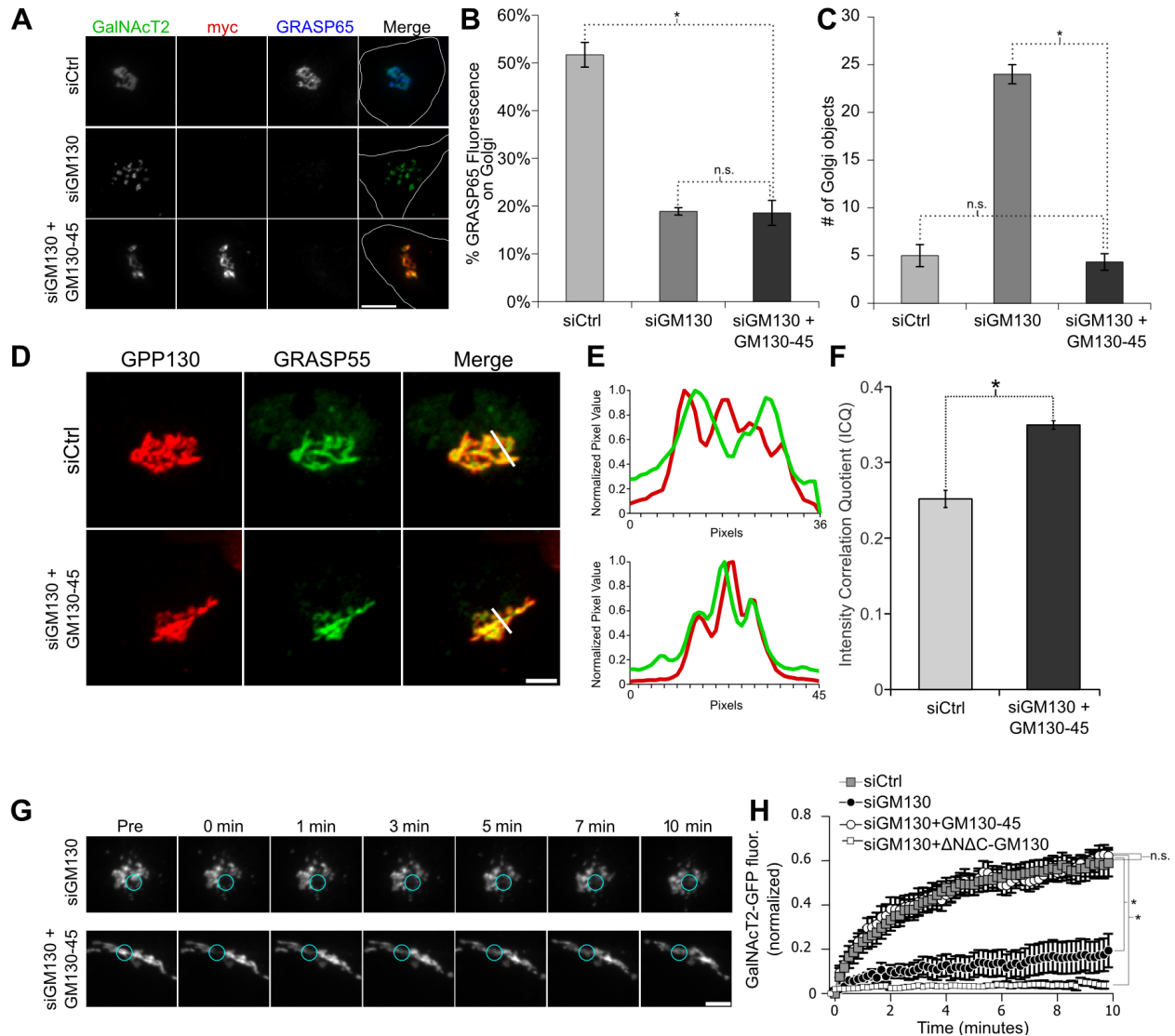


Figure 4.5: The GM130-45 chimera rescues Golgi ribbon integrity after GM130 knock-down. (A) Immunofluorescence staining is shown for cells stably expressing GalNAcT2-GFP that were transfected with control or GM130 specific siRNA 96 h prior to fixation. Where indicated, the cells were also transfected with the myc-tagged GM130-45 chimera 12 h prior to fixation. Bar = 5 μ m. (B) The amount of GRASP65 fluorescence present on the Golgi was determined using GalNAcT2-GFP as a mask. The percent of the total cellular pool that is present on the Golgi is shown for each condition. (n=10, mean \pm s.e.m., *P<0.05, n.s. = P>0.05) (C) The number of Golgi objects present for each condition was determined by counting discrete GalNAcT2-GFP positive objects. (n=10, mean \pm s.e.m., *P<0.05, n.s. = not significant) (D) Average value Z-projections of GRASP55 and GPP130 immunofluorescence images in control and mycGM130g45tail rescued expressing cells. Expression of GM130-45 increases colocalization of GRASP55 with cis Golgi marker GPP130 as shown by (E) profile plots and (F) the Intensity Correlation Quotient (ICQ) (G) Time course of Golgi fluorescence recovery after photo bleaching in siCtrl, siGM130, and GM130-45 rescued cells. Blue circles encompass the photobleached region. Bar = 5 μ m. (H) Fluorescence levels in bleached region is measured and is plotted versus time (n=10 cells, mean \pm s.e.m., *P<0.05, n.s. = not significant).

of resolvable Golgi objects (Figure 4.5C). The golgin-45 segment was taken from the last thirteen residues of the golgin-45 C-terminus. When targeted to the mitochondrial outer membrane, these residues were sufficient to recruit GRASP55 (Figure 4.6). Also, cells expressing the GM130-45 chimera showed a significant increase in GRASP55 on cis Golgi membranes as indicated by colocalization with endogenous GPP130 (Figure 4.5D-F). Thus, rescue of linking was presumably by recruiting GRASP55 instead of GRASP65 to the cis Golgi. Indeed, the reformed ribbon in these cells showed a dramatic recovery of GalNAcT2-GFP fluorescence after bleaching whereas little recovery occurred in GM130 depleted cells not expressing the rescue construct (Figure 4.5G-H). If full-length golgin-45 was expressed instead of the chimera there was no rescue of Golgi linking (our unpublished results). Also, if GRASP65 was depleted instead of GM130, the chimeric GM130-45 construct was still able to rescue linking (our unpublished results). In sum, a single GRASP protein localized to all Golgi cisternae is sufficient to stably link Golgi cisternae into a ribbon structure.

Based on this conclusion we tested whether there might be functional deficit in a HeLa cell Golgi ribbon linked by a single GRASP protein. To test for defective compartmentalization in the “single-GRASP” Golgi we first analyzed GPP130 and GalNAcT2-GFP by standard confocal microscopy. As expected, in control cells the Golgi markers showed significant side-by-side, rather than colocalized, staining that was evident in both the raw images (Figure 4.7A) and in profile plots taken across the Golgi ribbon (Figure 4.7B). In contrast, the markers coalesced in the Golgi ribbons of cells in which the GM130-45 chimera was expressed to replace the depleted GM130. Significantly, this was also the case for cells simply expressing the chimera. That is, expression of the chimera to recruit GRASP55 to the cis Golgi was dominant negative in the sense that it caused loss of compartmentalization without depletion of GM130. Quantification of marker colocalization across many cells using the Intensity Correlation Quotient (Li et al., 2004) supported the conclusion that the chimeric construct caused loss of compartmentalization whether expressed on its own or after depletion of GM130 with the latter condition yielding the greatest effect (Figure 4.7C).

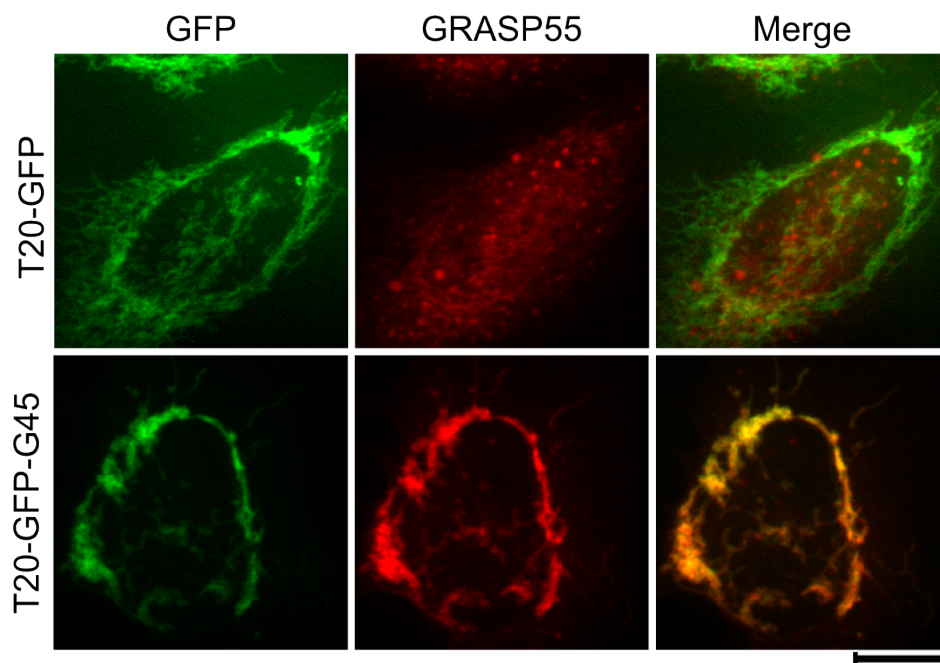


Figure 4.6: **C-terminus of golgin-45 recruits GRASP55 to mitochondrial membranes.** HeLa cells were transfected with mitochondrial localized T20-GFP or T20-GFP-G45 (green). These fusion proteins are targeted to the outer mitochondrial membrane by the N-terminal targeting sequence from Tom20. After 24 h, cells were treated with 20 $\mu\text{g}/\text{ml}$ brefeldin A for 20 min to collapse the Golgi into the ER. Cells were then fixed and stained for endogenous GRASP55 (red). The merged image shows GRASP55 overlap with mitochondria. Bar = 10 μm .

To substantiate these results we also analyzed cells expressing the GM130-45 chimera by SIM. Here, to accentuate the degree of compartmentalization in control cells and restrict the analysis to endogenous proteins, we compared GPP130 to the trans Golgi network marker golgin-97. In untransfected cells, or cells expressing wildtype GM130 as a control, the separation of the early and late Golgi markers was striking in both the raw images (Figure 4.7D) and in profile plots taken across the Golgi ribbon (Figure 4.7E). In cells expressing the GM130-45 chimera the side-by-side staining was greatly diminished and there was a much higher incidence of colocalization. This was supported by calculation of the Pearson's Coefficient (Figure 4.7F). Both the mean and the range of the data show the significant increase in colocalization in cells expressing the GM130-45 chimera.

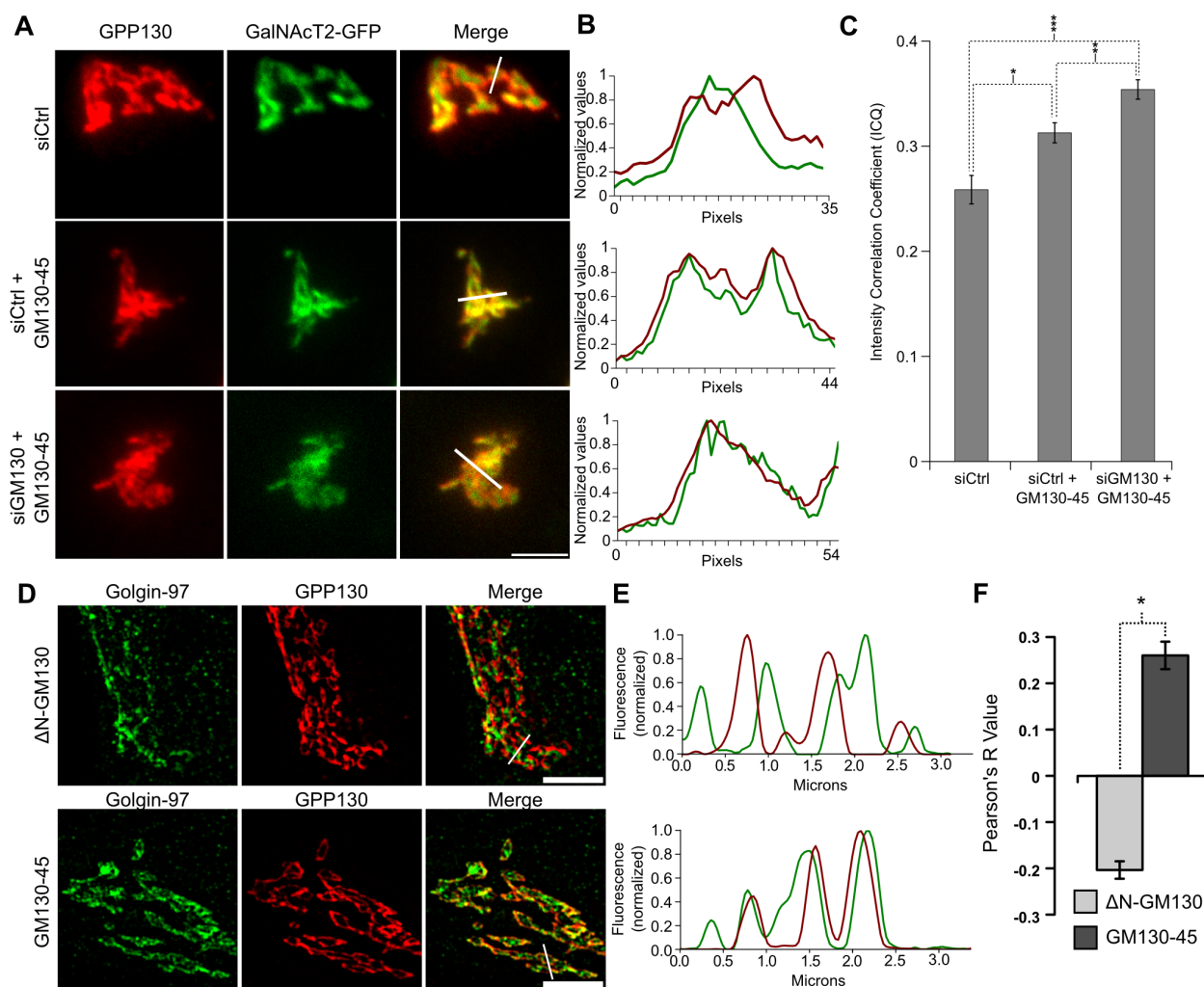


Figure 4.7: Expression of the GM130-45 chimera increases marker colocalization. (A) Average value Z-projections of immunofluorescence images of endogenous GPP130 and stably expressed GalNAcT2-GFP in control knockdown cells, control knockdown cells expressing GM130-45 and GM130 knockdown cells rescued with mycGM130g45tail. Bar = 5 μ m. (B) Profile plots of normalized pixel intensity of GPP130 (red) and GalNAcT2-GFP (green) corresponding to the region marked with white lines in A. (C) Colocalization of endogenous GPP130 and GalNAcT2-GFP across experimental conditions as measured by ICQ ($n \geq 15$ cells, mean \pm s.e.m., * $P=0.002$, ** $P=0.016$, *** $P=8.2 \times 10^{-7}$). (D) HeLa cells were transfected with mycGM130-WT or GM130-45. Shown is a representative single Z-slice of a 3D structured illumination image showing fluorescence patterns of endogenous GPP130 (red) and golgin-97 (green). Bar = 5 μ m. (E) Normalized values of pixel intensity for GPP130 (red) and golgin-97 (green) along the region indicated by the white lines in D. (F) Colocalization of endogenous GPP130 and golgin-97 is described by the Pearson's correlation coefficient for cells transfected with mycGM130-WT or GM130-45. ($n \geq 15$, mean \pm s.e.m., * $P=2.9 \times 10^{-11}$).

Perturbed compartmentalization is associated with glycan processing defects

To test whether the apparent loss of Golgi compartmentalization in these cells might cause a glycosylation defect we used a simple assay for efficient terminal glycosylation (Feinstein and Linstedt, 2008; Puthenveedu et al., 2006). The Alexa-647 conjugated GS-II lectin purified from *Griffonia simplicifolia* binds to terminal N-acetyl-D-glucosamine, which is rare on the cell surface due to the addition of galactose and sialic acid moieties in the late Golgi (Kornfeld and Kornfeld, 1985). Thus, a decrease in efficiency of these later steps leads to increased GS-II labeling at the cell surface. Consistent with a defect in processing efficiency upon chimera expression, control cells showed little surface GS-II staining whereas cells expressing the GM130-45 chimera yielded a clear signal (Figure 4.8A). Quantification indicated that surface levels more than doubled (Figure 4.8B). In conclusion, a single GRASP localized throughout the Golgi in HeLa cells is sufficient to maintain Golgi ribbon architecture but the resulting membranes are decompartmentalized and this likely causes inefficient glycosylation of cargo en route to the cell surface.

4.3 Discussion

The Golgi ribbon is dynamically maintained by the tubular membrane contacts linking analogous cisternae. These contacts continuously break and reform and they are also reversibly or irreversibly broken during processes such as cell division (Carcedo et al., 2004; Colanzi and Corda, 2007; Feinstein and Linstedt, 2007; Rabouille and Kondylis, 2007; Sengupta and Linstedt, 2010), directional changes in cell migration (Bisel et al., 2008a), apoptosis (Lane et al., 2002) and intracellular bacterial infection (Heuer et al., 2008). The precarious nature of the linkages is further highlighted by the many experimental manipulations (Marra et al., 2007; Mironov et al., 2004) that perturb them including microtubule depolymerization (Cole et al., 1996; Kreis, 1990). Our findings indicate that the GRASP proteins play direct and

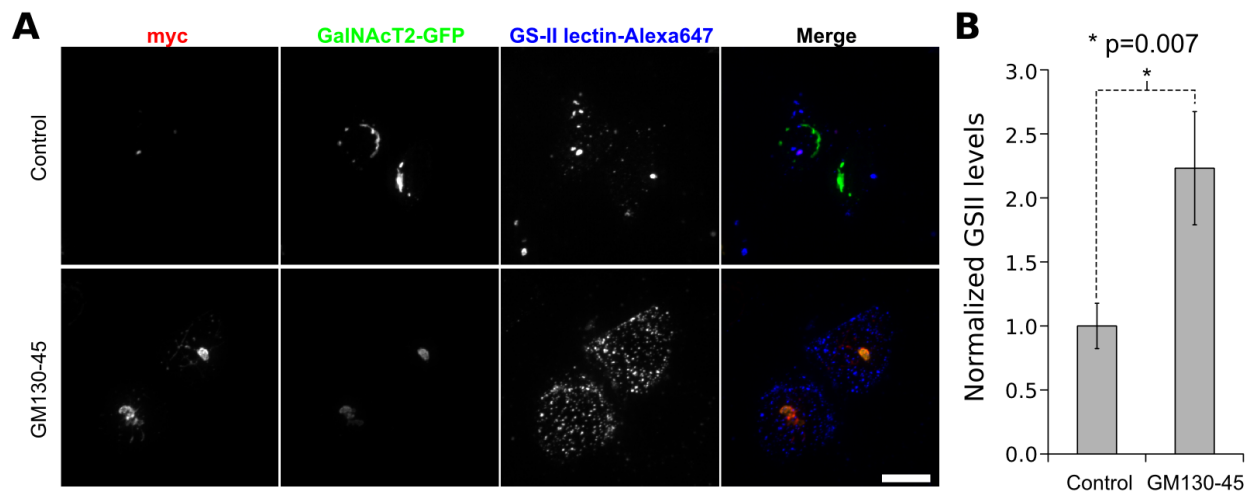


Figure 4.8: **Decreased glycan processing in cells expressing the GM130-45 chimera.** (A) Cell surface staining for terminal N-acetyl-D-glucosamine levels (blue) was performed using Alexa-647 conjugated GSII-lectin. Cells were transfected with the GM130-45 construct were grown for 84 h and then treated with trypsin and passed onto new coverslips for 12 h prior to fixation. The Golgi marked by GalNAc-T2GFP (green) and myc-tagged GM130-45 construct levels (red) are also shown. Representative average value Z-projections are shown for the indicated experiments. Bar = 20 μ m. (B) Graph showing the average staining of GSII-lectin normalized to the mean value of control cells ($n > 17$ cells, mean \pm s.e.m) Statistical significance was determined using a single-tailed paired Student's t-test (* $P = 0.007$).

cisternae specific roles in sustaining these linkages. Further, while a single GRASP, if localized throughout the Golgi, is capable of linking the membranes into a ribbon, the two GRASPs are needed to compartmentalize the membranes. Thus, Golgi ribbon formation involves lateral membrane contacts that require specificity conferred by the GRASP proteins to maintain compartmentalization.

Although the GRASP proteins are involved in other processes (reviewed in (Jarvela and Linstedt, 2012a; Vinke et al., 2011)), the evidence that they play a direct role in cisternae-specific tethering in cultured cells is now extensive. The localization of GRASP65 is biased to early cisternae and GRASP55 to late cisternae (Shorter and Warren, 1999). Inhibition of expression of either GRASP specifically disrupts Golgi ribbon formation (Feinstein and Linstedt, 2008; Puthenveedu et al., 2006; Xiang and Wang, 2010). That is, under these

conditions the Golgi membranes remain trafficking competent, stacked, compartmentalized and mostly juxtannuclear but fail to establish the ribbon-like membrane network. Perhaps most importantly, acute inactivation of GRASP65 has the immediate effect of unlinking cis cisternae, while rapid inhibition of GRASP55 first unlinks trans cisternae (Figure 4.4). The GRASP proteins exhibit tethering activity in assays using beads (Wang et al., 2005, 2003), mitochondria (Sengupta and Linstedt, 2010; Sengupta et al., 2009), and liposomes (our unpublished observations). The mechanism is homotypic oligomerization via a unique PDZ interaction (Truschel et al., 2011) such that either GRASP exclusively binds itself and trans interactions across membranes are favored over cis interactions in the same membrane (Bachert and Linstedt, 2010). Phosphorylation or phosphomimetic mutation of the GRASP proteins blocks tethering activity and prevents Golgi ribbon formation (Jesch and Linstedt, 1998; Wang et al., 2003; Preisinger et al., 2005; Feinstein and Linstedt, 2007, 2008; Sengupta and Linstedt, 2010; Tang et al., 2010; Truschel et al., 2012).

These experiments do not distinguish among the varied concepts of Golgi membrane dynamics. Nevertheless, the observation that ablation of either GRASP first yields a cisternae-specific loss of membrane continuity, followed by a loss of lateral continuity among all cisternae, is consistent with cisternal maturation in which GRASP65 establishes ribbon continuity and GRASP55 maintains it. Pre-cisternal membranes coalescing out of a multitude of ERGIC sites (Mironov et al., 2003) would use tethering by GRASP65 as part of their transformation into the interconnected cis cisternae of the Golgi ribbon. As these membranes mature, recycling of GRASP65 (Marra et al., 2001) would ensure further rounds of pre-cisternal membrane maturation. Also, as the cis membranes mature to medial they would acquire GRASP55 via recycling from later compartments so that the lateral connections established by GRASP65 are maintained in the medial and trans Golgi. Recycling of GRASP55 from medial membranes as they mature into trans cisternae may cause a reduced continuity among cisternae at the most trans position of the Golgi ribbon (Rambourg and Clermont, 1997; Jackson, 2009). As mentioned above, the ultimate loss of all ribbon

connectivity by acute inhibition of either GRASP agrees with RNA interference experiments showing that each GRASP is required. These findings imply interdependency in the function of the two GRASPs. It may be that, over time, net adhesivity within the non-compact zones is critical to the existence of stable connections. Thus, loss of either the initiating or the maintaining GRASP would ultimately cause full unlinking of the Golgi ribbon.

Why are there two GRASP proteins in mammalian cells? Our experiments show that in HeLa cells the GRASPs mediate cisternae specific linking within the Golgi ribbon and that establishment of the ribbon with a single GRASP cause defects in Golgi compartmentalization. Our interpretation is that the “single-GRASP” Golgi condition yielded net adhesivity that was sufficient to form the Golgi ribbon but that the presence of the single GRASP on all cisternae promoted an increase in contact between non-analogous cisternae. As a consequence, the rims of cis, medial and trans cisternae fused with one another at a sufficient level to cause mixing of what are normally compartmentalized Golgi proteins. In light of this view, its noteworthy that the number of cisternae per stack can vary greatly among differing cell types ([Rambourg and Clermont, 1997](#)) yet, to our knowledge, all cells with Golgi membranes express, at most, two GRASP proteins ([Shorter et al., 1999](#); [Kondylis et al., 2005](#); [Behnia et al., 2007](#); [Kinseth et al., 2007](#); [Struck et al., 2008](#); [Yelinek et al., 2009](#)). It follows that whether there are two or ten cisternae making up the stacks that are linked into a Golgi ribbon, there are, at most, two GRASPs available to maintain its compartmentalization. This can be understood, in part, due to the fact that Golgi proteins are distributed in gradients spanning multiple cisternae that probably define no more than three functional compartments ([Dunphy and Rothman, 1985](#); [Mellman and Simons, 1992](#); [Rabouille et al., 1995](#)). As stated in the previous paragraph, we hypothesize that GRASP65 initiates lateral contacts as cis cisternae form and that these contacts are maintained in later cisternae by GRASP55. Possibly, for Golgi ribbons with many cisternae, a gradient distribution of the GRASPs is sufficient to ensure separation of Golgi membranes into two or three functionally distinct domains. That is, multiple early cisternae may be in continuity at their rims

via GRASP65 homotypic connections and multiple late cisternae via GRASP55 homotypic connections.

What about cell types that express only a single GRASP and yet maintain a compartmentalized Golgi? These cell types have multiple, distributed Golgi stacks rather than a single ribbon-like membrane network. It may be that GRASPs are not needed to maintain compartmentalization if Golgi membranes are not brought together to form the Golgi ribbon. The Golgi rims of isolated Golgi stacks have little opportunity for tubule-mediated fusion, among analogous cisternae or not, because there are no adjacent stacks. In contrast, the potential for such fusion contacts is plentiful within a Golgi ribbon necessitating a mechanism ensuring homotypic fusion so that compartmentalization is not degraded.

In conclusion, rapid inactivation coupled with dynamic imaging and as well high-resolution microscopy revealed cisternal specific functions of GRASP65 and GRASP55 in continuity, compartmentalization and function of the Golgi ribbon.

4.4 Materials and Methods

Cloning. GRASP55-KR was created by PCR amplification of KR from pKillerRed-N (Evrogen) and replacing the myc tag at the ClaI and XbaI sites of pCS2-GRASP55myc (Jesch et al., 2001). GRASP65-KR was created by substituting its full-length cDNA generated by PCR, at the BamHI and ClaI sites of GRASP55-KR. KR-Gtn, Cyto-KR and GalT-YFP were as described (Jarvela and Linstedt, 2012b). GPP130-GFP (Mukhopadhyay et al., 2010) and T20-GFP (Sengupta et al., 2009) were as described. T20-GFP-G45 was created by inserting sequence of the last 13 amino acids of golgin-45 into T20-GFP. The myc-tagged GM130 rescue constructs Δ N-GM130 and Δ N Δ C-GM130, lacking the N-terminal p115 and C-terminal GRASP65 binding sites, respectively, were as described (Puthenveedu et al., 2006). The GM130-45 chimera was created by using a loop-in modification of the QuikChange protocol (Stratagene) to insert sequence encoding the last 13 amino acids of golgin-45 and a stop

codon in place of that encoding the last 13 residues of Δ N-GM130.

Cell culture and transfection. HeLa cells and HeLa cells stably expressing GalN-AcT2-GFP were cultured in MEM (Thermo Scientific) with 10% FBS (Atlanta Biologicals). Before experiments, cells were grown until 30-50% confluent in a 60mm dish and transfected with JetPEI (PolyPlus) according to the manufacturer's protocol. After 24 h, cells were suspended using trypsin and dispersed onto 35mm coverslips and 36-72 h post transfection the cells were imaged. SiRNA experiments were performed using Interferin (PolyPlus) according to manufacturer's protocol. Replacement constructs were transfected 24 h post knockdown using JetPrime (PolyPlus) and 72 h later cells were fixed or prepared for live imaging as needed. For Golgi assembly experiments, cells were treated with brefeldin A (Sigma) at 20 μ g/ml for 20 min. The cells were washed with 10 volumes of cold PBS and coverslips were then transferred to imaging chambers and imaging media was added. KR constructs were inactivated within 90 seconds of drug washout, prior to normal imaging.

Cell Imaging. Brefeldin A washout experiments and steady state Golgi inactivation were performed with a Zeiss Axiovert 200 at 37°C with a 100x Plan-Apo NA 1.4 oil objective (Zeiss, Thornwood, NY) attached to an UltraView spinning-disk confocal system (Perkin-Elmer, Shelton, CT). Photoinactivation was achieved with epifluorescence light at an intensity of 2W/cm² for 30 sec. Z-slices were acquired at 300nm intervals encompassing the full range of the cell, on average 18 slices encompassing approximately 5.4 μ m. FRAP experiments and immunofluorescence confocal images were acquired with Andor iQ2 spinning-disk confocal system at the Molecular Biosensors and Imaging Center at Carnegie Mellon University. CALI of KR constructs was achieved by drawing an ROI encompassing the perimeter of the cell. Each pixel was irradiated with 15.8 mW of a 561nm laser for 45 μ sec per pixel repeated six times. Photobleaching of GFP or YFP constructs was achieved using 27.3 mW of 488 nm laser power for 20 μ sec per pixel repeated 60 times, and fluorescence recovery was recorded for a further 10 min at 10 second intervals. Stacks of fluorescence were acquired for the full range of the cell with z-slices at 200 nm intervals. SIM images were

acquired with a Nikon A1 Structured Illumination Microscope using a CFI Apo TIRF 100x oil (NA 1.49) objective with Nikon Elements Software at the Center for Biologic Imaging at the University of Pittsburgh. Three-dimensional Z stacks were acquired of fixed cells with slices every 100nm, encompassing the Golgi fluorescence.

Immunofluorescence. Cells adhered to glass coverslips were fixed (3% paraformaldehyde in PBS at pH 7.4) at room temperature for 20 min. They were then rinsed five times in PBS then permeabilized and blocked in 0.5% Triton X-100, 50 mM glycine, 5% fetal bovine serum, in PBS for 30 min. Cells were incubated with one or two of the primary antibodies diluted in block for 30 minutes and washed again five times in PBS. Secondary antibodies diluted in block were then added to the cells for 30 min. Cells were again rinsed five times and mounted onto slides using either 80% glycerol in Tris pH 7.4 or gelvatol mounting media (10.5% Polyvinyl alcohol, 21% glycerol, in 100 mM Tris pH 8.5). Antibodies were: rabbit anti-GRASP55 (Feinstein and Linstedt, 2007), rabbit anti-GRASP65 (Bachert and Linstedt, 2010), rabbit anti-GPP130 (Puri and Linstedt, 2003), mouse anti-GPP130 (Linstedt et al., 1997), mouse anti-golgin-97 (Life Technologies), and mouse anti-myc (Evan et al., 1985). Secondary antibodies labeled with Alexa-488, Alexa-568, and Alexa-647 as well as Alexa-647 labeled GSII-lectin were obtained from Life technologies. GSII lectin surface staining was performed after washing cells 5x in ice-cold PBS. Cells were incubated with 10 μ g GSII lectin per ml of ice-cold PBS containing 0.5 mM MgCl₂ and 1 mM CaCl₂ for 30 min at 4^oC. Cells were then washed 5x with the same buffer prior to fixation as normal.

Image analysis. ImageJ (<http://rsbweb.nih.gov/ij>) was used to carry out most analysis. All images were background subtracted using the 'Subtract BG from ROI' plugin and selecting a region outside the cells. FRAP was measured using 'FRAP profiler' on average projections of confocal stacks using the freehand selection tool to select the bleached area post bleach and normalized to total cellular fluorescence. Largest objects and total number of objects were determined by using the 'Analyze particles' function in ImageJ. Colocalization of confocal images was performed using the 'Intensity correlation analysis' plugin (Li et

al., 2004). Colocalization analysis for SIM images was performed using the 'Coloc 2' plugin incorporated into Fiji (Schindelin et al., 2012) after background subtraction. GRASP65 on the Golgi was the summed fluorescence in the Golgi region, demarcated by GalNAcT2-GFP, as a percentage of the summed fluorescence in the entire cell.

4.5 Movie Legends

Movie 1. Golgi assembly after inactivation of KR constructs. Experiment as described in Figure 4.2. Each frame corresponds to 1 min of the experiment. Total time is 90 min.

Movie 2. Golgi ribbon integrity after inactivation of KR constructs. Experiment as described in Figure 4.3. White triangle at the top marks the frames surrounding the KR bleaching event. Total time is 70 min.

Conclusions and Future Directions

While acute inactivation of proteins as means of study is by no means novel—researchers working in yeast and bacteria have been using temperature sensitivity as a means of protein inactivation for over half a century—the results of this thesis show that Killer Red mediated CALI is a powerful and tractable tool in the mammalian cell biologist’s arsenal. Using our KillerRed in *trans* approach, we achieved inactivation of total cellular protein levels enough to inhibit functional activity. Importantly, we verified the efficacy of these inactivations using assays which replicated conditions of chronic inhibition, replicating results. Our KillerRed CALI approach revealed recycling of Golgi enzymes to peripheral ERGIC compartments, a key prediction of the maturation model of Golgi biogenesis. Additionally, by means of acute inactivation, GRASP proteins were shown to be directly responsible for the integrity of the Golgi ribbon at distinct levels of the Golgi stack. Thus, when coupled with diligent confocal microscopy acute inactivation at steady state phenotypes can achieve cogent results.

Chromophore Assisted Light Inactivation

Technical limitations have been a major deterrent of generalized CALI use over the years. Microinjection of antibodies, dangerous dyes, or high laser power were all hurdles that needed to be overcome. Here, we have used KillerRed which surmounts these hurdles and approaches the next set of obstacles including reproducibility, expression levels, descriptive inactivation.

Of paramount importance for KillerRed to be a mainstream technique is controlling for off target effects, specifically inactivation of adjacent proteins or binding partners. Through our own work, we have seen many times that over-expression of KillerRed can result in cell death upon inactivation. Further, some regions of the cell such as the nucleus or mitochondrial membrane, are susceptible to ROS damage that can result in apoptosis. CALI is therefore at a constant struggle between over-ablation resulting in off target effects and under inactivation resulting in functional copies of the protein still remaining in the cell. Eliminating endogenous copies of the target proteins through RNAi can further improve inactivation efficiency in some experiments. Indeed, this would be a necessity for target proteins which do not function as homotypic dimers or oligomers, to ensure full inactivation of the cellular pool.

The recent generation of more powerful photosensitizer should make these experiments amenable. MiniSOG (Qi et al., 2012; Shu et al., 2011) (mini singlet oxygen generator) is a protein of only 106 amino acids. This may allow it to be attached to proteins which do not accept larger, bulkier tags. With an excitation spectra similar to GFP, a miniSOG tagged protein can be combined with KillerRed tagged protein in the same cell and their inactivation can be controlled separately.

Golgi recycling to the cell periphery

A constant source of debate for many years was how separate the Golgi was from the ER. Evidence was presented for and against Golgi proteins constitutively recycling through the ER. When cells were treated with nocodazole to depolymerize microtubules, it was found that the Golgi did not gradually fragment and disperse to peripheral ER exit sites, but appear there gradually as de novo structures (Cole et al., 1996). Early live imaging of GalNAc-T2-GFP failed to show any directed movement of Golgi membranes to the periphery (Storrie et al., 1998). We now know that these recycling objects are transient and dim under normal conditions. Our use of sec13 inactivation allowed for observation of the recycling

intermediates prior to their eventual collapse into the ER. Microinjection of a dominant negative form of Sar1 showed a robust transfer of Golgi fluorescence to the ER on a similar time scale of 4 hours (Miles et al., 2001), though the researchers did not identify intermediate steps.

The total block of ER export by KillerRed inactivation of sec13 revealed the presence of a pathway that is not well understood. Our current model is that this pathway primes ERGIC derived Golgi carriers with cis-cisternae residents and tethers so they can be easily incorporated into the ribbon once they brought in to the perinuclear region. The retrograde recycling pathway is better understood for ER proteins that have escaped and need to be captured and returned (Letourneur et al., 1994). It is unclear if this is the same pathway or peripheral cycling is another pathway entirely.

Interestingly, recycling intermediates cannot make their way back to the Golgi without some ER derived factor adding to motility. The direct candidate for this factor is Golgin160, which is known to be necessary for minus end directed motility of Golgi objects (Yadav et al., 2009). Our unpublished data shows that the recycling intermediates are absent of Golgin160. It is likely however, that something upstream, (Arf1 most likely) requires ER exit to be continually renewed on the ERGIC membranes and allow for recruitment of Golgin160 and minus end motility. Additionally, further study will need to be done concerning the packaging and transport of these recycling components out of the Golgi. Our data suggest that this process is COPI mediated due to the sensitivity of the phenotype to CBM treatment. It is unknown if this is a directed secretory event or simple bulk flow of membrane and protein in a retrograde manner.

It is important to note that the observed recycling of early Golgi components to peripheral ERGIC sites is a prediction of the cisternal maturation model. However it is possible that this recycling to the periphery is purely to prime cells for transport to and fusion with already existing cis-cisternae. A definitive answer will require structural analysis of the recycling intermediates, most likely by electron microscopy. Recycling to the cell periphery provides

an advantage in studying Golgi structure and dynamics as it can be spatially resolved from the Golgi stack. KillerRed mediated inactivation should be used to further test key players in Golgi structure and dynamics.

The Golgi ribbon

Much controversy has surrounded the function of GRASP proteins, though they are now recognized as multi-functional proteins that play important roles formation of the Golgi ribbon, trafficking of cargoes, and regulation of the structure of the Golgi apparatus. One reason for controversy is that GRASP knockdowns have given conflicting results as to whether the Golgi remains stacked but fragmented or if it consists of unstacked cisternae. There is also potential for one of the phenotypes to be a primary one, while the other is a secondary side effect of prolonged Golgi perturbation. Our use of acute inactivation allowed for assaying the integrity of the Golgi immediately post loss of GRASP activity. The immediate effects on ribbon integrity suggest that GRASPs play a primary role in ribbon formation and that fragmentation is not a side effect of prolonged knockdown. Further, we have shown that GRASP65 maintains the early cis-Golgi compartment and GRASP55 maintains the later medial and trans compartments. This was not entirely unexpected as the proteins show differential localization across the Golgi stack ([Shorter et al., 1999](#)), though this differs remarkably from the complete fragmentation across all layers of the stack seen in chronic knockdowns ([Feinstein and Linstedt, 2008](#); [Puthenveedu et al., 2006](#); [Xiang and Wang, 2010](#)).

The rapid response to GRASP inactivation suggests that the connections between adjacent Golgi stacks have a high turnover rate. One reason for this may be from the activity of CtBP1/BARS, a known driver of Golgi membrane fission ([Bonazzi et al., 2005](#); [Weigert et al., 1999](#)). The requirement for two distinct GRASP tethers may stem from how often these connections are broken and need to be reformed.

Our identification that this separation of duties is necessary for maintaining sub-compartmentalization of the Golgi was surprising in several ways. Disruption of the Golgi ribbon has been shown to

negatively affect glycosylation efficiency (Feinstein and Linstedt, 2008; Puthenveedu et al., 2006; Xiang and Wang, 2010), but this is thought to be from unequal cargo and enzyme loading of the clustered stacks as Nocodazole induced fragmentation of the Golgi ribbon does not show any adverse effects on processing efficiency of secretory cargo. The ability of the chimeric GM130-45 construct to affect glycosylation in the presence of a contiguous ribbon must therefore be due to another mechanism.

It is possible that the GRASPs play a key role in establishing compartmental identity. Within an intra connected secretory pathway, tethers have been shown to be important in identifying membranes prior to fusions. It is known that both GRASP65 and GRASP55 are recruited to membranes by a joint effort of N-terminal myristoylation and binding to a cognate golgin (Bachert and Linstedt, 2010). GM130 and golgin45 each bind a different Rab partner, Rab1 for GM130 (Moyer et al., 2001) and Rab2 for golgin45 (Short et al., 2001). It is therefore possible that Rab cascades play a key role in establishing sub-compartmental identity within the Golgi apparatus. Establishing the sub-compartmental recruitment mechanism of GRASPs and their effectors will be crucial in determining how they help maintain sub-compartmentalization of the Golgi.

The use of KillerRed to rapidly inhibit the machinery of the endomembrane system will be a valuable resource in resolving ambiguous results left by chronic inhibition experiments. These findings demonstrate the utility of KillerRed as well as a framework for establishing proper controls for KillerRed inactivation. Further use of acute inactivation, especially when coupled with super-resolution imaging, will be essential for expanding our knowledge of the secretory pathway.

Appendix on the use of KillerRed for acute inactivation

Abstract

The lengthy waits between of gene knockdown or knockout experiments is source of ambiguity when studying cellular processes. Especially when considering dynamic systems, the tendency for acquired chronic effects or cellular adaptations to mask acute, direct effects is considerable. KillerRed is a genetically targetable photosensitizer, allowing for the easy tagging of target proteins. Protein inactivation mediated by KillerRed is a challenging but useful tool for understanding the role of proteins function in dynamic systems. Reactive oxygen species (ROS) are created when Killer Red is exposed to green light(Bulina et al., 2005). The high reactivity of the ROS causes them to react with the sidechains and peptide backbone of proteins, ultimately making the protein non-functional. In addition at high levels, ROS accumulation triggers many different pathways that could lead to cell death. Acute inactivation by Killer Red is a balancing act of getting adequate expression and inactivation of your protein without causing off target effects and cell death. In this appendix, I will discuss how to use Killer Red as a precision tool focusing on protein inactivation.

Equipment and reagent requirements:

- Metal imaging chamber – This will be used to contain the cover slip and media. Glass-bottomed dishes (MatTek) can also be used, but metal imaging chambers may provide for better thermal stability and less focal drift in some setups.

- Microscope – For KillerRed inactivation, a high powered mercury, xenon, or LED lamp with an excitation filter encompassing 535-580nm is best suited for irradiation of all cells present in the field of view. A high-magnification (60x or 100x) objective is preferred to provide the highest light intensity for irradiation. Irradiation can also be performed with a 561nm laser line through a galvo scanning beam to irradiate only specific cells or portions of cells.
- Our experiments used an Andor-Revolution iQ2 spinning disc confocal system equipped with an iXon3 EMCCD camera and 100x 1.49NA oil-immersion objective. A 50mW 561nm laser was used to illuminate and irradiate KillerRed.

Experimental Setup: Generation of constructs and optimization of KillerRed inactivation

1. **Generation of KillerRed construct:** Clone KillerRed into a vector with target protein of interest. Ideally KillerRed should be placed as close to the functional domain of the protein being targeted as possible, without interfering with the domain and usually joined by a flexible linker so as not to disrupt proper folding. KillerRed has a tendency to form dimers ([Bulina et al., 2005](#)) which may perturb localization and activity of your protein of interest. Proper localization of fusion protein should be ensured by comparing to endogenous proteins. Expression of an siRNA insensitive form of the fusion protein in an siRNA knockdown background can be used to verify that the fusion protein is functional. If aggregation of tagged proteins occurs, the generation of a KillerRed tag with two tandem copies can create a 'pseudo-monomer' that can self-interact and help restore proper protein localization and activity.
2. **Trans inactivation vs rescue:** The nature of ROS production suggests that all proteins closely bound to the photosensitizer tagged protein can be inactivated upon irradiation. This can be a boon for experiments as the KillerRed tagged protein can

be expressed in cells and inactivate endogenous protein. This is most effective when the target protein functions as a homotypic dimer, or is a limiting member of a protein complex. If this is not the case, the fusion protein should be expressed in an siRNA knockdown background, with proper silent mutations made to make the construct siRNA insensitive.

- 3. Controls for the off target effects of ROS:** While remaining relatively short lived, non-specific generation of reactive oxygen can effect surrounding proteins if generated in high enough levels. Ideally, a KillerRed control construct should be generated to control for the production of reactive oxygen in the target cellular environment. For instance, use a soluble untagged KillerRed to control for off target effects of a primarily cytosolic protein. Specific organelle tags can be used, such as localizing KillerRed to the Golgi by the c-terminus of Giantin ([Jarvela and Linstedt, 2012b](#)), to control for organelle specific effects.
- 4. Environmental conditions:** As previously stated, the use of CALI is at a balance between ineffective inactivation and off target effects. With a control KillerRed construct generated for a protein of interest, optimal conditions for inactivation can be determined. A good starting point is as follows:

Imaging Media

Minimal Essential Media

7% Fetal Bovine Serum

375 μ M Trolox

95% Air, 5% CO₂

Note: The use of 95% Air and 5% is useful to prevent hypoxic conditions in the experimental media which can reduce the phototoxicity of KillerRed.

- 5. Irradiation conditions:** Depending on the type of microscope used, irradiation can be performed with in widefield a mercury arc lamp or similar LED. Other setups include a focusing scan head in which the laser line will be used to irradiate the sample.

When using wide field light, an intensity of 535–580 nm light of $2\text{W}/\text{cm}^2$ for 30 sec was found to be suitable to bleach KillerRed fluorescence under the above conditions when performed through a 100x objective. For a scanning laser unit, irradiating each point with laser power at 15.6mW for 45µsec six times provides good bleaching without visible cellular damage. This should serve as a good place to start. Irradiation time and/or power may need to be changed depending on your specific settings and the power of your microscope

Widefield irradiation can allow for quicker inactivation times. Laser scanning irradiation can be targeted to a specific ROI, a cell or just part of a cell, for inactivation. Restricting irradiation to a subcellular region allows for spatial control of protein function, though if the target protein is freely diffusible, the irradiated region may quickly recover due to recovery from outside the bleached zone.

- 6. Determining proper inactivation conditions:** The bleaching of KillerRed is a good way of determining the efficacy of inactivation. To that end, control KillerRed constructs should be expressed in the assay chosen to be measured. For example, if one is investigating the Golgi ribbon integrity by observing fluorescence of a Golgi protein, the control KillerRed constructs would be expressed in that experimental background. This experimental setup should involve recording cellular activity prior to irradiation to establish a baseline measurement of activity. Proper conditions should result in bleaching of KillerRed fluorescence without causing deviation from your baseline measurements.

Problems	Potential solutions
Irradiation does not bleach KillerRed fluorescence	<p>(i) Increase power of light for irradiation</p> <p>(ii) Decrease antioxidants</p> <p>(iii) Increase irradiation time</p> <p>(iv) Increase oxygen content of media</p>
Inactivation of control construct causes cellular phenotypes	<p>(i) Increase antioxidant concentration</p> <p>(ii) Decrease light intensity</p>
KillerRed fluorescence quickly returns after bleaching	<p>(i) KillerRed production maybe be high due to recent transfection, wait longer after transfection before beginning experiment</p> <p>(ii) Treat cells with cyclohexamide for >4hrs prior to start of experiment to prevent further production of protein.</p>
Irradiation of control construct kills the cell	<p>(i) Expression of KillerRed construct is too high, decrease levels by allowing for more time to pass since the start of transfection or use a plasmid with a lower promoter</p> <p>(ii) If expression level is not too high, try decreasing illumination intensity and increasing illumination time to compensate</p>

7. **Assaying for inactivity:** When testing KillerRed inactivation on proteins that have known knockdown phenotypes, it is unexpected that a good experimental setup can replicate the chronic knockdown effect in the acute inactivation experiment. This can help assuage concerns of specificity and efficacy. These chronic knockdown effects can be replicated using certain treatments that force a process to rebuild from scratch. For example, the inactivation of Golgi assembly proteins can be verified using a Golgi assembly assay in which the Golgi reforms de novo after collapse into the ER, through the use of brefeldin A (as performed in [Jarvela and Linstedt \(2012b\)](#))

Experimental protocol:

1. Pass tissue culture cells into 60mm culture dish one to about 30-50% confluency one day prior to transfections.
2. Transiently transfect cells in 60mm dishes with the control or experimental KillerRed constructs according to transfection reagent protocols. If needed, co-transfect with markers for activity that will be assayed.
3. After 24-48 hours, pass cells into 35mm dishes containing 25mm glass cover slips.
**Note: this step allows for the initial burst of protein production to die down, thereby limiting the amount of KillerRed tagged protein still in production and the process of folding.*
4. Approximately 24 hrs later, move glass cover slip into metal imaging chamber and add imaging media to chamber.
5. Transfer imaging chamber to a confocal microscope with a heated stage setup for 37°C and 5% CO₂ .
6. Visualize KillerRed fluorescence with 561nm laser line and 600-650 nm emission filter under minimal intensity so as to prevent premature CALI.

7. Select cells for CALI based on proper localization and expression level of fusion protein.

**Note: it is important to keep the exposure of cells to green light wavelengths at a minimum prior to desired inactivation timepoint. This will prevent premature inactivation of constructs.*

8. Begin acquiring images of fluorescent protein that serves as the marker for the cellular event you are observing. Stacks of Z-slices may be required to fully observe the cellular process. Acquiring Z-stacks every 10 seconds is a good starting point, but you may wish to acquire more or less often depending on the specifics of your experiment. This establishes the baseline of cellular activity.

9. Acquire pre-bleach image of KillerRed fluorescence. Irradiate cells to induce CALI, under conditions previously optimized. Acquire post-bleach image of KillerRed fluorescence.

**This step can be helpful when troubleshooting experiments in the future.*

10. Return to acquiring periodic Z-stacks of marker proteins to observe changes in cellular dynamics.

Bibliography

Usha Acharya, Richard Jacobs, Jan-Michael Peters, Nicki Watson, Marilyn G Farquhar, and Vivek Malhotra. The formation of golgi stacks from vesiculated golgi membranes requires two distinct fusion events. *Cell*, 82(6):895–904, 1995. [2.2](#)

Usha Acharya, Arrate Mallabiabarrena, Jairaj K Acharya, and Vivek Malhotra. Signaling via mitogen-activated protein kinase kinase (mek1) is required for golgi fragmentation during mitosis. *Cell*, 92(2):183–192, 1998. [2.2](#)

Bernard B Allan and William E Balch. Protein sorting by directed maturation of golgi compartments. *Science*, 285(5424):63–66, 1999. URL <http://www.sciencemag.org/content/285/5424/63.short>. [3.1](#)

Nihal Altan-Bonnet, Rachid Sougrat, and Jennifer Lippincott-Schwartz. Molecular basis for golgi maintenance and biogenesis. *Curr. Opin. Cell Biol.*, 16(4):364–372, 2004. URL <http://www.sciencedirect.com/science/article/pii/S0955067404000808>. [3.3](#)

Christian Appenzeller-Herzog and Hans-Peter Hauri. The er-golgi intermediate compartment (ergic): in search of its identity and function. *J. Cell Sci.*, 119(11):2173–2183, 2006. URL <http://jcs.biologists.org/content/119/11/2173.short>. [2.1](#)

Meir Aridor and William E Balch. Kinase signaling initiates coat complex ii (copii) recruitment and export from the mammalian endoplasmic reticulum. *J. Biol. Chem.*, 275(46):35673–35676, 2000. URL <http://www.jbc.org/content/275/46/35673.short>. 3.2

Collin Bachert and Adam D Linstedt. Dual anchoring of the grasp membrane tether promotes trans pairing. *J. Biol. Chem.*, 285(21):16294–16301, 2010. URL <http://www.jbc.org/content/285/21/16294.short>. 2.2, 2.3, 3.4, 4.1, 4.3, 5

Francis A Barr, Nobuhiro Nakamura, and Graham Warren. Mapping the interaction between grasp65 and gm130, components of a protein complex involved in the stacking of golgi cisternae. *The EMBO journal*, 17(12):3258–3268, 1998. URL <http://www.nature.com/emboj/journal/v17/n12/abs/7591031a.html>. 2.2, 2.2, 2.3, 2.4, 4.1

Francis A Barr, Christian Preisinger, Robert Kopajtich, and Roman Körner. Golgi matrix proteins interact with p24 cargo receptors and aid their efficient retention in the golgi apparatus. *J cell biol*, 155(6):885–892, 2001. URL <http://jcb.rupress.org/content/155/6/885.abstract>. 2.5

Francis A Barr, Herman HW Silljé, and Erich A Nigg. Polo-like kinases and the orchestration of cell division. *Nat. Rev. Mol. Cell Biol.*, 5(6):429–441, 2004. URL <http://www.nature.com/nrm/journal/v5/n6/abs/nrm1401.html>. 2.2

Rudy Behnia, Francis A Barr, John J Flanagan, Charles Barlowe, and Sean Munro. The yeast orthologue of grasp65 forms a complex with a coiled-coil protein that contributes to er to golgi traffic. *J cell biol*, 176(3):255–261, 2007. URL <http://jcb.rupress.org/content/176/3/255.short>. 2.2, 2.5, 4.3

John E Bergmann, Abraham Kupfer, and SJ Singer. Membrane insertion at the leading edge of motile fibroblasts. *Proceedings of the National Academy of Sciences*, 80(5):1367–1371, 1983. URL <http://www.pnas.org/content/80/5/1367.short>. 1, 2.1

-
- Roger H Bisby, Christopher G Morgan, Ian Hamblett, and Anthony A Gorman. Quenching of singlet oxygen by trolox c, ascorbate, and amino acids: effects of ph and temperature. *The Journal of Physical Chemistry A*, 103(37):7454–7459, 1999. URL <http://pubs.acs.org/doi/abs/10.1021/jp990838c>. 3.2
- Blaine Bisel, Yanzhuang Wang, Jen-Hsuan Wei, Yi Xiang, Danming Tang, Miguel Miron-Mendoza, Shin-ichiro Yoshimura, Nobuhiro Nakamura, and Joachim Seemann. Erk regulates golgi and centrosome orientation towards the leading edge through grasp65. *J cell biol*, 182(5):837–843, 2008a. URL <http://jcb.rupress.org/content/182/5/837.short>. 4.3
- Blaine Bisel, Yanzhuang Wang, Jen-Hsuan Wei, Yi Xiang, Danming Tang, Miguel Miron-Mendoza, Shin-ichiro Yoshimura, Nobuhiro Nakamura, and Joachim Seemann. Erk regulates golgi and centrosome orientation towards the leading edge through grasp65. *J cell biol*, 182(5):837–843, 2008b. URL <http://jcb.rupress.org/content/182/5/837.short>. 2.1, 2.4, 2.4
- Matteo Bonazzi, Stefania Spanò, Gabriele Turacchio, Claudia Cericola, Carmen Valente, Antonino Colanzi, Hee Seok Kweon, Victor W Hsu, Elena V Polishchuck, Roman S Polishchuck, et al. Ctbp3/bars drives membrane fission in dynamin-independent transport pathways. *Nat. Cell Biol.*, 7(6):570–580, 2005. URL <http://www.nature.com/ncb/journal/v7/n6/abs/ncb1260.html>. 2.3, 5
- Lidia Bonfanti, Alexander A Mironov Jr, Jose A Martinez-Menarguez, Oliviano Martella, Aurora Fusella, Massimiliano Baldassarre, Roberto Buccione, Hans J Geuze, and Alberto Luini. Procollagen traverses the golgi stack without leaving the lumen of cisternae: evidence for cisternal maturation. *Cell*, 95(7):993–1003, 1998. 1, 3.1
- Juan S Bonifacino and Benjamin S Glick. The mechanisms of vesicle budding and fusion. *Cell*, 116(2):153–166, 2004. 2.1

Annika Budnik and David J Stephens. Er exit sites–localization and control of copii vesicle formation. *FEBS Lett.*, 583(23):3796–3803, 2009. [3.3](#)

Maria E Bulina, Dmitriy M Chudakov, Olga V Britanova, Yurii G Yanushevich, Dmitry B Staroverov, Tatyana V Chepurnykh, Ekaterina M Merzlyak, Maria A Shkrob, Sergey Lukyanov, and Konstantin A Lukyanov. A genetically encoded photosensitizer. *Nat. Biotechnol.*, 24(1):95–99, 2005. URL <http://www.nature.com/nbt/journal/vaop/ncurrent/full/nbt1175.html>. [1](#), [3.1](#), [3.2](#), [4.2](#), [6](#), [1](#)

Matthew Cabral, Christophe Anjard, Vivek Malhotra, William F Loomis, and Adam Kuspa. Unconventional secretion of acba in dictyostelium discoideum through a vesicular intermediate. *Eukaryot. Cell*, 9(7):1009–1017, 2010. URL <http://ec.asm.org/content/9/7/1009.short>. [2.1](#), [2.6](#)

Cristina Hidalgo Carcedo, Matteo Bonazzi, Stefania Spanò, Gabriele Turacchio, Antonino Colanzi, Alberto Luini, and Daniela Corda. Mitotic golgi partitioning is driven by the membrane-fissioning protein ctbp3/bars. *Science*, 305(5680):93–96, 2004. URL <http://www.sciencemag.org/content/305/5680/93.short>. [4.3](#)

Philippe Carpentier, Sebastien Violot, Laurent Blanchoin, and Dominique Bourgeois. Structural basis for the phototoxicity of the fluorescent protein killerred. *FEBS Lett.*, 583(17):2839–2842, 2009. [3.1](#)

JPX Cheng, VMS Betin, H Weir, GMA Shelmani, DK Moss, and JD Lane. Caspase cleavage of the golgi stacking factor grasp65 is required for fas/cd95-mediated apoptosis. *Cell death & disease*, 1(10):e82, 2010. URL <http://www.nature.com/cddis/journal/v1/n10/abs/cddis201059a.html>. [2.2](#)

Antonino Colanzi and Daniela Corda. Mitosis controls the golgi and the golgi controls mitosis. *Curr. Opin. Cell Biol.*, 19(4):386–393, 2007. URL <http://www.sciencedirect.com/science/article/pii/S0955067407000956>. [1](#), [4.3](#)

Antonino Colanzi, Cristina Hidalgo Carcedo, Angela Persico, Claudia Cericola, Gabriele Turacchio, Matteo Bonazzi, Alberto Luini, and Daniela Corda. The golgi mitotic checkpoint is controlled by bars-dependent fission of the golgi ribbon into separate stacks in g2. *The EMBO journal*, 26(10):2465–2476, 2007. URL <http://www.nature.com/emboj/journal/v26/n10/abs/7601686a.html>. 2.1

Nelson B Cole, N Sciaky, Alex Marotta, Jia Song, and J Lippincott-Schwartz. Golgi dispersal during microtubule disruption: regeneration of golgi stacks at peripheral endoplasmic reticulum exit sites. *Mol. Biol. Cell*, 7(4):631, 1996. URL <http://www.ncbi.nlm.nih.gov/pmc/articles/PMC275914/>. 1, 4.3, 5

Nelson B Cole, Jan Ellenberg, Jia Song, Diane DiEuliis, and Jennifer Lippincott-Schwartz. Retrograde transport of golgi-localized proteins to the er. *J cell biol*, 140(1):1–15, 1998. URL <http://jcb.rupress.org/content/140/1/1.abstract>. 3.1, 3.3

Pamela L Connerly, Masatoshi Esaki, Elisabeth A Montegna, Daniel E Strongin, Stephanie Levi, Jon Soderholm, and Benjamin S Glick. Sec16 is a determinant of transitional er organization. *Curr. Biol.*, 15(16):1439–1447, 2005. 2.3

DN Cooper and Samuel H Barondes. Evidence for export of a muscle lectin from cytosol to extracellular matrix and for a novel secretory mechanism. *J cell biol*, 110(5):1681–1691, 1990. URL <http://jcb.rupress.org/content/110/5/1681.abstract>. 2.1

Giovanni D’Angelo, Libera Prencipe, Luisa Iodice, Galina Beznoussenko, Marco Savarese, PierFrancesco Marra, Giuseppe Di Tullio, Gianluca Martire, Maria Antonietta De Matteis, and Stefano Bonatti. Grasp65 and grasp55 sequentially promote the transport of c-terminal valine-bearing cargos to and through the golgi complex. *J. Biol. Chem.*, 284(50):34849–34860, 2009. URL <http://www.jbc.org/content/284/50/34849.short>. 2.5, 2.6

Froylan Calderon DeAnda, Giulia Pollarolo, Jorge Santos Da Silva, Paola G Camoletto, Fabian Feiguin, and Carlos G Dotti. Centrosome localization determines neuronal polarity. *Nature*, 436(7051):704–708, 2005. URL <http://www.nature.com/nature/journal/vaop/ncurrent/full/nature03811.html>. 2.1

Olivier Destaing, Emmanuelle Planus, Daniel Bouvard, Christiane Oddou, Cedric Badowski, Valentine Bossy, Aurelia Raducanu, Bertrand Fourcade, Corinne Albiges-Rizo, and Marc R Block. β 1a integrin is a master regulator of invadosome organization and function. *Mol. Biol. Cell*, 21(23):4108–4119, 2010. URL <http://www.molbiolcell.org/content/21/23/4108.short>. 3.1

Michel Dominguez, Kurt Dejgaard, Joachim Füllekrug, Sophie Dahan, Ali Fazel, Jean-Pierre Paccard, David Y Thomas, John JM Bergeron, and Tommy Nilsson. gp251/emp24/p24 protein family members of the cis-golgi network bind both cop i and ii coatomer. *J cell biol*, 140(4):751–765, 1998. URL <http://jcb.rupress.org/content/140/4/751.abstract>. 2.5

William G Dunphy and James E Rothman. Compartmental organization of the golgi stack. *Cell*, 42(1):13–21, 1985. 4.3

Nicolas Dupont, Shanya Jiang, Manohar Pilli, Wojciech Ornatowski, Dhruva Bhattacharya, and Vojo Deretic. Autophagy-based unconventional secretory pathway for extracellular delivery of il-1 β . *The EMBO journal*, 30(23):4701–4711, 2011. URL <http://www.nature.com/emboj/journal/vaop/ncurrent/full/emboj2011398a.html>. 2.1, 2.6, 2.6

Juan M Duran, Christophe Anjard, Chris Stefan, William F Loomis, and Vivek Malhotra. Unconventional secretion of acb1 is mediated by autophagosomes. *J cell biol*, 188(4):527–536, 2010. URL <http://jcb.rupress.org/content/188/4/527.short>. 2.1, 2.6

Kaitlyn M Dykstra, Jacqueline E Pokusa, Joseph Suhan, and Tina H Lee. Yip1a structures

-
- the mammalian endoplasmic reticulum. *Mol. Biol. Cell*, 21(9):1556–1568, 2010. URL <http://www.molbiolcell.org/content/21/9/1556.short>. 3.4
- Andrew EH Elia, Lewis C Cantley, and Michael B Yaffe. Proteomic screen finds pser/pthr-binding domain localizing plk1 to mitotic substrates. *Science*, 299(5610):1228–1231, 2003. URL <http://www.sciencemag.org/content/299/5610/1228.short>. 2.2
- Scott Emr, Benjamin S Glick, Adam D Linstedt, Jennifer Lippincott-Schwartz, Alberto Luini, Vivek Malhotra, Brad J Marsh, Akihiko Nakano, Suzanne R Pfeffer, Catherine Rabouille, et al. Journeys through the golgi: taking stock in a new era. *J cell biol*, 187(4):449–453, 2009. URL <http://jcb.rupress.org/content/187/4/449.short>. 3.1, 3.3
- Gerard I Evan, George K Lewis, Gary Ramsay, and J Michael Bishop. Isolation of monoclonal antibodies specific for human c-myc proto-oncogene product. *Mol. Cell. Biol.*, 5(12):3610–3616, 1985. URL <http://mcb.asm.org/content/5/12/3610.short>. 3.4
- Timothy N Feinstein and Adam D Linstedt. Mitogen-activated protein kinase kinase 1-dependent golgi unlinking occurs in g2 phase and promotes the g2/m cell cycle transition. *Mol. Biol. Cell*, 18(2):594–604, 2007. URL <http://www.molbiolcell.org/content/18/2/594.short>. 2.2, 2.4, 4.3
- Timothy N Feinstein and Adam D Linstedt. Grasp55 regulates golgi ribbon formation. *Mol. Biol. Cell*, 19(7):2696–2707, 2008. URL <http://www.molbiolcell.org/content/19/7/2696.short>. 1, 2.1, 2.2, 2.3, 2.4, 4.2, 4.2, 4.2, 4.2, 4.3, 5, 5
- Heon Yung Gee, Shin Hye Noh, Bor Luen Tang, Kyung Hwan Kim, and Min Goo Lee. Rescue of delta-f508-cftr trafficking via a grasp-dependent unconventional secretion pathway. *Cell*, 146(5):746–760, 2011. 2.2, 2.6
- Fabrizio Giuliani, Adam Grieve, and Catherine Rabouille. Unconventional secretion: a stress on grasp. *Curr. Opin. Cell Biol.*, 23(4):498–504, 2011. URL <http://www.sciencedirect.com/science/article/pii/S0955067411000536>. 2.1, 2.6, 2.6

Benjamin S Glick and Akihiko Nakano. Membrane traffic within the golgi apparatus. *Annu. Rev. Cell Dev. Biol.*, 25:113, 2009. [2.3](#), [3.1](#)

Benjamin S Glick, Timothy Elston, and George Oster. A cisternal maturation mechanism can explain the asymmetry of the golgi stack. *FEBS Lett.*, 414(2):177–181, 1997. [3.1](#)

Jennifer Greaves and Luke H Chamberlain. Palmitoylation-dependent protein sorting. *J cell biol*, 176(3):249–254, 2007. URL <http://jcb.rupress.org/content/176/3/249.short>. [2.2](#)

Yusong Guo and Adam D Linstedt. Copii–golgi protein interactions regulate copii coat assembly and golgi size. *J cell biol*, 174(1):53–63, 2006. URL <http://jcb.rupress.org/content/174/1/53.short>. [2.5](#)

John A Hamilton. Colony-stimulating factors in inflammation and autoimmunity. *Nat. Rev. Immunol.*, 8(7):533–544, 2008. URL <http://www.nature.com/nri/journal/vaop/ncurrent/full/nri2356.html>. [2.4](#)

Georges Herbein, Audrey Varin, et al. The macrophage in hiv-1 infection: from activation to deactivation. *Retrovirology*, 7(33):1–15, 2010. [2.4](#)

Dagmar Heuer, Anette Rejman Lipinski, Nikolaus Machuy, Alexander Karlas, Andrea Wehrens, Frank Siedler, Volker Brinkmann, and Thomas F Meyer. Chlamydia causes fragmentation of the golgi compartment to ensure reproduction. *Nature*, 457(7230):731–735, 2008. URL <http://www.nature.com/nature/journal/vaop/ncurrent/full/nature07578.html>. [4.3](#)

Brian J Hillier, Karen S Christopherson, Kenneth E Prehoda, David S Bredt, and Wendell A Lim. Unexpected modes of pdz domain scaffolding revealed by structure of nnos-syntrophin complex. *Science*, 284(5415):812–815, 1999. URL <http://www.sciencemag.org/content/284/5415/812.short>. [2.2](#)

-
- Masateru Hiyoshi, Shinya Suzu, Yuka Yoshidomi, Ranya Hassan, Hideki Harada, Naomi Sakashita, Hirofumi Akari, Kazuo Motoyoshi, and Seiji Okada. Interaction between hck and hiv-1 nef negatively regulates cell surface expression of m-csf receptor. *Blood*, 111(1):243–250, 2008. URL <http://bloodjournal.hematologylibrary.org/content/111/1/243.short>. 2.4
- Masateru Hiyoshi, Naoko Takahashi-Makise, Yuka Yoshidomi, Nopporn Chutiwitoonchai, Takashi Chihara, Masato Okada, Nobuhiro Nakamura, Seiji Okada, and Shinya Suzu. Hiv-1 nef perturbs the function, structure, and signaling of the golgi through the src kinase hck. *J. Cell. Physiol.*, 227(3):1090–1097, 2012. URL <http://onlinelibrary.wiley.com/doi/10.1002/jcp.22825/full>. 2.4
- Tonghuan Hu, Chia-Yi Kao, Robert Tod Hudson, Alice Chen, and Rockford K Draper. Inhibition of secretion by 1, 3-cyclohexanebis (methylamine), a dibasic compound that interferes with coatomer function. *Mol. Biol. Cell*, 10(4):921–933, 1999. URL <http://www.molbiolcell.org/content/10/4/921.short>. 3.2
- R Colin Hughes. Secretion of the galectin family of mammalian carbohydrate-binding proteins. *Biochimica et Biophysica Acta (BBA)-General Subjects*, 1473(1):172–185, 1999. URL <http://www.sciencedirect.com/science/article/pii/S0304416599001774>. 2.1
- Catherine L Jackson. Mechanisms of transport through the golgi complex. *J. Cell Sci.*, 122(4):443–452, 2009. URL <http://jcs.biologists.org/content/122/4/443.short>. 4.3
- Timothy Jarvela and AD Linstedt. Golgi grasps: moonlighting membrane tethers. *Cell Health and Cytoskeleton*, 4:37–47, 2012a. 1, 4.3
- Timothy Jarvela and Adam D Linstedt. Irradiation-induced protein inactivation reveals golgi enzyme cycling to cell periphery. *J. Cell Sci.*, 125(4):973–980, 2012b. URL <http://jcs.biologists.org/content/125/4/973.short>. 1, 4.2, 4.2, 4.2, 3, 7

Daniel G Jay. Selective destruction of protein function by chromophore-assisted laser inactivation. *Proceedings of the National Academy of Sciences*, 85(15):5454–5458, 1988. URL <http://www.pnas.org/content/85/15/5454.short>. 1, 3.1, 4.2

Daniel G Jay and Takashi Sakurai. Chromophore-assisted laser inactivation (cali) to elucidate cellular mechanisms of cancer. *Biochimica et Biophysica Acta (BBA)-Reviews on Cancer*, 1424(2):M39–M48, 1999. URL <http://www.sciencedirect.com/science/article/pii/S0304419X99000220>. 3.1, 3.3

Stephen A Jesch and Adam D Linstedt. The golgi and endoplasmic reticulum remain independent during mitosis in hela cells. *Mol. Biol. Cell*, 9(3):623–635, 1998. URL <http://www.molbiolcell.org/content/9/3/623.short>. 2.1, 4.3

Stephen A Jesch, Timothy S Lewis, Natalie G Ahn, and Adam D Linstedt. Mitotic phosphorylation of golgi reassembly stacking protein 55 by mitogen-activated protein kinase erk2. *Mol. Biol. Cell*, 12(6):1811–1817, 2001. URL <http://www.molbiolcell.org/content/12/6/1811.short>. 2.2, 2.4

Fumi Kano, Katsuya Takenaka, Akitsugu Yamamoto, Kuniaki Nagayama, Eisuke Nishida, and Masayuki Murata. Mek and cdc2 kinase are sequentially required for golgi disassembly in mdck cells by the mitotic xenopus extracts. *J cell biol*, 149(2):357–368, 2000. URL <http://jcb.rupress.org/content/149/2/357.abstract>. 2.2

Martin Keller, Andreas Rüegg, Sabine Werner, and Hans-Dietmar Beer. Active caspase-1 is a regulator of unconventional protein secretion. *Cell*, 132(5):818–831, 2008. 2.1

Matthew A Kinseth, Christophe Anjard, Danny Fuller, Gianni Guizzunti, William F Loomis, and Vivek Malhotra. The golgi-associated protein grasp is required for unconventional protein secretion during development. *Cell*, 130(3):524–534, 2007. 2.1, 2.6, 4.3

-
- Judith Klumperman. Architecture of the mammalian golgi. *Cold Spring Harbor Perspectives in Biology*, 3(7), 2011. URL <http://cshperspectives.cshlp.org/content/3/7/a005181.short>. 4.1
- Vangelis Kondylis, Kirsten M Spoorendonk, and Catherine Rabouille. dgrasp localization and function in the early exocytic pathway in drosophila s2 cells. *Mol. Biol. Cell*, 16(9):4061–4072, 2005. URL <http://www.molbiolcell.org/content/16/9/4061.short>. 2.3, 4.3
- Rosalind Kornfeld and Stuart Kornfeld. Assembly of asparagine-linked oligosaccharides. *Annu. Rev. Biochem.*, 54(1):631–664, 1985. URL <http://www.annualreviews.org/doi/pdf/10.1146/annurev.bi.54.070185.003215>. 4.2
- Thomas E Kreis. Role of microtubules in the organisation of the golgi apparatus. *Cell Motil. Cytoskeleton*, 15(2):67–70, 1990. URL <http://onlinelibrary.wiley.com/doi/10.1002/cm.970150202/abstract>. 4.3
- Alfred Kuo, Cuiling Zhong, William S Lane, and Rik Derynck. Transmembrane transforming growth factor- α tethers to the pdz domain-containing, golgi membrane-associated protein p59/grasp55. *The EMBO journal*, 19(23):6427–6439, 2000. URL <http://www.nature.com/emboj/journal/v19/n23/abs/7593456a.html>. 2.2, 2.4, 2.5
- Abraham Kupfer, Daniel Louvard, and SJ Singer. Polarization of the golgi apparatus and the microtubule-organizing center in cultured fibroblasts at the edge of an experimental wound. *Proceedings of the National Academy of Sciences*, 79(8):2603–2607, 1982. URL <http://www.pnas.org/content/79/8/2603.short>. 2.1
- Abraham Kupfer, Gunther Dennert, and SJ Singer. Polarization of the golgi apparatus and the microtubule-organizing center within cloned natural killer cells bound to their targets. *Proceedings of the National Academy of Sciences*, 80(23):7224–7228, 1983. URL <http://www.pnas.org/content/80/23/7224.short>. 2.1

- Mark S Ladinsky, David N Mastrorarde, J Richard McIntosh, Kathryn E Howell, and L Andrew Staehelin. Golgi structure in three dimensions: functional insights from the normal rat kidney cell. *J cell biol*, 144(6):1135–1149, 1999. URL <http://jcb.rupress.org/content/144/6/1135.abstract>. 4.1
- Jon D Lane, John Lucocq, James Pryde, Francis A Barr, Philip G Woodman, Victoria J Allan, and Martin Lowe. Caspase-mediated cleavage of the stacking protein grasp65 is required for golgi fragmentation during apoptosis. *J cell biol*, 156(3):495–509, 2002. URL <http://jcb.rupress.org/content/156/3/495.short>. 2.1, 2.2, 4.3
- Joel Lanoix, Joke Ouwendijk, Annika Stark, Edith Szafer, Dan Cassel, Kurt Dejgaard, Matthias Weiss, and Tommy Nilsson. Sorting of golgi resident proteins into different subpopulations of copi vesicles a role for arfgap1. *J cell biol*, 155(7):1199–1212, 2001. URL <http://jcb.rupress.org/content/155/7/1199.abstract>. 3.1
- Tina H Lee and Adam D Linstedt. Potential role for protein kinases in regulation of bidirectional endoplasmic reticulum-to-golgi transport revealed by protein kinase inhibitor h89. *Mol. Biol. Cell*, 11(8):2577–2590, 2000. URL <http://www.molbiolcell.org/content/11/8/2577.short>. 3.2
- François Letourneur, Erin C Gaynor, Silke Hennecke, Corinne Démollière, Rainer Duden, Scott D Emr, Howard Riezman, and Pierre Cosson. Coatomer is essential for retrieval of dilysine-tagged proteins to the endoplasmic reticulum. *Cell*, 79(7):1199–1207, 1994. URL <http://www.sciencedirect.com/science/article/pii/0092867494900116>. 5
- Stephanie K Levi, Dibyendu Bhattacharyya, Rita L Strack, Jotham R Austin, and Benjamin S Glick. The yeast grasp grh1 colocalizes with copii and is dispensable for organizing the secretory pathway. *Traffic*, 11(9):1168–1179, 2010. 2.3, 2.5
- Qi Li, Anthony Lau, Terence J Morris, Lin Guo, Christopher B Fordyce, and Elise F Stanley. A syntaxin 1, gao, and n-type calcium channel complex at a presynaptic nerve terminal:

-
- analysis by quantitative immunocolocalization. *The Journal of neuroscience*, 24(16):4070–4081, 2004. URL <http://www.jneurosci.org/content/24/16/4070.short>. 4.2
- Joseph C Liao, Johann Roider, and Daniel G Jay. Chromophore-assisted laser inactivation of proteins is mediated by the photogeneration of free radicals. *Proceedings of the National Academy of Sciences*, 91(7):2659–2663, 1994. URL <http://www.pnas.org/content/91/7/2659.short>. 1, 3.1, 4.2
- Chung-Chih Lin, Harold D Love, Jennifer N Gushue, John JM Bergeron, and Joachim Ostermann. Er/golgi intermediates acquire golgi enzymes by brefeldin a-sensitive retrograde transport in vitro. *The Journal of cell biology*, 147(7):1457–1472, 1999. URL <http://jcb.rupress.org/content/147/7/1457.abstract>. 3.2
- AD Linstedt, A Mehta, J Suhan, H Reggio, and HP Hauri. Sequence and overexpression of gpp130/gimpc: evidence for saturable ph-sensitive targeting of a type ii early golgi membrane protein. *Mol. Biol. Cell*, 8(6):1073, 1997. URL <http://www.ncbi.nlm.nih.gov/pmc/articles/PMC305715/>. 3.4
- Adam D Linstedt and Hans-Peter Hauri. Giantin, a novel conserved golgi membrane protein containing a cytoplasmic domain of at least 350 kda. *Mol. Biol. Cell*, 4(7):679, 1993. URL <http://www.ncbi.nlm.nih.gov/pmc/articles/PMC300978/>. 3.4
- Jennifer Lippincott-Schwartz, Lydia C Yuan, Juan S Bonifacino, and Richard D Klausner. Rapid redistribution of golgi proteins into the er in cells treated with brefeldin a: evidence for membrane cycling from golgi to er. *Cell*, 56(5):801–813, 1989. URL <http://www.sciencedirect.com/science/article/pii/0092867489906855>. 3.2
- Nadia Litterman, Yoshiho Ikeuchi, Gilbert Gallardo, Brenda C O’Connell, Mathew E Sowa, Steven P Gygi, J Wade Harper, and Azad Bonni. An obsl1-cul7fbxw8 ubiquitin ligase signaling mechanism regulates golgi morphology and dendrite patterning. *PLoS Biol.*, 9(5):e1001060, 2011. 2.4

- Eugene Losev, Catherine A Reinke, Jennifer Jellen, Daniel E Strongin, Brooke J Bevis, and Benjamin S Glick. Golgi maturation visualized in living yeast. *Nature*, 441(7096):1002–1006, 2006. URL <http://www.nature.com/nature/journal/vaop/ncurrent/full/nature04717.html>. 3.1
- Harold D Love, Chung-Chih Lin, Craig S Short, and Joachim Ostermann. Isolation of functional golgi-derived vesicles with a possible role in retrograde transport. *The Journal of cell biology*, 140(3):541–551, 1998. URL <http://jcb.rupress.org/content/140/3/541.abstract>. 3.2
- Martin Lowe. Structural organization of the golgi apparatus. *Curr. Opin. Cell Biol.*, 23(1):85–93, 2011. URL <http://www.sciencedirect.com/science/article/pii/S0955067410001754>. 2.1
- Drew M Lowery, Daniel Lim, and Michael B Yaffe. Structure and function of polo-like kinases. *Oncogene*, 24(2):248–259, 2005. URL <http://www.nature.com/onc/journal/v24/n2/abs/1208280a.html>. 2.2
- Vivek Malhotra, Tito Serafini, Lelio Orci, James C Shepherd, and James E Rothman. Purification of a novel class of coated vesicles mediating biosynthetic protein transport through the golgi stack. *Cell*, 58(2):329–336, 1989. URL <http://www.sciencedirect.com/science/article/pii/0092867489908477>. 3.1
- Jörg Malsam, Ayano Satoh, Laurence Pelletier, and Graham Warren. Golgin tethers define subpopulations of cop1 vesicles. *Science*, 307(5712):1095–1098, 2005. URL <http://www.sciencemag.org/content/307/5712/1095.short>. 3.1
- Ravi Manjithaya, Christophe Anjard, William F Loomis, and Suresh Subramani. Unconventional secretion of pichia pastoris acb1 is dependent on grasp protein, peroxisomal functions, and autophagosome formation. *J cell biol*, 188(4):537–546, 2010. URL <http://jcb.rupress.org/content/188/4/537.short>. 2.1, 2.6

-
- Gonzalo A Mardones, Christopher M Snyder, and Kathryn E Howell. Cis-golgi matrix proteins move directly to endoplasmic reticulum exit sites by association with tubules. *Molecular biology of the cell*, 17(1):525–538, 2006. URL <http://www.molbiolcell.org/content/17/1/525.short>. 3.3
- Pierfrancesco Marra, Tania Maffucci, Tiziana Daniele, Giuseppe Di Tullio, Yukio Ikehara, Edward KL Chan, Alberto Luini, Gala Beznoussenko, Alexander Mironov, and Maria Antonietta De Matteis. The gm130 and grasp65 golgi proteins cycle through and define a subdomain of the intermediate compartment. *Nat. Cell Biol.*, 3(12):1101–1113, 2001. URL <http://www.nature.com/ncb/journal/v3/n12/abs/ncb1201-1101.html>. 3.2, 3.3, 4.3
- Pierfrancesco Marra, Lorena Salvatore, Alexander Mironov, Antonella Di Campi, Giuseppe Di Tullio, Alvar Trucco, Galina Beznoussenko, and Maria Antonietta De Matteis. The biogenesis of the golgi ribbon: the roles of membrane input from the er and of gm130. *Mol. Biol. Cell*, 18(5):1595–1608, 2007. URL <http://www.molbiolcell.org/content/18/5/1595.short>. 4.3
- José A Marti nez Menárguez, Hans J Geuze, Jan W Slot, and Judith Klumperman. Vesicular tubular clusters between the er and golgi mediate concentration of soluble secretory proteins by exclusion from copi-coated vesicles. *Cell*, 98(1):81–90, 1999. 3.1
- Kumi Matsuura-Tokita, Masaki Takeuchi, Akira Ichihara, Kenta Mikuriya, and Akihiko Nakano. Live imaging of yeast golgi cisternal maturation. *Nature*, 441(7096):1007–1010, 2006. URL <http://www.nature.com/nature/journal/vaop/ncurrent/full/nature04737.html>. 3.1
- Bruno Mehul, Sulemana Bawumia, and R Colin Hughes. Cross-linking of galectin 3, a galactose-binding protein of mammalian cells, by tissue-type transglutaminase. *FEBS Lett.*, 360(2):160–164, 1995. 2.1

I Mellman and KS Simons. The golgi complex: in vitro veritas? *Cell*, 68(5):829–840, March 1992. ISSN 00928674. [1](#), [2.1](#), [2.5](#), [3.1](#), [4.3](#)

Suzanne Miles, Heather McManus, Kimberly E Forsten, and Brian Storrie. Evidence that the entire golgi apparatus cycles in interphase hela cells sensitivity of golgi matrix proteins to an er exit block. *J cell biol*, 155(4):543–556, 2001. URL <http://jcb.rupress.org/content/155/4/543.abstract>. [1](#), [3.1](#), [3.3](#), [5](#)

Alexander A Mironov, Galina V Beznoussenko, Alvar Trucco, Pietro Lupetti, Jeffrey D Smith, Willie JC Geerts, Abraham J Koster, Koert NJ Burger, Maryann E Martone, Thomas J Deerinck, et al. Er-to-golgi carriers arise through direct en bloc protrusion and multistage maturation of specialized er exit domains. *Dev. Cell*, 5(4):583–594, 2003. [4.3](#)

Alexander A Mironov, Antonino Colanzi, Roman S Polishchuk, Galina V Beznoussenko, Alexander A Mironov Jr, Aurora Fusella, Giuseppe Di Tullio, Maria Giuseppina Silletta, Daniela Corda, Maria Antonietta De Matteis, et al. Dicumarol, an inhibitor of adp-ribosylation of ctbp3/bars, fragments golgi non-compact tubular zones and inhibits intra-golgi transport. *Eur. J. Cell Biol.*, 83(6):263–279, 2004. URL <http://www.sciencedirect.com/science/article/pii/S0171933504703957>. [4.3](#)

Hilton H Mollenhauer and D James Morr e. Perspectives on golgi apparatus form and function. *Journal of electron microscopy technique*, 17(1):2–14, 1991. URL <http://onlinelibrary.wiley.com/doi/10.1002/jemt.1060170103/abstract>. [3.1](#)

Bryan D Moyer, Bernard B Allan, and William E Balch. Rab1 interaction with a gm130 effector complex regulates copii vesicle cis-golgi tethering. *Traffic*, 2(4):268–276, 2001. [5](#)

Somshuvra Mukhopadhyay, Collin Bachert, Donald R Smith, and Adam D Linstedt. Manganese-induced trafficking and turnover of the cis-golgi glycoprotein gpp130. *Mol. Biol. Cell*, 21(7):1282–1292, 2010. URL <http://www.molbiolcell.org/content/21/7/1282.short>. [3.4](#), [4.2](#)

-
- Walter Nickel. The mystery of nonclassical protein secretion. *European Journal of Biochemistry*, 270(10):2109–2119, 2003. [2.1](#)
- Walter Nickel. Unconventional secretory routes: direct protein export across the plasma membrane of mammalian cells. *Traffic*, 6(8):607–614, 2005. [2.1](#)
- Claire Nourry, Seth GN Grant, and Jean-Paul Borg. PdZ domain proteins: plug and play! *Science Signaling*, 2003(179):re7, 2003. URL <http://stke.sciencemag.org/cgi/content/abstract/2003/179/re7>. [2.2](#)
- Hartmut Oschkinat et al. A new type of pdz domain recognition. *Nat. Struct. Biol.*, 6(5):408–410, 1999. [2.2](#)
- George H Patterson, Koret Hirschberg, Roman S Polishchuk, Daniel Gerlich, Robert D Phair, and Jennifer Lippincott-Schwartz. Transport through the golgi apparatus by rapid partitioning within a two-phase membrane system. *Cell*, 133(6):1055–1067, 2008. [1](#), [3.3](#)
- Matt Yasuo Pecot and Vivek Malhotra. Golgi membranes remain segregated from the endoplasmic reticulum during mitosis in mammalian cells. *Cell*, 116(1):99–107, 2004. [3.1](#), [3.3](#)
- Matthew Y Pecot and Vivek Malhotra. The golgi apparatus maintains its organization independent of the endoplasmic reticulum. *Molecular biology of the cell*, 17(12):5372–5380, 2006. URL <http://www.molbiolcell.org/content/17/12/5372.short>. [3.1](#), [3.3](#)
- Hugh RB Pelham and James E Rothman. The debate about transport in the golgi two sides of the same coin? *Cell*, 102(6):713–719, 2000. [3.1](#)
- Laurence Pelletier, Charlene A Stern, Marc Pypaert, David Sheff, Huân M Ngô, Nitin Roper, Cynthia Y He, Ke Hu, Derek Toomre, Isabelle Coppens, et al. Golgi biogenesis in *Toxoplasma gondii*. *Nature*, 418(6897):548–552, 2002. URL <http://www.nature.com/nature/journal/v418/n6897/abs/nature00946.html>. [2.3](#)

Anne Peyroche, Bruno Antony, Sylviane Robineau, Joel Acker, Jacqueline Cherfils, and Catherine L Jackson. Brefeldin a acts to stabilize an abortive arf-gdp-sec7 domain protein complex: involvement of specific residues of the sec7 domain. *Molecular cell*, 3(3):275–285, 1999. [3.2](#)

Sergei Pletnev, Nadya G Gurskaya, Nadya V Pletneva, Konstantin A Lukyanov, Dmitri M Chudakov, Vladimir I Martynov, Vladimir O Popov, Mikhail V Kovalchuk, Alexander Wlodawer, Zbigniew Dauter, et al. Structural basis for phototoxicity of the genetically encoded photosensitizer killerred. *J. Biol. Chem.*, 284(46):32028–32039, 2009. URL <http://www.jbc.org/content/284/46/32028.short>. [3.1](#)

Christian Preisinger, Roman Körner, Mathias Wind, Wolf D Lehmann, Robert Kopajtich, and Francis A Barr. Plk1 docking to grasp65 phosphorylated by cdk1 suggests a mechanism for golgi checkpoint signalling. *The EMBO journal*, 24(4):753–765, 2005. URL <http://www.nature.com/emboj/journal/v24/n4/abs/7600569a.html>. [2.2](#), [2.4](#), [4.3](#)

John F Presley, Nelson B Cole, Trina A Schroer, Koret Hirschberg, Kristien JM Zaal, and Jennifer Lippincott-Schwartz. Er-to-golgi transport visualized in living cells. *Nature*, 389(6646):81–85, 1997. URL <http://www.nature.com/nature/journal/v389/n6646/full/389081a0.html>. [1](#), [2.1](#), [3.2](#)

Igor Prudovsky, Cinzia Bagala, Francesca Tarantini, Anna Mandinova, Raffaella Soldi, Stephen Bellum, and Thomas Maciag. The intracellular translocation of the components of the fibroblast growth factor 1 release complex precedes their assembly prior to export. *J cell biol*, 158(2):201–208, 2002. URL <http://jcb.rupress.org/content/158/2/201.short>. [2.1](#), [2.2](#)

Sapna Puri and Adam D Linstedt. Capacity of the golgi apparatus for biogenesis from the endoplasmic reticulum. *Mol. Biol. Cell*, 14(12):5011–5018, 2003. URL <http://www.molbiolcell.org/content/14/12/5011.short>. [1](#)

-
- Manojkumar A Puthenveedu and Adam D Linstedt. Evidence that golgi structure depends on a p115 activity that is independent of the vesicle tether components giantin and gm130. *J cell biol*, 155(2):227–238, 2001. URL <http://jcb.rupress.org/content/155/2/227.abstract>. 1, 3.2, 3.2
- Manojkumar A Puthenveedu and Adam D Linstedt. Subcompartmentalizing the golgi apparatus. *Current opinion in cell biology*, 17(4):369–375, 2005. URL <http://www.sciencedirect.com/science/article/pii/S0955067405000785>. 3.1
- Manojkumar A Puthenveedu, Collin Bachert, Sapna Puri, Frederick Lanni, and Adam D Linstedt. Gm130 and grasp65-dependent lateral cisternal fusion allows uniform golgi-enzyme distribution. *Nat. Cell Biol.*, 8(3):238–248, 2006. URL <http://www.nature.com/ncb/journal/v8/n3/abs/ncb1366.html>. 1, 1, 2.1, 2.2, 2.3, 2.4, 4.1, 4.2, 4.2, 4.2, 4.2, 4.2, 4.3, 5, 5
- Yingchuan B Qi, Emma J Garren, Xiaokun Shu, Roger Y Tsien, and Yishi Jin. Photo-inducible cell ablation in caenorhabditis elegans using the genetically encoded singlet oxygen generating protein minisog. *Proceedings of the National Academy of Sciences*, 109(19):7499–7504, 2012. URL <http://www.pnas.org/content/109/19/7499.short>. 5
- Catherine Rabouille and Vangelis Kondylis. Golgi ribbon unlinking: an organelle-based g2/m checkpoint. *Cell Cycle*, 6(22):2723–2729, 2007. URL <http://www.landesbioscience.com/journals/cc/abstract.php?id=4896>. 4.3
- Catherine Rabouille, Norman Hui, Felicia Hunte, Regina Kieckbusch, Eric G Berger, Graham Warren, and Tommy Nilsson. Mapping the distribution of golgi enzymes involved in the construction of complex oligosaccharides. *J. Cell Sci.*, 108(4):1617–1627, 1995. URL <http://jcs.biologists.org/content/108/4/1617.short>. 4.3
- A Rambourg and Y Clermont. Three-dimensional structure of the golgi apparatus in

- mammalian cells. In *The Golgi Apparatus*, pages 37–61. Springer, 1997. URL http://link.springer.com/chapter/10.1007/978-3-0348-8876-9_2. 4.3
- A Rambourg, Y Clermont, L Hermo, and D Segretain. Tridimensional structure of the golgi apparatus of nonciliated epithelial cells of the ductuli efferentes in rat: an electron microscope stereoscopic study. *Biol. Cell*, 60(2):103–115, 1987. URL <http://onlinelibrary.wiley.com/doi/10.1111/j.1768-322X.1987.tb00550.x/abstract>. 4.1
- Sung Wu Rhee, Tregui Starr, Kimberly Forsten-Williams, and Brian Storrie. The steady-state distribution of glycosyltransferases between the golgi apparatus and the endoplasmic reticulum is approximately 90: 10. *Traffic*, 6(11):978–990, 2005. 3.1, 3.3
- Christian Roghi, Louise Jones, Matthew Gratian, William R English, and Gillian Murphy. Golgi reassembly stacking protein 55 interacts with membrane-type (mt) 1-matrix metalloprotease (mmp) and furin and plays a role in the activation of the mt1-mmp zymogen. *FEBS J.*, 277(15):3158–3175, 2010. 2.5
- Steven T Runyon, Yingnan Zhang, Brent A Appleton, Stephen L Sazinsky, Ping Wu, Borlan Pan, Christian Wiesmann, Nicholas J Skelton, and Sachdev S Sidhu. Structural and functional analysis of the pdz domains of human htra1 and htra3. *Protein Sci.*, 16(11):2454–2471, 2007. 2.2
- Daniel Sage, Franck R Neumann, Florence Hediger, Susan M Gasser, and Michael Unser. Automatic tracking of individual fluorescence particles: application to the study of chromosome dynamics. *Image Processing, IEEE Transactions on*, 14(9):1372–1383, 2005. URL http://ieeexplore.ieee.org/xpls/abs_all.jsp?arnumber=1495509. 3.4
- Sachiko Sato, Ian Burdett, and R Colin Hughes. Secretion of the baby hamster kidney 30-kda galactose-binding lectin from polarized and nonpolarized cells: a pathway independent of the endoplasmic reticulum-golgi complex. *Exp. Cell Res.*, 207(1):8–18, 1993. URL <http://www.sciencedirect.com/science/article/pii/S0014482783711572>. 2.1

-
- Hans Schotman, Leena Karhinen, and Catherine Rabouille. dgrasp-mediated noncanonical integrin secretion is required for drosophila epithelial remodeling. *Dev. Cell*, 14(2):171–182, 2008. [2.1](#), [2.6](#)
- A Schweizer, JA Fransen, K Matter, TE Kreis, L Ginsel, and HP Hauri. Identification of an intermediate compartment involved in protein transport from endoplasmic reticulum to golgi apparatus. *European journal of cell biology*, 53(2):185–196, 1990. URL <http://europepmc.org/abstract/MED/1964413>. [3.4](#)
- Debrup Sengupta and Adam D Linstedt. Mitotic inhibition of grasp65 organelle tethering involves polo-like kinase 1 (plk1) phosphorylation proximate to an internal pdz ligand. *J. Biol. Chem.*, 285(51):39994–40003, 2010. URL <http://www.jbc.org/content/285/51/39994.short>. [2.2](#), [2.2](#), [2.4](#), [4.3](#)
- Debrup Sengupta, Steven Truschel, Collin Bachert, and Adam D Linstedt. Organelle tethering by a homotypic pdz interaction underlies formation of the golgi membrane network. *J cell biol*, 186(1):41–55, 2009. URL <http://jcb.rupress.org/content/186/1/41.short>. [2.2](#), [2.3](#), [2.3](#), [4.1](#), [4.3](#)
- Ekaterina O Serebrovskaya, Eveline F Edelweiss, Oleg A Stremovskiy, Konstantin A Lukyanov, Dmitry M Chudakov, and Sergey M Deyev. Targeting cancer cells by using an antireceptor antibody-photosensitizer fusion protein. *Proceedings of the National Academy of Sciences*, 106(23):9221–9225, 2009. URL <http://www.pnas.org/content/106/23/9221.short>. [3.1](#)
- Benjamin Short, Christian Preisinger, Roman Körner, Robert Kopajtich, Olwyn Byron, and Francis A Barr. A grasp55-rab2 effector complex linking golgi structure to membrane traffic. *J cell biol*, 155(6):877–884, 2001. URL <http://jcb.rupress.org/content/155/6/877.short>. [2.2](#), [4.1](#), [5](#)

- James Shorter, Rose Watson, Maria-Eleni Giannakou, Mairi Clarke, Graham Warren, and Francis A Barr. Grasp55, a second mammalian grasp protein involved in the stacking of golgi cisternae in a cell-free system. *The EMBO journal*, 18(18):4949–4960, 1999. URL <http://www.nature.com/emboj/journal/v18/n18/abs/7591904a.html>. 2.1, 4.1, 4.3, 5
- Xiaokun Shu, Varda Lev-Ram, Thomas J Deerinck, Yingchuan Qi, Ericka B Ramko, Michael W Davidson, Yishi Jin, Mark H Ellisman, and Roger Y Tsien. A genetically encoded tag for correlated light and electron microscopy of intact cells, tissues, and organisms. *PLoS Biol.*, 9(4):e1001041, 2011. 5
- Brian Storrie, Jamie White, Sabine Röttger, Ernst HK Stelzer, Tatsuo Sukanuma, and Tommy Nilsson. Recycling of golgi-resident glycosyltransferases through the er reveals a novel pathway and provides an explanation for nocodazole-induced golgi scattering. *J cell biol*, 143(6):1505–1521, 1998. URL <http://jcb.rupress.org/content/143/6/1505.abstract>. 3.1, 3.2, 3.2, 3.3, 4.2, 4.2, 5
- Nicole S Struck, Susann Herrmann, Christine Langer, Andreas Krueger, Bernardo J Foth, Klemens Engelberg, Ana L Cabrera, Silvia Haase, Moritz Treeck, Matthias Marti, et al. Plasmodium falciparum possesses two grasp proteins that are differentially targeted to the golgi complex via a higher-and lower-eukaryote-like mechanism. *J. Cell Sci.*, 121(13):2123–2129, 2008. URL <http://jcs.biologists.org/content/121/13/2123.short>. 2.2, 4.3
- Thomas Surrey, Michael B Elowitz, Pierre-Etienne Wolf, Feng Yang, FRANCois NEdelec, Kevan Shokat, and Stanislas Leibler. Chromophore-assisted light inactivation and self-organization of microtubules and motors. *Proceedings of the National Academy of Sciences*, 95(8):4293–4298, 1998. URL <http://www.pnas.org/content/95/8/4293.short>. 1, 3.1, 3.3, 4.2
- Danming Tang, Hebao Yuan, and Yanzhuang Wang. The role of grasp65 in golgi cisternal stacking and cell cycle progression. *Traffic*, 11(6):827–842, 2010. 4.3

Cathleen Teh, Dmitry Chudakov, Kar-Lai Poon, Ilgar Mamedov, Jun-Yan Sek, Konstantin Shidlovsky, Sergey Lukyanov, and Vladimir Korzh. Optogenetic in vivo cell manipulation in killerred-expressing zebrafish transgenics. *BMC developmental biology*, 10(1):110, 2010.

3.1

Gro Thorne-Tjomsland, Michel Dumontier, and James C Jamieson. 3d topography of non-compact zone golgi tubules in rat spermatids: A computer-assisted serial section reconstruction study. *The Anatomical Record*, 250(4):381–396, 1998. 4.1

Anna K Townley, Yi Feng, Katy Schmidt, Deborah A Carter, Robert Porter, Paul Verkade, and David J Stephens. Efficient coupling of sec23-sec24 to sec13-sec31 drives copii-dependent collagen secretion and is essential for normal craniofacial development. *Journal of cell science*, 121(18):3025–3034, 2008. URL <http://jcs.biologists.org/content/121/18/3025.short>.

3.2

Alvar Trucco, Roman S Polishchuk, Oliviano Martella, Alessio Di Pentima, Aurora Fusella, Daniele Di Giandomenico, Enrica San Pietro, Galina V Beznoussenko, Elena V Polishchuk, Massimiliano Baldassarre, et al. Secretory traffic triggers the formation of tubular continuities across golgi sub-compartments. *Nat. Cell Biol.*, 6(11):1071–1081, 2004. URL <http://www.nature.com/ncb/journal/v6/n11/abs/ncb1180.html>.

2.5, 3.1

Steven T Truschel, Debrup Sengupta, Adam Foote, Annie Heroux, Mark R Macbeth, and Adam D Linstedt. Structure of the membrane-tethering grasp domain reveals a unique pdz ligand interaction that mediates golgi biogenesis. *J. Biol. Chem.*, 286(23):20125–20129, 2011. URL <http://www.jbc.org/content/286/23/20125.short>.

2.2, 2.2, 2.3, 4.1, 4.3

Steven T Truschel, Ming Zhang, Collin Bachert, Mark R Macbeth, and Adam D Linstedt. Allosteric regulation of grasp protein-dependent golgi membrane tethering by mitotic phosphorylation. *J. Biol. Chem.*, 287(24):19870–19875, 2012. URL <http://www.jbc.org/content/287/24/19870.short>.

4.3

F Vinke, A Grieve, and Catherine Rabouille. The multiple facets of the golgi reassembly stacking proteins. *Biochem. J*, 433:423–433, 2011. URL <http://www.biochemj.org/bj/433/bj4330423.htm>. 4.1, 4.3

Thiennu H Vu and Zena Werb. Matrix metalloproteinases: effectors of development and normal physiology. *Science Signaling*, 14(17):2123, 2000. URL <http://stke.sciencemag.org/cgi/reprint/genesdev;14/17/2123.pdf>. 2.5

Conan K Wang, Lifeng Pan, Jia Chen, and Mingjie Zhang. Extensions of pdz domains as important structural and functional elements. *Protein & cell*, 1(8):737–751, 2010. URL <http://link.springer.com/article/10.1007/s13238-010-0099-6>. 2.2, 2.2

Yanzhuang Wang. Golgi apparatus inheritance. pages 580–607, 2008. URL http://link.springer.com/chapter/10.1007/978-3-211-76310-0_34. 2.4

Yanzhuang Wang, Joachim Seemann, Marc Pypaert, James Shorter, and Graham Warren. A direct role for grasp65 as a mitotically regulated golgi stacking factor. *The EMBO journal*, 22(13):3279–3290, 2003. URL <http://www.nature.com/emboj/journal/v22/n13/abs/7595227a.html>. 2.2, 2.3, 2.3, 4.3

Yanzhuang Wang, Ayano Satoh, and Graham Warren. Mapping the functional domains of the golgi stacking factor grasp65. *J. Biol. Chem.*, 280(6):4921–4928, 2005. URL <http://www.jbc.org/content/280/6/4921.short>. 2.2, 2.3, 4.1, 4.3

Theresa H Ward, Roman S Polishchuk, Steve Caplan, Koret Hirschberg, and Jennifer Lippincott-Schwartz. Maintenance of golgi structure and function depends on the integrity of er export. *The Journal of cell biology*, 155(4):557–570, 2001. URL <http://jcb.rupress.org/content/155/4/557.short>. 3.3

Jen-Hsuan Wei and Joachim Seemann. Mitotic division of the mammalian golgi apparatus. In *Seminars in cell & developmental biology*, volume 20, pages 810–816. Elsevier, 2009. URL <http://www.sciencedirect.com/science/article/pii/S1084952109000494>. 3.3

-
- Jen-Hsuan Wei and Joachim Seemann. Unraveling the golgi ribbon. *Traffic*, 11(11):1391–1400, 2010. [4.2](#)
- Roberto Weigert, Maria Giuseppina Silletta, Stefania Spanò, Gabriele Turacchio, Claudia Cericola, Antonino Colanzi, Silvia Senatore, Raffaella Mancini, Elena V Polishchuk, Mario Salmona, et al. Ctbp/bars induces fission of golgi membranes by acylating lysophosphatidic acid. *Nature*, 402(6760):429–433, 1999. URL <http://www.nature.com/nature/journal/v402/n6760/abs/402429a0.html>. [5](#)
- Jamie White, Ludger Johannes, Frédéric Mallard, Andreas Girod, Stephan Grill, Sigrid Reinsch, Patrick Keller, Barbara Tzschaschel, Arnaud Echard, Bruno Goud, et al. Rab6 coordinates a novel golgi to er retrograde transport pathway in live cells. *The Journal of cell biology*, 147(4):743–760, 1999. URL <http://jcb.rupress.org/content/147/4/743.short>. [3.2](#)
- James RC Whyte and Sean Munro. Vesicle tethering complexes in membrane traffic. *J. Cell Sci.*, 115(13):2627–2637, 2002. URL <http://jcs.biologists.org/content/115/13/2627.short>. [4.1](#)
- Cathal Wilson, Rossella Venditti, L Rega, Antonino Colanzi, Giovanni D’Angelo, and M De Matteis. The golgi apparatus: an organelle with multiple complex functions. *Biochem. J.*, 433:1–9, 2011. URL <http://www.biochemj.org/bj/433/bj4330001.htm>. [4.1](#)
- Yi Xiang and Yanzhuang Wang. Grasp55 and grasp65 play complementary and essential roles in golgi cisternal stacking. *J cell biol*, 188(2):237–251, 2010. URL <http://jcb.rupress.org/content/188/2/237.short>. [2.3](#), [4.2](#), [4.3](#), [5](#), [5](#)
- Smita Yadav, Sapna Puri, and Adam D Linstedt. A primary role for golgi positioning in directed secretion, cell polarity, and wound healing. *Mol. Biol. Cell*, 20(6):1728–1736, 2009. URL <http://www.molbiolcell.org/content/20/6/1728.short>. [1](#), [5](#)

Jordan T Yelinek, Cynthia Y He, and Graham Warren. Ultrastructural study of golgi duplication in trypanosoma brucei. *Traffic*, 10(3):300–306, 2009. [4.3](#)

Shin-ichiro Yoshimura, Katsuji Yoshioka, Francis A Barr, Martin Lowe, Kazuhisa Nakayama, Shoji Ohkuma, and Nobuhiro Nakamura. Convergence of cell cycle regulation and growth factor signals on grasp65. *J. Biol. Chem.*, 280(24):23048–23056, 2005. URL <http://www.jbc.org/content/280/24/23048.short>. [2.2](#)

Christoph Zehe, André Engling, Sabine Wegehingel, Tobias Schäfer, and Walter Nickel. Cell-surface heparan sulfate proteoglycans are essential components of the unconventional export machinery of fgf-2. *Proceedings of the National Academy of Sciences*, 103(42):15479–15484, 2006. URL <http://www.pnas.org/content/103/42/15479.short>. [2.1](#)

Leiliang Zhang, Stella Y Lee, Galina V Beznoussenko, Peter J Peters, Jia-Shu Yang, Hui-ya Gilbert, Abraham L Brass, Stephen J Elledge, Stuart N Isaacs, Bernard Moss, et al. A role for the host coatomer and kdel receptor in early vaccinia biogenesis. *Proceedings of the National Academy of Sciences*, 106(1):163–168, 2009. URL <http://www.pnas.org/content/106/1/163.short>. [2.2](#), [3.2](#)